

# **Ionogels for Sodium Rechargeable Batteries**

**Asier Fernández De Añastro Arrieta**

**University of the Basque Country UPV/EHU**

**Donostia-San Sebastián**

**2019**



Universidad del País Vasco Euskal Herriko Unibertsitatea

**POLYMAT**

Basque Center for  
Macromolecular Design and Engineering



# Contents

## Chapter 1. Introduction 1

---

1.1. Batteries -----	3
1.2. Lithium-ion batteries limitations -----	6
1.3. Sodium based batteries -----	10
1.4. Electrolytes for sodium batteries -----	13
1.5. Organic conventional electrolytes -----	14
1.6. Ionic liquids -----	15
1.7. Polymer electrolytes -----	17
1.7.1. Gel polymer electrolytes -----	18
1.7.2. Ionogels -----	19
1.7.2.1. Poly(ionic liquid)´s based electrolytes -----	21
1.7.2.2. Block copolymer based electrolytes -----	23
1.7.2.3. UV-light cross-linked electrolytes -----	24
1.8. Motivation and objectives -----	25
1.9. Outline of the thesis -----	26
1.10. References -----	28

---

## **Chapter 2. Poly(ionic liquid ) ionogel membranes for all solid-state rechargeable sodium-batteries 39**

---

<b>2.1.</b>	Introduction -----	39
<b>2.2.</b>	Optimizing of ionic conductivity and sodium transference number -----	42
<b>2.2.1.</b>	Membrane preparation -----	42
<b>2.2.2.</b>	Ionic conductivity of the membranes -----	43
<b>2.3.</b>	Rheological properties of poly(ionic liquid) based ionogels -----	49
<b>2.4.</b>	Sodium plating and stripping -----	51
<b>2.5.</b>	Electrochemical performance of the Na/NaFePO <sub>4</sub> sodium solid-state battery -----	53
<b>2.6.</b>	Conclusions -----	56
<b>2.7.</b>	Experimental part -----	57
<b>2.7.1.</b>	Materials and sample preparation -----	57
<b>2.7.2.</b>	Characterization -----	58
<b>2.7.2.1.</b>	Ionic conductivity and sodium transference number ---	58
<b>2.7.2.2.</b>	Rheology -----	59
<b>2.7.2.3.</b>	Electrochemical window -----	59
<b>2.7.2.4.</b>	Electrode preparation -----	60
<b>2.7.2.5.</b>	Sodium plating and stripping -----	60
<b>2.7.2.6.</b>	Electrochem. characterization of solid-state battery ----	61
<b>2.8.</b>	References -----	62

---

# Chapter 3. Poly(diallyldimethylammonium)-Polystyrene Block Copolymers based ionogels

69

---

3.1.	Introduction-----	69
3.2.	Synthesis of MADIX CTA-----	72
3.3.	MADIX polymerization of DADMAC-----	73
3.4.	PISA of Styrene-----	74
3.5.	PDADMA-based Ionogel Membranes-----	79
3.6.	Ionic conductivity-----	81
3.7.	Dynamic mechanical thermal analysis (DMTA) of the ionogel membranes-----	83
3.8.	Conclusions-----	86
3.9.	Experimental part-----	86
3.9.1.	Materials-----	86
3.9.2.	Nuclear Magnetic Spectroscopy (NMR) analysis-----	87
3.9.3.	Gravimetric analysis-----	87
3.9.4.	DMF LiTFSI Size Exclusion Chromatography (SEC)-----	88
3.9.5.	Transmission Electron Microscopy (TEM)-----	88
3.9.6.	Dynamic Mechanical Thermal Analysis (DMTA)-----	89
3.9.7.	Synthesis of Monofunctional Chain Transfer Agent (CTA): Ethoxythiocarbonyl Mercaptoacetic Acid (XAA)-----	89
3.9.8.	Synthesis of Difunctional CTA: X-Pam-DiEst-Pam-X (X-AdA-X)- -----	90
3.9.9.	MADIX/RAFT Polymerization of DADMAC in water-----	95
3.9.10.	Synthesis of Poly(Styrene) block copolymer latexes by Polymerization Induced Self-Assembly (PISA) using PDADMAC macro CTA-----	97

3.9.11.	Ionogels membrane preparation-----	100
3.9.12.	Ionic conductivity-----	100
3.10.	References-----	102

---

## Chapter 4. UV-crosslinked Ionogels for All Solid-State Rechargeable Sodium Batteries 111

---

4.1.	Introduction-----	111
4.2.	Membrane preparation-----	113
4.3.	Mechanical properties and thermal stability-----	116
4.4.	Ionic conductivity and sodium transference number-----	117
4.5.	Symmetric sodium cell-----	120
4.6.	Sodium metal solid state battery-----	122
4.7.	Versatility of UV-crosslinked ionogels-----	125
4.7.1.	UV-crosslinked ionogels for Na-O <sub>2</sub> batteries-----	125
4.7.2.	Phosponium ionic liquid based ionogels-----	128
4.8.	Conclusions-----	130
4.9.	Experimental part-----	131
4.9.1.	Materials and sample preparation-----	131
4.9.2.	Photo-Differential Scanning Calorimetry (DSC) and FTIR---	132
4.9.3.	Thermo-mechanical properties-----	132
4.9.4.	Electrochemical characterization-----	133
4.9.5.	Electrode preparation-----	134
4.9.6.	Sodium plating and stripping-----	135
4.9.7.	Solid state battery-----	136
4.10.	References-----	137

---

<b>Chapter 5. Conclusions</b>	<b>143</b>
-------------------------------	------------

---

<b>List of acronyms</b>	<b>151</b>
-------------------------	------------

---

<b>List of publications, conference presentations and collaborations</b>	<b>153</b>
--	------------

---







# Chapter 1. Introduction

## 1.1. Batteries

Batteries are often mentioned in the news these days, especially as the result of several safety-related issues, but also because of their increasing use for different applications, such as, electric vehicles or electric grid for wind and solar energy sources. This means that the requirements for the batteries are wide and demanding. In case of electric vehicles, energy and power per unit weight and size are the biggest concern and safety and cost as well. However, stationary applications require mostly safety and cost, but also a long lifetime and high charge and discharge rates. Size and weight are secondary considerations.

It is surprising that battery development has progressed much more slowly than other fields of electronics<sup>1</sup>. This slow progress is due to the lack of suitable electrolyte and electrode materials adding difficulties in the interfaces between the components. Batteries have not been a linear development of a single technology, but the emergence of several, with different characteristics and applications.

Ni/Cd are considered to be the first type of batteries when they were used and developed during World War II in German aircrafts but they were not

introduced and spread all over the world after the war. These first batteries had been replaced slowly by metal hybrid/Ni because of environmental concerns, which were firstly introduced in the 1980's by Ovonic Battery Co. in the United States and a number of Japanese companies. Little by little this technology was developed and finally was dominated worldwide by Japanese companies. These batteries are very reliable and they possess very long cycle life, they are now currently used in different applications and vehicles like the Toyota Prius.

It is interesting to mention that the metal hydride materials used in this type of batteries were founded by accident in the Netherlands in the Phillips laboratories. Researchers of this company were investigating the magnetic properties of rare earth alloys and they left some of these alloys in a furnace under hydrogen atmosphere for annealing. Next morning they found that the hydrogen reacted with the alloy and turned into fine powder. They quickly found out that this phenomenon could be used in a new type of battery with a hydrogen storage electrode. Finally, the company did not pursue its commercialization.

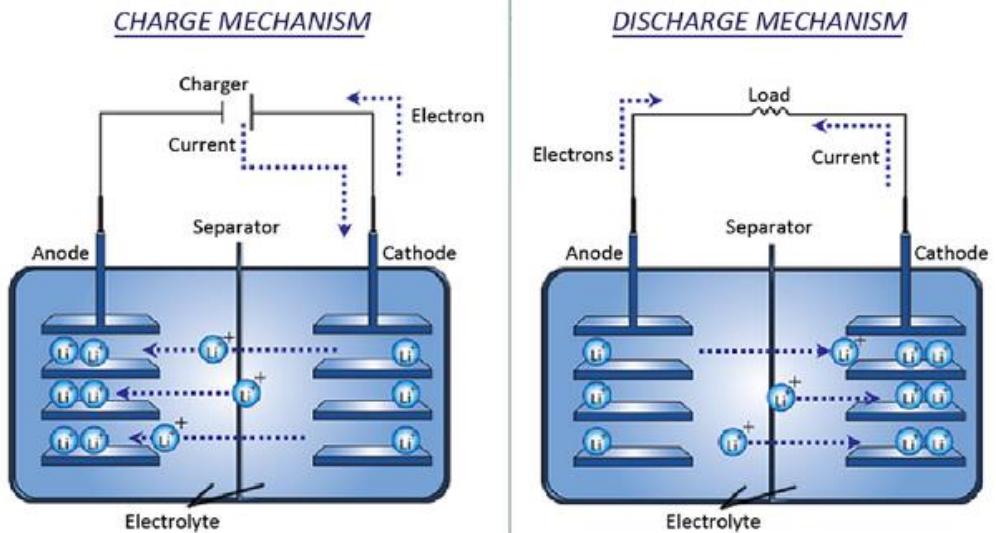
A big innovation was introduced using solid electrolytes, not only for all solid systems but also for liquid/solid/liquid systems like the Na/S high temperature battery. This battery was invented at Ford Motor Co. 1967 while they were investigating the ionic conductivity of the beta phase of aluminium oxide. Researchers and the director of Ford knew that this material could be used to make a new type of batteries but Ford was not interested in battery production so finally the commercialization of these batteries took place in Europe and Japan and not in the United States.

Another innovation in high temperature batteries was the development of Na/NiCl<sub>2</sub> or "Zebra" battery. This type of battery was developed in secret in

South Africa and it first became popular in the United States in 1986. The Zebra battery was developed for use in electric vehicles until testing showed to be unsafe. Later, the further development of these batteries continues in Japan and was recently revived by General Electric in the United States.

But how does a battery work? Since the first battery invented by Alessandro Volta in 1800<sup>2</sup> all batteries are compound of two electrodes separated by an ionic conductive material called electrolyte. These two electrodes have different chemical potential, which depends on the chemistry that occurs at each. When these electrodes are connected by an external circuit (a device), electrons spontaneously flow from the more negative electrode to the positive one creating a flow of electrons that feed the device, at the same time, ions are transported through the electrolyte to balance the charge in both electrodes.

Two scenarios are possible in a battery, charge and discharge. When a battery is discharging, the electrons flow from the anode to the cathode through an external circuit feeding the device connected to it. Batteries that can only be discharged are called primary batteries. On the other hand, secondary batteries are those one than applying an external current source they can be recharged, in other words, the electrons flow from cathode to anode through an external circuit while the ions move towards the anode in order to balance the charge in both electrodes.



**Figure 1.1.** Scheme of a battery in charge and discharge mode.

The amount of electrical energy (per mass or volume) that a battery can deliver is a function of the capacity and the voltage of the battery, which depend directly on the chemistry of the system.

## 1.2. Lithium-ion batteries limitations

However, this battery overview cannot be completed without mentioning lithium-ion batteries. Some researchers in an inorganic chemistry lab in Oxford showed for the first time that it is possible to insert and remove lithium ions from two layer structured oxides as  $\text{LiCoO}_2$  and  $\text{LiNiO}_2$ . In the following years in Bell Labs in the United States and in Grenoble, France, was discovered that lithium ions could be inserted between layers of graphite. Finally, in 1990 SONY

produced the first high voltage rechargeable battery basing in these last discoveries.

The foundation of the lithium-ion battery was laid during the oil crisis in the 1970s. Stanley Whittingham worked on developing methods that could lead to fossil fuel-free energy technologies. While His research was focused in superconductors, he discovered an extremely energy-rich material, which he used to create an innovative cathode for a lithium battery. This was made from titanium disulphide which, at a molecular level, has spaces that can house – intercalate – lithium ions.

The battery's anode was made from metallic lithium, which has a strong drive to release electrons. Finally, this resulted in a battery that had great potential, just over two volts. However, metallic lithium is reactive and the battery was too explosive to be viable.

After that, John Goodenough predicted that the cathode would have even greater potential if it was made using a metal oxide instead of using a metal sulphide. After a big search, in 1980 he demonstrated that cobalt oxide with intercalated lithium ions could produce as much as four volts. This was an important breakthrough and would lead to much more powerful batteries.

Finally, basing on Goodenough's cathode, Akira Yoshino created the first commercially viable lithium-ion battery in 1985. Rather than using reactive lithium in the anode, he used petroleum coke, a carbon material that, like the cathode's cobalt oxide, can intercalate lithium ions.

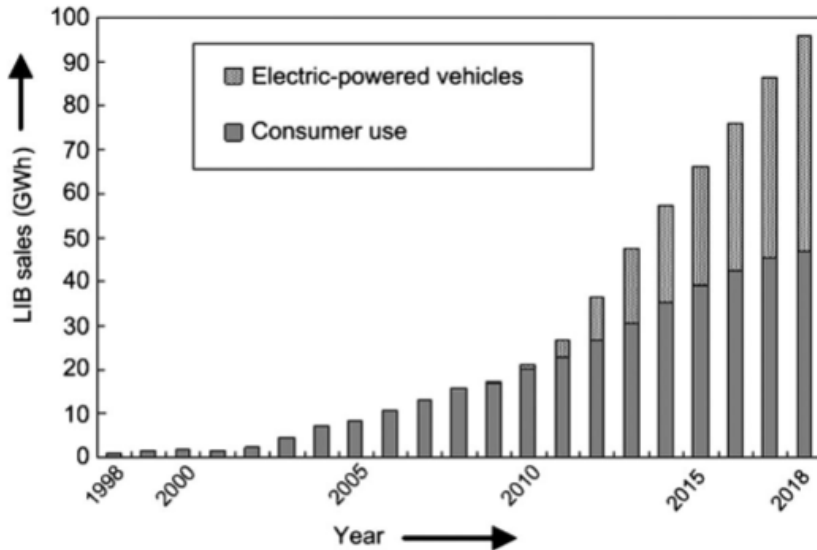
As a result, this year, the Royal Swedish Academy of Science has decided to award the Nobel Prize in chemistry 2019 John B. Goodenough, M. Stanley

Whittingham and Akira Yoshino for the development of lithium ion batteries. The effort and predictions of these three researchers made this technology possible changing our lives since they were first entered in the market in 1991.

Lithium-ion batteries are one of the most advanced rechargeable batteries. They are currently dominating the world of mobile power sources for portable electronic devices<sup>3</sup>. But, why are they more popular? These batteries are more advanced than other commercially available rechargeable batteries mentioned before in this chapter, they have higher energy densities, higher specific energy<sup>4</sup> and they are still expected to dominate the market of rechargeable battery market. Lithium-ion batteries can be formed in a wide variety of size and shapes; they are very flexible in terms of manufacturing. They do not suffer from the problem of memory effect as the Ni/Cd does. Lithium batteries possess very low discharge rate (less than 5% per month versus around 30% of Ni-based batteries).

As it is mentioned before, lithium-ion batteries are widely used in many applications such as cell phones as laptops as well as in hybrid and fully electric cars. But not only energy related applications, but also, lithium is widely used in for ceramics and glasses, is becoming a key ingredient for the pharmaceutical industry<sup>5</sup> and is extensively used in the next generation of nuclear power plants. However, among all applications and advanced properties of lithium-ion batteries, the growing demand of lithium metal is becoming a big problem. Even if lithium elemental abundance is rather big in the crust of the earth, its availability is not as simple as considering only its abundance on the crust, measuring lithium reserves is much more complex.





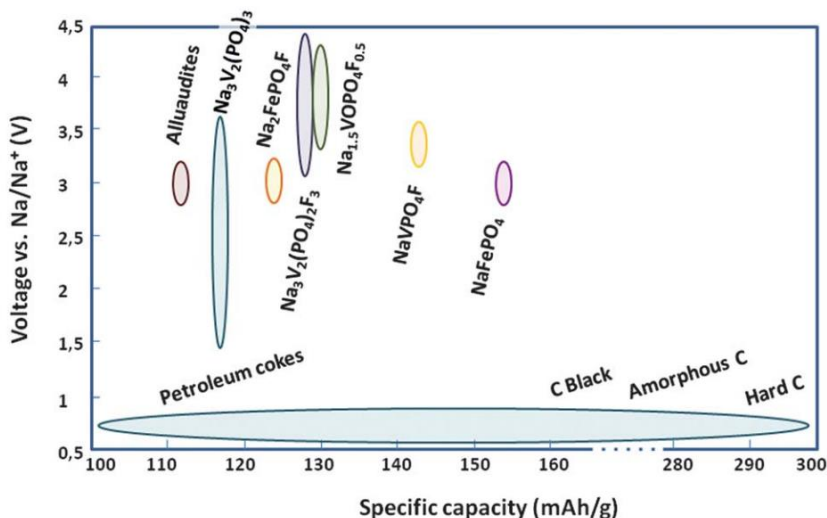
**Figure 1.2.** The increasing lithium-ion batteries sales over the last twenty years.

The measure of lithium reserve is a complex interplay of production, availability, recycling, geographical/political constraints and cost issues making lithium “the new gold”, thus, the actual lithium reserves are dynamic, with the resources being the absolute maximum<sup>5, 6 7</sup>. As an example, replacing each of the world’s 800 million cars with electric vehicles 15kWh lithium-ion batteries would be required and this would be up to 30% of the world’s lithium reserve. New cheaper and more available materials are required to substitute this unsustainable lithium demand.

### 1.3. Sodium based batteries

One of the alternatives is to use sodium instead of lithium. Sodium is an “unlimited”, abundant in the earth’s crust as well as in seawater, low cost and geographically well distributed resource and it can be used in similar technologies than lithium-ion batteries due to its similar chemistry. Another advantage of sodium-ion batteries over the lithium-ion ones is that they do not form alloys with aluminum, meaning that aluminum can be used as current collector minimizing the weight and the cost of the overall battery.

Historically, in the 1980’s and 1990’s sodium-ion batteries and lithium-ion batteries were parallel developed and several electrochemical cells were assembled using different systems like  $\text{TiS}_2$ <sup>8</sup> or  $\text{Na}_x\text{CoO}_2$ <sup>9</sup> as positive electrode using either solid or liquid electrolytes. Unfortunately, this research was quickly abandoned due to the popularity and more generalized field of application of the lithium-ion batteries. The field of sodium-ion battery started to re-emerge in 2010 and is rapidly increasing (more than 250 scientific papers published in 2013).



**1.4. Figure** Screening of the different cathode and anodic materials proposed for sodium batteries in the literature.

Figure 1.4. shows the big variety of cathode and anodic materials proposed for sodium in the literature. The best candidates to be used as cathode materials in a sodium ion battery are phosphate based materials.  $\text{NaFePO}_4$  is the one with highest theoretical capacity among many other phosphate based materials like  $\text{NaVPO}_4\text{F}$ ,  $\text{Na}_3\text{V}_2(\text{PO}_4)_2\text{F}_3$ ,  $\text{Na}_2\text{FePO}_4\text{F}$  and  $\text{Na}_3\text{V}_2(\text{PO}_4)_3$ . These electroactive materials require conductive coating and nanostructured morphology to improve their electrochemical properties.

Among the different anodic materials there has been emerging interest into sodium metal to be used as anode due to its high theoretical capacity (1165 mAh/g) and low electrochemical potential (-2.71 V), maximizing its energy density over different anode materials. Sodium metal batteries started in 1960s using both sulfur and sodium metal in molten state known as high-temperature batteries (operating temperature of 300°C to 350°C)<sup>10, 11</sup>. However, lower

operating temperature batteries are required as well for many different applications.

Different Na based battery systems have been appeared in recent years offering advantages in terms of cost and energy density, such as, sodium-ion, sodium sulfur or sodium-air based on conventional cathodes, S cathodes, halide cathodes and O<sub>2</sub> cathodes.

Na metal batteries have many potential advantages and enable new and different types of cell chemistries, different in terms of service life or efficiency. Like other metals, sodium metal tends to deposit in dendrites. This type of formation can cause many issues related with the safety or/and the efficiency of the battery<sup>12</sup>. Moreover, its high reactivity can degradate the electrolyte or the cell surroundings, and the constant formation/breaking of the solid electrolyte interphase (SEI) lead to a lower Coulombic efficiency and shortened cycling life<sup>13</sup>.

Finding and optimizing new electrode materials and electrolytes is essential to develop and produce sodium-ion batteries in a safer and more economic way. Probably within the next 10 years, sodium-ion batteries will have more attention from the scientific community and they will be pushed and developed rapidly until approaching lithium-ion technology and aiming new niches in the market.

## 1.5. Electrolytes for sodium batteries

While the electrode active material attracts the more attention, the electrolyte has other, equally important roles to play in the cell. This thesis will be mainly focused in new electrolytes for sodium batteries so a screening of the newest and more advanced electrolyte for sodium batteries will be described in this chapter.

But first, some electrolyte basics are described next. The electrolyte is the material located between the cathode and the anode, the electrolyte does not necessarily conduct electricity, but it need to allow the free movement of ions through it. There are some properties that an electrolyte for sodium batteries needs to fulfill<sup>14</sup>:

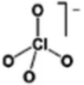
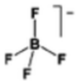

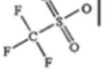
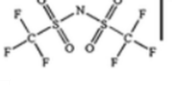
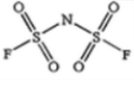
- ✓ Ionic conductivity: The electrolyte must be ionically conductive and electronically insulating material, to sustain battery operation by easy  $\text{Na}^+$  transport. This is one of the most studied and critical property of electrolytes.
- ✓ Chemical stability: The electrolyte must be chemically stable, no chemical reactions during cell operation including both within itself, separator, electrodes used, current collectors or any material employed in the packaging.
- ✓ Electrochemically stable: The electrolyte must have a wide electrochemical window, which means that it need to be stable at any oxidation or reduction process involve in the operational range of potential of the battery.
- ✓ Thermally stable: The electrolyte both the melting and boiling points should be well outside the operation temperatures of the battery.

## 1.6. Organic conventional electrolytes

Organic conventional electrolytes are the most extensive type of electrolyte used either for lithium-ion or for sodium-ion batteries. They usually consist of a sodium salt dissolved in a non-polar solvent.

Historically propylene carbonate (PC) was one of the first organic electrolytes used in lithium and sodium batteries, due to its large liquid range and high dielectric constant. However, it was quickly replaced by ethylene carbonate (EC) as EC passivates on the surface of the graphene based electrodes while the PC caused exfoliation of the graphene. Apart of EC and PC Many different combination of organic electrolytes have been used combining different carbonate organic solvent such as, diethyl carbonate (DEC), ethylmethyl carbonate (EMC) or dimethyl carbonate (DMC) always looking to enhance the ionic conductivity of the sodium ion and to decrease the viscosity of the system.

Normally organic solvents base electrolytes are not only composed by organic solvents but also sodium salts. The most commonly sodium salt used combined with organic solvents is  $\text{NaClO}_4$ , due to a combination of historical and cost reasons. But many other sodium salts are becoming more popular like  $\text{NaPF}_6$ ,  $\text{NaBF}_4$ , NaFSI or NaTFSI due to the roles of these anions in creating suitable ionic liquid matrixes<sup>15, 16</sup>.

SALT	STRUCTURE	SOLVENT
NaClO <sub>4</sub>		3 Ethylene carbonate (EC)
NaBF <sub>4</sub>		Propylene carbonate (PC)
NaPF <sub>6</sub>		Dimethyl carbonate (DMC)
NaTf		Diethyl carbonate (DEC)
NaTFSI		Ethylmethyl carbonate (EMC)
NaFSI		Dimethoxyethane (DME)

**1.5.Figure** Chemical structures of the most common sodium salt and organic solvent used in sodium batteries.

Despite their good battery performance in sodium batteries, this type of electrolyte is highly flammable and volatile and it causes many catastrophic fires and explosions<sup>17-19</sup>. Another type of safer electrolyte is required maintaining the best electrochemical performance.

## 1.7. Ionic liquids

Ionic liquids are novel solvents with unique properties that out perform in many aspects the conventional organic electrolytes<sup>20</sup>. These solvents are composed of structurally asymmetric bulky organic salts. They are able to dissolve a wide range of metal salts at even high concentrations. Comparing with conventional organic electrolytes, ionic liquids are considered the “safer” alternative because of their low flammability, higher stability with sodium metal and their almost negligible vapor pressure. Ionic liquids are intrinsically ionic conductors, being composed entirely of ions, and they possess a wide electrochemical stability. The properties of the ionic liquids can vary and adapt to the application due to the enormous amount of possible cation and anion pairings. As expected ionic liquids have found applications in a big variety of fields<sup>21-24</sup>.

Ionic liquid electrolytes consist in a sodium salt dissolved in an ionic liquid. Many types of salt-ionic liquid have been tried along last decade like NaFSI in C<sub>3</sub>mpyrFSI or NaTFSI in C<sub>4</sub>mpyrTFSI reporting high ionic conductivities of 15,6 mS·cm<sup>-1</sup> and 2 mS·cm<sup>-1</sup> respectively<sup>25</sup>, being some of the most popular ones due to its good electrochemical performance<sup>26-28</sup>. But not only pyrrolidinium based ionic liquids but also, imidazolium, ammonium or phosphonium based ionic liquids mostly combined with NaTFSI or NaFSI salts<sup>29-31</sup>.

Among the different ionic liquid families pyrrolidinium cations, such as *N*-butyl-*N*-methylpyrrolidinium [C<sub>4</sub>mpyr]<sup>+</sup> and *N*-methyl-*N*-propylpyrrolidinium [C<sub>3</sub>mpyr]<sup>+</sup>, are appealing to be excellent candidates to use them in sodium metal batteries especially combined with imide-based anions, such as bis(trifluoromethanesulfonyl)imide [TFSI]<sup>-</sup> and the bis(fluorosulfonyl)imide [FSI]<sup>-</sup> anions<sup>32, 33</sup> due to their good ionic conductivity (0.1-5 mS·cm<sup>-1</sup>), wide



electrochemical window and very low vapor pressure. Although ionic liquids have in general higher viscosity and lower ionic conductivities than the conventional organic electrolytes, some groups reported promising results in terms of enhanced specific capacity and cycle life of LIBs and SIBs employing ionic liquid as electrolytes<sup>34, 35</sup>.

One of the main reason to chose ionic liquids to develop this thesis is because their high stability with sodium metal. Ionic liquids consisting of FSI<sup>-</sup> anion are known for their ability to stabilize the Na metal anode. FSI<sup>-</sup> anion is currently considered as the “magic anion” for film formation because of its low reactivity and the ability to generate radical anions that stabilizes the metal surface<sup>29, 36</sup>. Hosokawa et al. performed an experiment comparing the stability of sodium metal towards FSI<sup>-</sup> and TFSI<sup>-</sup> based ionic liquids<sup>37</sup>. They stored sodium metal in the C<sub>2</sub>C<sub>1</sub>im-FSI (1-ethyl-3-methylimidazolium bis(fluorosulfonyl)imide) and C<sub>2</sub>C<sub>1</sub>im-TFSI (1-ethyl-3-methylimidazolium bis(trifluoromethanesulfonyl)imide) electrolyte for 4 weeks. After this period of time they observed the metal surface was still smooth and shiny with its metallic appear. Furthermore, they observed a much thicker SEI layer in presence of TFSI<sup>-</sup> based electrolyte than for the FSI<sup>-</sup> based counterpart.

But not only the anion influences the stability of the sodium metal, but also the salt concentration, water content or temperature. Many studies are currently focused in studying these different parameters and their influence to sodium metal but still more studies are required to improve to performance of the electrolyte and the metal battery<sup>38, 39</sup>.

In this thesis C<sub>3</sub>mpyrFSI has been used. This ionic liquid has shown excellent behavior in sodium metal batteries. This ionic liquids has an excellent ability to dissolve a wide range of concentration of NaFSI salt, being able to cycle sodium metal batteries from room temperature to elevated temperatures<sup>25</sup>,

<sup>28</sup>. In addition, some studies using similar pyrrolidinium based ionic liquids like buthyl methyl pyrrolidinium bis(fluorosulfonimide) has demonstrated their ability to support sodium chemistry achieving an optimal  $\text{NaFePO}_4$  capacity of 152  $\text{mAh}\cdot\text{g}^{-1}$  (at 1/20C) in a sodium metal battery configuration<sup>40</sup>.

Despite their wide and excellent physico-chemical and electrochemical characteristics, because of their liquid nature, leakage of the electrolyte can cause the failure of the battery or can cause other safety related issue, so still a much more robust and safer electrolyte material is required.

## 1.8. Polymer electrolytes

Polymer electrolytes could be a solution to overcome the poor mechanical properties and the safety issues of liquid electrolytes. Polymers in general are bad solvents for ions ( they have low dielectric constants and very high viscosities), that is why polymers used as electrolytes often had strongly solvating groups such as, carbonyl groups, etheric oxygen atoms or nitrile groups. Poly(ethylene oxide), PEO, was the first polymer used in 1973<sup>41</sup>. PEO was founded to be a conductive polymer with an alkali metal ion in 1973. Moreover, solid polymer electrolytes compared to liquid electrolytes are much less reactive and can be used in sodium batteries. Polymer electrolytes were originally proposed for lithium metal batteries because of their ability to stabilize the anode surface. PEO was used already in 1979 in lithium batteries and still remains at the centre of solid polymer electrolytes<sup>42</sup>.

During the 80's, the study of polymer electrolytes for sodium batteries was based in PEO- $\text{NaClO}_4$  system<sup>43</sup> while in the 90's they focused also in PEO-

$\text{NaCF}_3\text{SO}_3$  and PEO- $\text{NaTFSI}$ <sup>44, 45</sup>. However, PEO system need to operate at least at above 60-80 °C in order to approach to ionic conductivity values that can be useful in practical operation rates. Moreover, sodium metal melts at 98 °C, very close to this temperature limiting the performance of the sodium-ion battery, that contrast with lithium-ion batteries based on solid polymer electrolytes used in the “bluecar” battery by Batscap.

Other polymers like poly(vinylidene fluoride –hexafluoro propylene) PVDF/HFP or poly(methyl meta)acrylate PMMA have been proposed as well to be used in sodium-ion batteries but they are much less studied than PEO based polymer electrolytes<sup>46-48</sup>.

Solid polymer electrolytes have many advantages such as, mechanical strength, dimensional stability or ability to prevent sodium dendrite growth leading to a “safer” type of electrolytes comparing with those liquid electrolytes. However, the low ionic conductivity ( $10^{-4}\text{S}\cdot\text{cm}^{-2}$  -  $10^{-5}\text{S}\cdot\text{cm}^{-2}$ ) limit the performance of the battery and several alternatives have been taken to solve this problem.

### **1.8.1. Gel polymer electrolyte**

One interesting alternative is to try to join the best properties of solid and liquid electrolytes in a single material; these types of materials are known as gel polymer electrolytes. Gel polymer electrolytes are a combination of both materials, the polymer acts as a matrix giving mechanical support while the liquid electrolyte is swollen providing ion transport in liquid manner<sup>49</sup>. If we compare gel polymer electrolytes with the solid polymer electrolytes, they have

lower mechanical strength, but at the same time they offer high ionic conductivities ( $10^{-2}\text{S}\cdot\text{cm}^{-2}$  -  $10^{-3}\text{S}\cdot\text{cm}^{-2}$ ) and better contact with the electrodes. In addition, gel polymer electrolyte have become popular because of its their low volatility, high thermal stability and safety<sup>50</sup>.

The concept of gel polymer electrolyte allows for the applications of a wide range of polymer such as, PEO, PAN, PMMA and Poly(vinylidene fluoride)(PVDF) being the more commonly used<sup>46-48</sup>.

Different type of liquid electrolytes can be used to make gel polymer electrolytes like conventional organic solvents or ionic liquids. As we mentioned before conventional organic liquid electrolyte have many drawbacks in terms of safety so a different electrolyte system is required to full fill the safety and the operational requirements of a good polymer electrolyte for sodium batteries.

### **1.8.2. Ionogels**

One of the approaches for the safer sodium battery is the introduction of ionic liquids into polymer electrolytes. Ionogels usually present the unique properties of the ionic liquids, such as, nonflammability, good chemical and electrochemical stability or high ionic conductivity. Furthermore the polymer is responsible to give to the material the strength and robustness<sup>51, 52</sup>. The use of an ionic liquid in the ionogel can increase the ionic conductivity up to  $6\cdot 10^{-3}\text{S}\cdot\text{cm}^{-1}$ .



**1.6. Figure** Ionogel membrane and the chemical structure of the components used to elaborate it. PIL is used as hosting polymer, pyr<sub>14</sub>TFSI ionic liquid and LiTFSI for Li<sup>+</sup> conduction.

As in other field of polymer electrolytes ionogels were firstly introduced for lithium ion batteries, but are much less studied for sodium-ion batteries<sup>53</sup>. Among all the host polymers that we can find PVDF-HFP as copolymer matrix has been deeply studied<sup>54-56</sup>. The conductivity of the ionogel depends on the ionic liquid and the sodium salt dissolved but it can be very close to the ionic conductivity of the neat ionic liquid, close to  $10^{-3} \text{ S}\cdot\text{cm}^{-1}$ <sup>57</sup>.

Even if ionogels have higher ionic conductivity than solid polymer electrolytes still is one of the limitations of these materials. Normally ionic conductivity of the ionogels are below the neat ionic liquid and there is always a tend to approach as much as possible to this value.

$$\sigma_{\text{solid polymer elect.}} < \sigma_{\text{ionogels}} < \sigma_{\text{gel elect.}} < \sigma_{\text{ionic liquids}} < \sigma_{\text{organic liquid}}$$

Different strategies have been used to increase the ionic conductivity like adding inorganic fillers<sup>58, 59</sup>, increasing the ionic liquid fraction in the ionogel or even using poly ionic liquid<sup>59</sup>. It has been already seen that the the ionic conductivity of the ionogel is limited by the amount of ionic liquid in the polymer. The more ionic liquid the higher will be the ionic conductivity<sup>58, 59</sup>.

One of the most studied approaches to enhance the ionic conductivity is to adjust the amount of the ionic liquid in the polymer or vary the polymer matrix in the ionogel. Furthermore, by increasing the content of ionic liquid the ionic conductivity can be enhanced as well. Marcilla et al. reported several ion gels with different conductivities varying from  $10^{-7}$  to  $10^{-2}$  S·cm<sup>-1</sup> demonstrating that the ionic conductivity depends on the poly(ionic liquid) to ionic liquid ratio<sup>60</sup>.

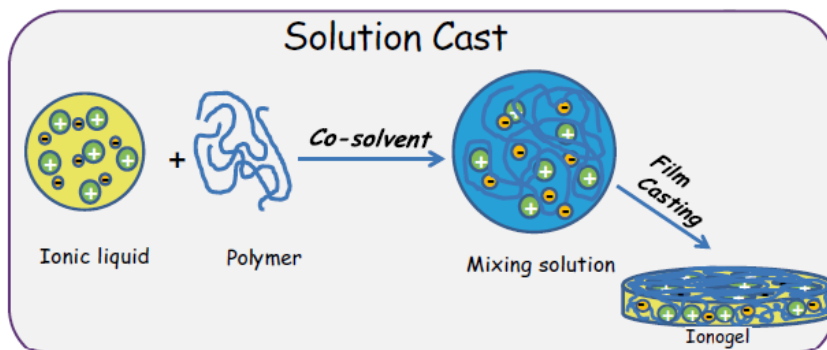
In this thesis we will focus in the development of new ionogels for sodium batteries, trying to approach the ionic conductivity of neat ionic liquids. For that purpose, different ways to prepare ionogels will be described always trying to elaborate a solid ionogel with the highest ionic liquid content. This is a field that is not exhaustively investigated and at the same time very promising due to the interest in developing new safer electrolytes for sodium batteries.

### **1.8.2.1. Poly(ionic liquid)s based ionogels**

As it is mentioned before, one of the approaches to enhance the ionic liquid content of the ionogel is to synthesize new polymeric materials through polymerization of ionic liquid monomers to be used as hosting polymer for the electrolyte system<sup>60-62</sup>. This type of polymer are named poly(ionic liquids).

These materials, exhibit interesting properties as tunable solubility, good ionic conductivity and chemical compatibility towards ionic liquids. Thus, the use of poly(ionic liquids) as hosting polymer to elaborate ionogels present some advantages comparing with other polymer hosts. The chemical affinity between poly(ionic liquids) and ionic liquids affords a completely compatible combination resulting in stable polymer electrolytes. This allows a completely well suited and tunable blend, minimizing and leakage phenomena and phase separation<sup>60</sup>.

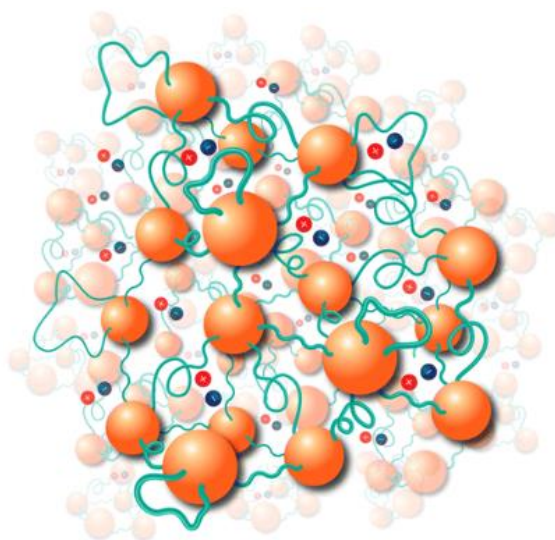
One of the most commonly method of elaboration of this type of ionogels is the solvent mediated method<sup>38, 50</sup>. This elaboration method consist on the mixture of a host polymer with an ionic liquid with the help of a cosolvent in order to form a homogeneous solution that lately is casted and dried to remove the cosolvent. Using this method, the properties of the final material can be adjusted very easily controlling the polymer, ionic liquid and their proportion<sup>51</sup>. However, this method is limited to the compatibility of the polymer and the ionic liquid adding the difficulties of finding a cosolvent able to dissolve the polymer and the ionic liquid at the same time.



**1.7.Figure** Schematic representation of the solution casting method.

### 1.8.2.2. Block copolymers based ionogels

Another type of polymer that it has been used already to make ionogels are the block copolymers. The association of block copolymers with ionic liquids opens an unlimited number of combinations to be explored and exploited. ABA triblock copolymers have been already successfully used to elaborate ionogels immobilizing a large amount of ionic liquids. Furthermore, due to the selective solubility of each block in the ionic liquid the macromolecules can self-assemble providing highly elastic solid with typical mesh sizes in the range of 10–100 nm<sup>63</sup>.



**1.8.Figure** Schematic representation of an ABA triblock copolymer based ionogel.

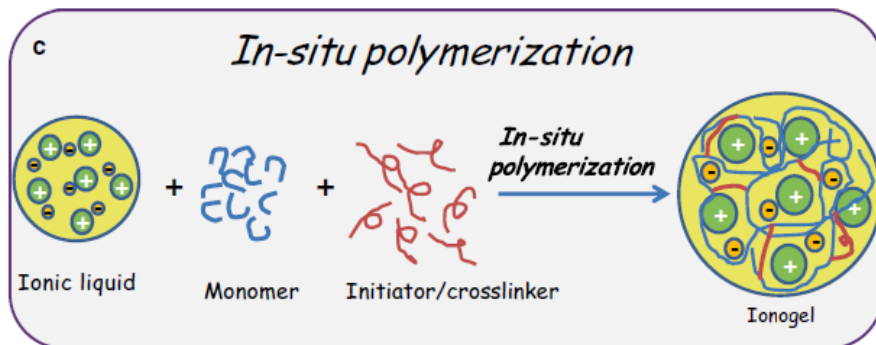


The chemical structure or the molar mass of each block and the concentration of the copolymer are tunable to attain desired properties. For example, the modulus of the resulting ionogel can change between 100 Pa to 1 MPa, with little sacrifice of the ionic conductivity<sup>64</sup>.

### **1.8.2.3. UV-light Cross linked ionogels**

UV-polymerization is a well known polymerization technique, which takes place at room temperature, under UV light: a liquid poly-functional monomer in the presence of a proper photo-initiator, upon irradiation, a solid highly cross-linked film is obtained. The biggest advantages of this process is that is known to be fast and environmentally friendly, as the energy consumption is low and there is no emission of volatile organic compounds.

However the polymer and the ionic liquid need to be carefully chosen since the loss of miscibility during polymerization may be a limitation to obtain the ionogel membrane<sup>65</sup>. Vinyl monomers have been deeply studied since many of them show high compatibility/miscibility with different ionic liquids<sup>66-68</sup>. In this way, mechanically strong, transparent and highly conductive polymer electrolyte films have been obtained. Watanabe and coworkers reported for the first time the in situ radical polymerization of a vinyl monomer 2-hydroxyethyl methacrylate (HEMA) in an ionic liquid 1-butylpyridinium tetrafluoroborate [C<sub>4</sub>py][BF<sub>4</sub>] obtaining an ionogel with an ionic conductivity of 10<sup>-3</sup> S·cm<sup>-1</sup><sup>67</sup>. Using this polymerization technique high ionic liquid loading ionogels can be obtained, close to 90 wt%, obtaining almost same conductivity than the neat ionic liquid<sup>69</sup>.



1.9. **Figure** Schematic representation of the cross linking process.

## 1.10. Motivation and objectives

These days, the approach to make safer and more economic batteries relies on the discovery and development of new components or alternatives to lithium-ion batteries. Sodium seems to be the next generation battery approach but still new electrolytes are required to make this type of battery safer devices.

In this context, ionogels are a very promising type of material because they possess the unique properties of the ionic liquids contained in a tunable solid matrix, giving robustness to the system and making possible to assemble safer sodium batteries.

The main goal of this thesis is to synthesize new ionogels to be used as solid electrolyte in sodium metal batteries. Within this scope, the specific objectives of this thesis are:

- Synthesis and characterization of new ionogels with enhanced physico-chemical and electrochemical properties.

- To Explore different preparation methods of ionogels as self standing membranes.
- Enhance the ionic liquid fraction in the ionogel using different polymers and synthesis methods, to approach as much as possible to the ionic conductivity of the neat ionic liquid.
- Use the optimized ionogels with most promising properties in sodium batteries.

## 1.11. Outline of the thesis

In **chapter 1**, a brief introduction to the history of the batteries is presented. The most advanced battery technologies like lithium-ion and sodium-ion batteries are described and the need of suitable and safer electrolyte materials. The chapter has also introduced the actual electrolytes used in sodium batteries as well as solid electrolytes. Among those we focused in ionogels, their characteristics and different preparation methods, as it will be the main topic of this thesis.

In **chapter 2**, we show the synthesis and characterization of an ionogel membrane based on the poly(dimethyldiallylammonium) polyDADMA-TFSI poly(ionic liquid), N-Propyl-N-methylpyrrolidinium bis(fluorosulfonyl)imide ( $C_3\text{mpyrFSI}$ ) and sodium bis (fluorosulfonyl)imide (NaFSI) the salt. Several parameters are measured like ionic conductivity, transference number or electrochemical window. Finally, the electrochemical performance of the optimum composition ionogel is evaluated in sodium all solid-state battery using sodium metal anode and  $\text{NaFePO}_4$  as the cathode material.

In **chapter 3**, we described the synthesis and characterization of different new ABA triblock copolymer based on polystyrene and poly(dimethyldiallylammonium) (PDADMA-TFSI). The block copolymer show excellent ionic liquid retention and some ionogel membranes are elaborated with them. Different parameters have been analyzed and finally ionic conductivity is measured.

In **chapter 4**, A simple method to prepare a mechanically robust ionogel film by fast (<1 min) UV photopolymerization of poly(ethylenglycol diacrylate) in the presence of an ionic liquid electrolyte (ILE) based on N-Propyl-N-methylpyrrolidinium bis(fluorosulfonyl)imide (C<sub>3</sub>mpyrFSI) IL and sodium bis(fluorosulfonyl)imide (NaFSI) salt is demonstrated. Furthermore, Na/ionogel/NaFePO<sub>4</sub> full cells are easily assembled with the high ILE loading of the ionogel.

In **chapter 5**, materials synthesized in chapter 2, 3 and 4 are summarized and compared. Finally, the most relevant conclusions of this thesis are summarized.

## 1.12. References

1. Armand, M., Tarascon, J. M., Building Better Batteries, *Nature*, **2008**, 451, 652-657.
2. Scrosati, B., History of lithium batteries, *Journal of Solid State Electrochemistry - J SOLID STATE ELECTROCHEM*, **2011**, 15.
3. Deng, D., Kim, M. G., Lee, J. Y., Cho, J., Green energy storage materials: Nanostructured TiO<sub>2</sub> and Sn-based anodes for lithium-ion batteries, *Energy & Environmental Science*, **2009**, 2, 818-837.
4. Tarascon, J. M., Armand, M., Issues and challenges facing rechargeable lithium batteries, *Nature*, **2001**, 414, 359.
5. Tarascon, J.-M., Is lithium the new gold?, *Nature Chemistry*, **2010**, 2, 510.
6. Vikström, H., Davidsson, S., Höök, M., Lithium availability and future production outlooks, *Applied Energy*, **2013**, 110, 252-266.
7. Grosjean, C., Miranda, P. H., Perrin, M., Poggi, P., Assessment of world lithium resources and consequences of their geographic distribution on the expected development of the electric vehicle industry, *Renewable and Sustainable Energy Reviews*, **2012**, 16, 1735-1744.
8. Nagelberg, A. S., Worrell, W. L., A thermodynamic study of sodium-intercalated TaS<sub>2</sub> and TiS<sub>2</sub>, *Journal of Solid State Chemistry*, **1979**, 29, 345-354.
9. Mendiboure, A., Delmas, C., Hagenmüller, P., Electrochemical intercalation and deintercalation of Na<sub>x</sub>MnO<sub>2</sub> bronzes, *Journal of Solid State Chemistry*, **1985**, 57, 323-331.
10. Morachevskii, A. G., Demidov, A. I., Sodium–sulfur system: Phase diagram, thermodynamic properties, electrochemical studies, and use in

- chemical current sources in the molten and solid states, *Russian Journal of Applied Chemistry*, **2017**, 90, 661-675.
11. Lu, X., Lemmon, J. P., Sprenkle, V., Yang, Z., Sodium-beta alumina batteries: Status and challenges, *JOM*, **2010**, 62, 31-36.
  12. Kim, H., Jeong, G., Kim, Y.-U., Kim, J.-H., Park, C.-M., Sohn, H.-J., Metallic anodes for next generation secondary batteries, *Chemical Society Reviews*, **2013**, 42, 9011-9034.
  13. Bieker, G., Winter, M., Bieker, P., Electrochemical in situ investigations of SEI and dendrite formation on the lithium metal anode, *Physical Chemistry Chemical Physics*, **2015**, 17, 8670-8679.
  14. Xu, K., Nonaqueous Liquid Electrolytes for Lithium-Based Rechargeable Batteries, *Chem. Rev.*, **2004**, 104, 4303-4418.
  15. Bhide, A., Hofmann, J., Katharina Dürr, A., Janek, J., Adelhelm, P., Electrochemical stability of non-aqueous electrolytes for sodium-ion batteries and their compatibility with  $\text{Na}_{0.7}\text{CoO}_2$ , *Physical Chemistry Chemical Physics*, **2014**, 16, 1987-1998.
  16. Basile, A., Ferdousi, S. A., Makhlooghiyazad, F., Yunis, R., Hilder, M., Forsyth, M., Howlett, P. C., Beneficial effect of added water on sodium metal cycling in super concentrated ionic liquid sodium electrolytes, *Journal of Power Sources*, **2018**, 379, 344-349.
  17. Wang, J., Yamada, Y., Sodeyama, K., Watanabe, E., Takada, K., Tateyama, Y., Yamada, A., Fire-extinguishing organic electrolytes for safe batteries, *Nature Energy*, **2018**, 3, 22-29.
  18. Grünebaum, M., Hiller, M. M., Jankowsky, S., Jeschke, S., Pohl, B., Schürmann, T., Vettikuzha, P., Gentschev, A.-C., Stolina, R., Müller, R., Wiemhöfer, H.-D., Synthesis and electrochemistry of polymer based electrolytes for lithium batteries, *Progress in Solid State Chemistry*, **2014**, 42, 85-105.

19. Schmitz, R. W., Murmann, P., Schmitz, R., Müller, R., Krämer, L., Kasnatscheew, J., Isken, P., Niehoff, P., Nowak, S., Röschenthaler, G.-V., Ignatiev, N., Sartori, P., Passerini, S., Kunze, M., Lex-Balducci, A., Schreiner, C., Cekic-Laskovic, I., Winter, M., Investigations on novel electrolytes, solvents and SEI additives for use in lithium-ion batteries: Systematic electrochemical characterization and detailed analysis by spectroscopic methods, *Progress in Solid State Chemistry*, **2014**, 42, 65-84.
20. Basile, A., Hilder, M., Makhlooghiyazad, F., Pozo-Gonzalo, C., MacFarlane, D. R., Howlett, P. C., Forsyth, M., Ionic Liquids and Organic Ionic Plastic Crystals: Advanced Electrolytes for Safer High Performance Sodium Energy Storage Technologies, *Advanced Energy Materials*, **2018**, 8, 1703491.
21. MacFarlane, D. R., Forsyth, M., Izgorodina, E. I., Abbott, A. P., Annat, G., Fraser, K., On the concept of ionicity in ionic liquids, *Physical Chemistry Chemical Physics*, **2009**, 11, 4962-4967.
22. Watanabe, M., Thomas, M. L., Zhang, S., Ueno, K., Yasuda, T., Dokko, K., Application of Ionic Liquids to Energy Storage and Conversion Materials and Devices, *Chem. Rev.*, **2017**, 117, 7190-7239.
23. Crowhurst, L., Mawdsley, P. R., Perez-Arlandis, J. M., Salter, P. A., Welton, T., Solvent–solute interactions in ionic liquids, *Physical Chemistry Chemical Physics*, **2003**, 5, 2790-2794.
24. Endres, F., Zein El Abedin, S., Air and water stable ionic liquids in physical chemistry, *Physical Chemistry Chemical Physics*, **2006**, 8, 2101-2116.
25. Ding, C., Nohira, T., Kuroda, K., Hagiwara, R., Fukunaga, A., Sakai, S., Nitta, K., Inazawa, S., NaFSA–C1C3pyrFSA ionic liquids for sodium

- secondary battery operating over a wide temperature range, *Journal of Power Sources*, **2013**, 238, 296-300.
26. Pozo-Gonzalo, C., Johnson, L. R., Jónsson, E., Holc, C., Kerr, R., MacFarlane, D. R., Bruce, P. G., Howlett, P. C., Forsyth, M., Understanding of the Electrogenerated Bulk Electrolyte Species in Sodium-Containing Ionic Liquid Electrolytes During the Oxygen Reduction Reaction, *The Journal of Physical Chemistry C*, **2017**, 121, 23307-23316.
27. Casado, N., Hilder, M., Pozo-Gonzalo, C., Forsyth, M., Mecerreyes, D., Electrochemical Behavior of PEDOT/Lignin in Ionic Liquid Electrolytes: Suitable Cathode/Electrolyte System for Sodium Batteries, *ChemSusChem*, **2017**, 10, 1783-1791.
28. Ding, C., Nohira, T., Hagiwara, R., Matsumoto, K., Okamoto, Y., Fukunaga, A., Sakai, S., Nitta, K., Inazawa, S., Na[FSA]-[C3C1pyrr][FSA] ionic liquids as electrolytes for sodium secondary batteries: Effects of Na ion concentration and operation temperature, *Journal of Power Sources*, **2014**, 269, 124-128.
29. Matsumoto, K., Taniki, R., Nohira, T., *Inorganic-Organic Hybrid Ionic Liquid Electrolytes for Na Secondary Batteries*, 2014.
30. Wongittharom, N., Lee, T.-C., Wang, C.-H., Wang, Y.-C., Chang, J.-K., Electrochemical performance of Na/NaFePO<sub>4</sub> sodium-ion batteries with ionic liquid electrolytes, *Journal of Materials Chemistry A*, **2014**, 2, 5655-5661.
31. Makhlooghiyazad, F., Guazzagaloppa, J., O'Dell, L. A., Yunis, R., Basile, A., Howlett, P. C., Forsyth, M., The influence of the size and symmetry of cations and anions on the physicochemical behavior of organic ionic plastic crystal electrolytes mixed with sodium salts, *Physical Chemistry Chemical Physics*, **2018**, 20, 4721-4731.



32. Hasa, I., Passerini, S., Hassoun, J., Characteristics of an ionic liquid electrolyte for sodium-ion batteries, *Journal of Power Sources*, **2016**, 303, 203-207.
33. Eshetu, G., Jeong, S., Pandard, P., Lecocq, A., Marlair, G., Passerini, S., Comprehensive Insights into the Thermal Stability, Biodegradability, and Combustion Chemistry of Pyrrolidinium-Based Ionic Liquids, *ChemSusChem*, **2017**, 10.
34. Chagas, L. G., Buchholz, D., Wu, L., Vortmann, B., Passerini, S., Unexpected performance of layered sodium-ion cathode material in ionic liquid-based electrolyte, *Journal of Power Sources*, **2014**, 247, 377-383.
35. Li, J., Jeong, S., Kloepsch, R., Winter, M., Passerini, S., Improved electrochemical performance of LiMO<sub>2</sub> (M=Mn, Ni, Co)–Li<sub>2</sub>MnO<sub>3</sub> cathode materials in ionic liquid-based electrolyte, *Journal of Power Sources*, **2013**, 239, 490-495.
36. Fukunaga, A., Nohira, T., Kozawa, Y., Hagiwara, R., Sakai, S., Nitta, K., Inazawa, S., Intermediate-temperature ionic liquid NaFSA-KFSA and its application to sodium secondary batteries, *Journal of Power Sources*, **2012**, 209, 52-56.
37. Matsumoto, K., Okamoto, Y., Nohira, T., Hagiwara, R., Thermal and Transport Properties of Na[N(SO<sub>2</sub>F)<sub>2</sub>]-[N-Methyl-N-propylpyrrolidinium][N(SO<sub>2</sub>F)<sub>2</sub>] Ionic Liquids for Na Secondary Batteries, *The Journal of Physical Chemistry C*, **2015**, 119, 7648-7655.
38. Fukunaga, A., Nohira, T., Hagiwara, R., Numata, K., Itani, E., Sakai, S., Nitta, K., Performance validation of sodium-ion batteries using an ionic liquid electrolyte, *J. Appl. Electrochem.*, **2016**, 46, 487-496.
39. Chen, C. Y., Matsumoto, K., Nohira, T., Hagiwara, R., Full utilization of superior charge-discharge characteristics of Na<sub>1.56</sub>Fe<sub>1.22</sub>P<sub>2</sub>O<sub>7</sub>

- positive electrode by using ionic liquid electrolyte, *Journal of the Electrochemical Society*, **2015**, 162, A176-A180.
40. Wongittharom, N., Wang, C.-H., Wang, Y.-C., Yang, C.-H., Chang, J.-K., Ionic Liquid Electrolytes with Various Sodium Solutes for Rechargeable Na/NaFePO<sub>4</sub> Batteries Operated at Elevated Temperatures, *ACS Applied Materials & Interfaces*, **2014**, 6, 17564-17570.
41. Fenton, D. E., Parker, J. M., Wright, P. V., Complexes of alkali metal ions with poly(ethylene oxide), *Polymer*, **1973**, 14, 589.
42. Hashmi, S. A., Chandra, S., Experimental investigations on a sodium-ion-conducting polymer electrolyte based on poly(ethylene oxide) complexed with NaPF<sub>6</sub>, *Materials Science and Engineering: B*, **1995**, 34, 18-26.
43. West, K., Zachau-Christiansen, B., Jacobsen, T., Skaarup, S., Solid-state sodium cells — An alternative to lithium cells?, *Journal of Power Sources*, **1989**, 26, 341-345.
44. Rhodes, C. P., Frech, R., Local Structures in Crystalline and Amorphous Phases of Diglyme–LiCF<sub>3</sub>SO<sub>3</sub> and Poly(ethylene oxide)–LiCF<sub>3</sub>SO<sub>3</sub> Systems: Implications for the Mechanism of Ionic Transport, *Macromolecules*, **2001**, 34, 2660-2666.
45. Edman, L., Doeff, M. M., Ferry, A., Kerr, J., De Jonghe, L. C., Transport Properties of the Solid Polymer Electrolyte System P(EO)<sub>n</sub>LiTFSI, *The Journal of Physical Chemistry B*, **2000**, 104, 3476-3480.
46. Gao, H., Guo, B., Song, J., Park, K., Goodenough, J. B., A Composite Gel–Polymer/Glass–Fiber Electrolyte for Sodium-Ion Batteries, *Advanced Energy Materials*, **2015**, 5, 1402235.
47. Gao, H., Zhou, W., Park, K., Goodenough, J. B., A Sodium-Ion Battery with a Low-Cost Cross-Linked Gel-Polymer Electrolyte, *Advanced Energy Materials*, **2016**, 6, 1600467.

48. Yang, Y. Q., Chang, Z., Li, M. X., Wang, X. W., Wu, Y. P., A sodium ion conducting gel polymer electrolyte, *Solid State Ionics*, **2015**, 269, 1-7.
49. Ponrouch, A., Monti, D., Boschini, A., Steen, B., Johansson, P., Palacín, M. R., Non-aqueous electrolytes for sodium-ion batteries, *Journal of Materials Chemistry A*, **2015**, 3, 22-42.
50. Fasciani, C., Panero, S., Hassoun, J., Scrosati, B., Novel configuration of poly(vinylidene difluoride)-based gel polymer electrolyte for application in lithium-ion batteries, *Journal of Power Sources*, **2015**, 294, 180-186.
51. Ye, Y.-S., Rick, J., Hwang, B.-J., Ionic liquid polymer electrolytes, *Journal of Materials Chemistry A*, **2013**, 1, 2719-2743.
52. Imaizumi, S., Kokubo, H., Watanabe, M., Polymer Actuators Using Ion-Gel Electrolytes Prepared by Self-Assembly of ABA-Triblock Copolymers, *Macromolecules*, **2012**, 45, 401-409.
53. Manuel Stephan, A., Nahm, K. S., Review on composite polymer electrolytes for lithium batteries, *Polymer*, **2006**, 47, 5952-5964.
54. Li, M., Yang, L., Fang, S., Dong, S., Jin, Y., Hirano, S.-i., Tachibana, K., Li/LiFePO<sub>4</sub> batteries with gel polymer electrolytes incorporating a guanidinium-based ionic liquid cycled at room temperature and 50 °C, *Lancet*, **2011**, 196, 6502-6506.
55. Fergus, J., Ceramic and Polymeric Solid Electrolytes for Lithium-Ion Batteries, *Journal of Power Sources - J POWER SOURCES*, **2010**, 195, 4554-4569.
56. Lewandowski, A., Swiderska-Mocek, A., Waliszewski, L., Li<sup>+</sup> conducting polymer electrolyte based on ionic liquid for lithium and lithium-ion batteries, *Electrochimica Acta*, **2013**, 92, 404-411.
57. Hofmann, A., Schulz, M., Hanemann, T., Gel electrolytes based on ionic liquids for advanced lithium polymer batteries, *Electrochimica Acta*, **2013**, 89, 823-831.

58. Fdz De Anastro, A., Casado, N., Wang, X., Rehmen, J., Evans, D., Mecerreyes, D., Forsyth, M., Pozo-Gonzalo, C., Poly(ionic liquid) iongels for all-solid rechargeable zinc/PEDOT batteries, *Electrochimica Acta*, **2018**, 278, 271-278.
59. Fdz De Anastro, A., Lago, N., Berlanga, C., Galcerán, M., Hilder, M., Forsyth, M., Mecerreyes, D., Poly(ionic liquid) iongel membranes for all solid-state rechargeable sodium-ion battery, *Journal of Membrane Science*, **2019**.
60. Marcilla, R., Alcaide, F., Sardon, H., Pomposo, J. A., Pozo-Gonzalo, C., Mecerreyes, D., Tailor-made polymer electrolytes based upon ionic liquids and their application in all-plastic electrochromic devices, *Electrochemistry Communications*, **2006**, 8, 482-488.
61. Ohno, H., Molten salt type polymer electrolytes, *Electrochimica Acta*, **2001**, 46, 1407-1411.
62. Pont, A.-L., Marcilla, R., De Meazza, I., Grande, H., Mecerreyes, D., Pyrrolidinium-based polymeric ionic liquids as mechanically and electrochemically stable polymer electrolytes, *Journal of Power Sources*, **2009**, 188, 558-563.
63. Lodge, T. P., A Unique Platform for Materials Design, *Science*, **2008**, 321, 50-51.
64. Lodge, T. P., Ueki, T., Mechanically Tunable, Readily Processable Ion Gels by Self-Assembly of Block Copolymers in Ionic Liquids, *Accounts of Chemical Research*, **2016**, 49, 2107-2114.
65. Le Bideau, J., Viau, L., Vioux, A., Ionogels, ionic liquid based hybrid materials, *Chemical Society Reviews*, **2011**, 40, 907-925.
66. Jiang, J., Gao, D., Li, Z., Su, G., Gel polymer electrolytes prepared by in situ polymerization of vinyl monomers in room-temperature ionic liquids, *Reactive and Functional Polymers*, **2006**, 66, 1141-1148.

67. Noda, A., Watanabe, M., Highly conductive polymer electrolytes prepared by in situ polymerization of vinyl monomers in room temperature molten salts, *Electrochimica Acta*, **2000**, 45, 1265-1270.
68. Susan, M. A. B. H., Kaneko, T., Noda, A., Watanabe, M., Ion Gels Prepared by in Situ Radical Polymerization of Vinyl Monomers in an Ionic Liquid and Their Characterization as Polymer Electrolytes, *Journal of the American Chemical Society*, **2005**, 127, 4976-4983.
69. Vioux, A., Viau, L., Volland, S., Le Bideau, J., Use of ionic liquids in sol-gel; ionogels and applications, *Comptes Rendus Chimie*, **2010**, 13, 242-255.



# **Chapter 2. Poly(ionic liquid) ionogel membranes for all solid-state rechargeable sodium-batteries**

## **2.1. Introduction**

Driven by the need of increasing the security of batteries, the area of polymer electrolyte membranes is growing exponentially. Pioneering work on the development of polymer electrolytes for lithium batteries was expended in the last two decades to other types of battery technologies and energy storage devices such as supercapacitors or fuel cells. In each particular case, the requirements of the polymer electrolyte such as ionic conductivity, cation/anion conduction, electrochemical stability or electrochemical window are completely different. For this reason, new polymer electrolytes membranes need to be developed and adapted for the emerging and future energy storage technologies.<sup>1</sup>

Among the emerging battery technologies, sodium-ion is seen as one of the most promising alternative technologies to the current lithium batteries which are used to run portable electronics and the electric vehicles. Nowadays, lithium is expensive and resources are unevenly distributed across the planet. On the

other hand, sodium is cheap and widely available. However, sodium is a larger ion than lithium and the current electrode materials do not work in the case of sodium as in the lithium case. For this reason, new electrode materials need to be found to act as battery components in order to compete with lithium for capacity, speed of charge, energy and power density.<sup>2</sup> Among the different battery components that need to be developed, the polymer electrolyte membrane is a crucial one in particular in a battery configuration which uses sodium metal as anode. The use of sodium as anode brings advantages in terms of specific capacity and power density of the battery, however brings about important safety issues due to the high reactivity of sodium metal. For this reason, electrolytes with low or zero flammability such as ionic liquids<sup>3-5</sup> and polymers<sup>6-9</sup> are ideal candidates in the case of sodium metal batteries.

In the last years, ionic liquid based electrolytes have been developed showing excellent performance in both Na-ion and Na-metal batteries. Several electrolyte formulations have been reported using ammonium, phosphonium, imidazolium and pyrrolidonium ionic liquids having mostly fluorinated sulphonamide anions such as TFSI and FSI combined with NaFSI or NaTFSI salts showing excellent ability to support sodium chemistry.<sup>3</sup> Particularly the ionic liquids including pyrrolidinium cation and sulfonimide type anion combined with sodium salts like C<sub>4</sub>mpyrTFSI/NaTFSI<sup>4, 5</sup> and C<sub>3</sub>mpyrFSI/FSI<sup>6</sup> have been deeply investigated due to their good electrochemical performance. However, their liquid nature brings about some disadvantages such as the need of a porous separator and potential leaking of the electrolyte. To overcome this issue, the preparation of ionogel electrolytes encapsulating the ionic liquid within a polymer network would be an ideal. Although, the use of ionogels is a very popular solution for lithium batteries and other devices such as supercapacitors, to the best of our knowledge there is no report about the development of such



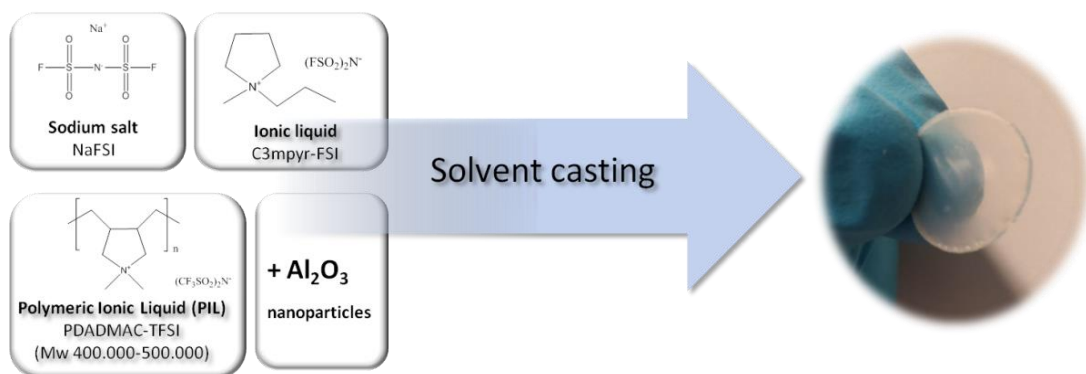
type of polymer electrolyte membrane for Na-ion or Na-metal batteries.<sup>7</sup> It is worth to mention that ionogels membranes are considered as the most promising type of soft solid polymer electrolytes due to their high ionic conductivity and high thermal stability.

In this paper we report the first ionogel membrane which can be used as solid electrolyte in a solid-state sodium rechargeable battery. The ionogels were prepared by using as a polymer matrix the poly(ionic liquid) poly(dimethyldiallylammonium) also known as polyDADMA. This poly(ionic liquid) is known to produce excellent membranes with ionic liquids and it has been previously used as a matrix to design ionogel membranes for lithium<sup>8</sup> and Zn-batteries<sup>9</sup>, supercapacitors<sup>10</sup>, electronics or gas separation.<sup>11, 12</sup> In this work, we present a new ionogel membrane based on polyDADMA-TFSI and the ionic liquid electrolyte formed by N-Propyl-N-methylpyrrolidinium bis(fluorosulfonyl)imide (C<sub>3</sub>mpyrFSI) and sodium bis(fluorosulfonyl)imide (NaFSI). This combination of polymer-ionic liquid has been selected because of the excellent mechanical properties of polyDADMA-TFSI and the good performance of the ionic liquid electrolyte in sodium batteries. This paper focused in understanding and optimizing key parameters of the new ionogel membrane, including ionic conductivity, sodium transference number and rheology. Finally, symmetrical and full-cell sodium batteries were assembled and demonstrated the potential of these ionogels as electrolytes for all solid-state rechargeable sodium ion batteries.

## 2.2. Optimizing of ionic conductivity and sodium transference number of the ionogel membranes.

### 2.2.1. Membrane preparation

Ionogel membranes were formulated with four different components: (1) the polyDADMA-TFSI poly(ionic liquid) (PIL) matrix, which gives the solid and flexible character to the membranes; (2) the ionic liquid  $C_3\text{mpyrFSI}$ , (3) the NaFSI which brings about the  $\text{Na}^+$  ionic conductivity; and (4) an optional component being alumina nanoparticles to further improve in some cases the ionic conductivity or mechanical properties of the polymer electrolyte membranes. The membranes were prepared by dissolving first the polyDADMA-TFSI,  $C_3\text{mpyrFSI}$ , NaFSI and  $\text{Al}_2\text{O}_3$  nanoparticles in acetone. Then the solution was casted and dried on a silicon mould obtaining self-standing flexible membranes as shown in figure 2.1.



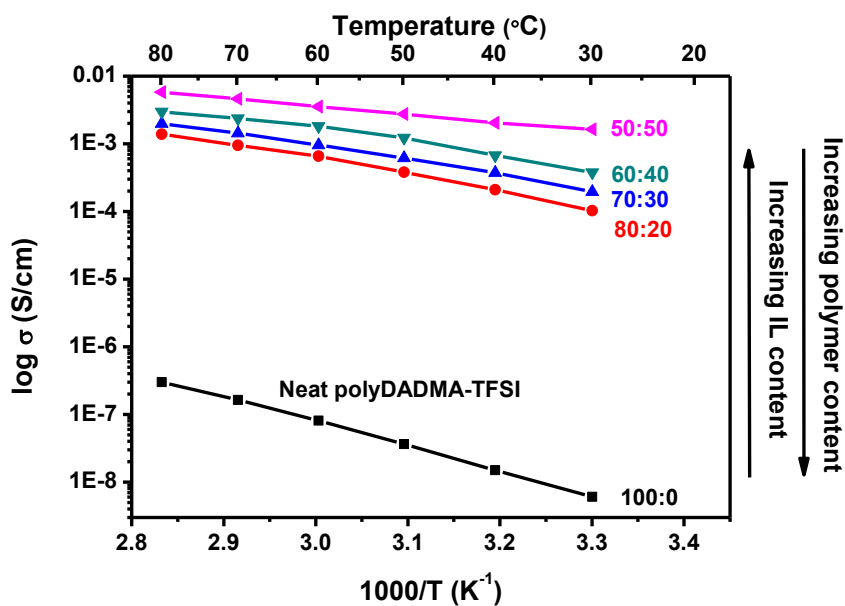
**Figure 2.1.** Schematic preparation method of the ionogel membranes

The composition/properties dependence of the ionogel was initially examined by systematic variation of the different components. As a first observation, increasing the ionic liquid concentration in the membrane, results in more flexible and softer membranes. The polyDADMA-TFSI poly(ionic liquid) matrix can withstand a maximum amount of 50-60 wt.% ionic liquid in a self-standing membrane. At higher amounts of ionic liquid, the membranes were too soft to be handled becoming as honey. The addition of the third component, Al<sub>2</sub>O<sub>3</sub> nanoparticles helps to incorporate a slightly higher amount of ionic liquid fraction and allows improved handling of the self-standing membranes. It was observed that after addition of the alumina nanoparticles the membranes became white and improved their handling as free-standing membranes.

### **2.2.2. Ionic conductivity of the membranes**

To begin with, we carried out a systematic study of the effect of the composition of the ionogel membranes on ionic conductivity at different temperatures. First, we investigated the effect of the content of ionic liquid in the membrane. For this purpose, different composition membranes were prepared varying the amount of IL (C<sub>3</sub>mpyrFSI) that contains 18 mol % of NaFSI salt and mixing it with polyDADMA-TFSI. These membranes were compared with the neat polyDADMAC-TFSI without ionic liquid electrolyte. Four additional ionogel compositions were prepared varying the content of ionic (100:0, 80:20, 70:30, 60:40 and 50:50) in presence of polyDADMA-TFSI as hosting polymer. Whereas, the polyDADMAC-TFSI was brittle, the ionogel membranes were easily handled and flexible; however, by increasing the ionic liquid content beyond 50 wt % a non self-standing viscous liquid electrolyte was obtained. According to figure 2.2., the ionic conductivity measured by impedance

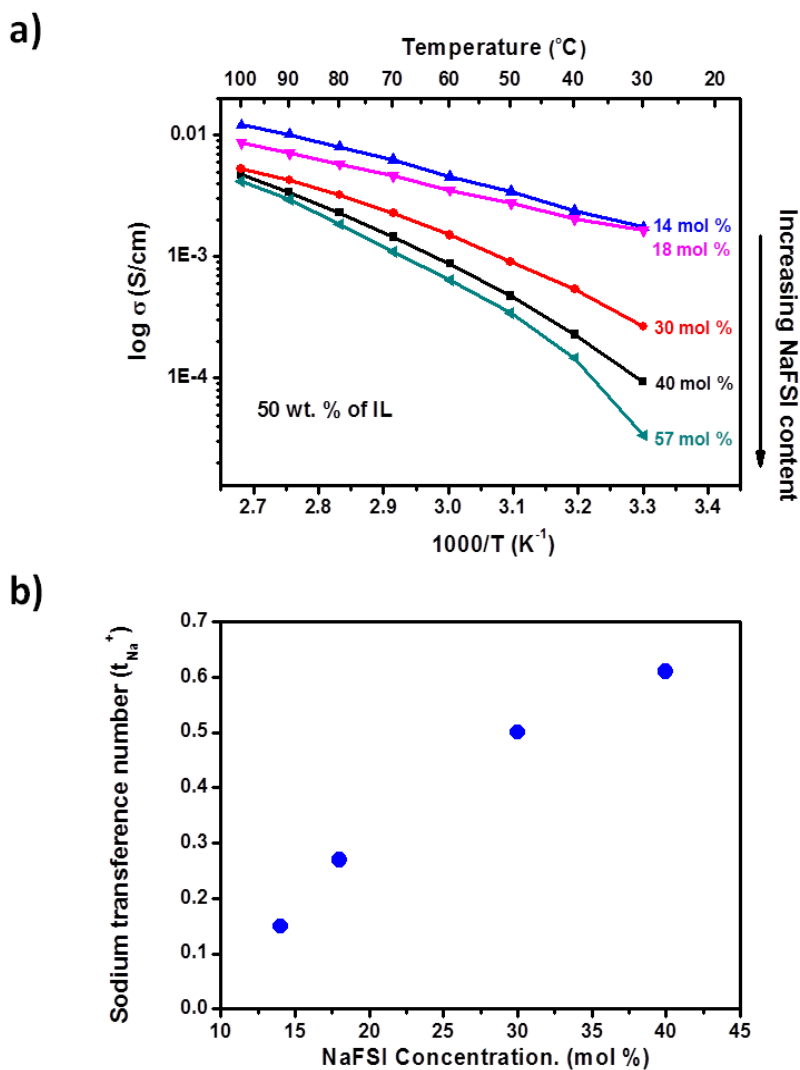
spectroscopy, shows a strong dependence with the IL content. An increase of the %IL content in the ionogel leads to increase the ionic conductivity. The ionic conductivity increases steadily when increases the IL content until approaching  $1.6 \cdot 10^{-3}$  S/cm at  $30^\circ\text{C}$  when 50 wt% of  $\text{C}_3\text{mpyrFSI}$  is added. It is remarkable that the ionic conductivity of the ionogel increases 5 orders of magnitude when adding only a 20 wt % of  $\text{C}_3\text{mpyrFSI}$  to the neat polyDADMA-TFSI (from  $6.1 \cdot 10^{-9}$  S/cm to  $1.1 \cdot 10^{-4}$  S/cm at  $30^\circ\text{C}$ ).



**Figure 2.2.** Ionic conductivity vs temperature of neat polyDADMATFSI and Ionogel membranes having 20, 30, 40, 50 wt. % of  $\text{C}_3\text{mpyrFSI}$  ionic liquid (with 18 mol % of NaFSI)

Second, we investigated the effect of the concentration of NaFSI salt in the poly(ionic liquid) membranes. Thus five different NaFSI salt concentration ionogels were prepared (57 mol %, 40 mol %, 30 mol %, 18 mol % and 14 mol

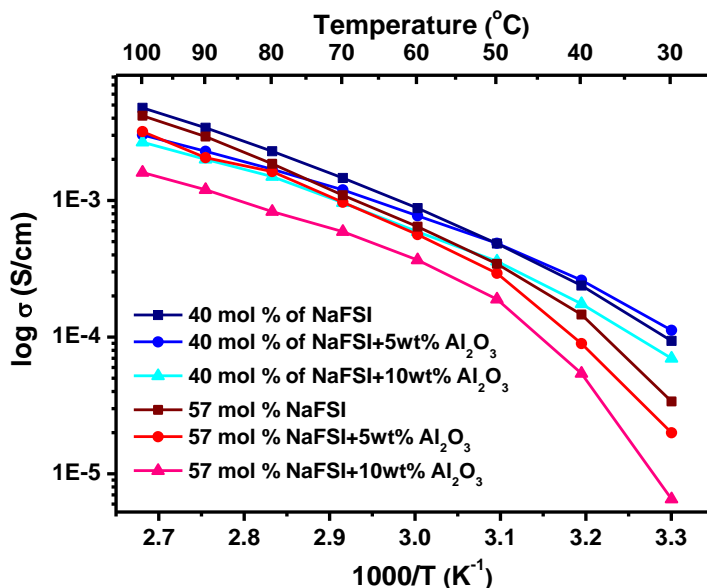
% NaFSI) dissolving the salt into the C<sub>3</sub>mpyrFSI. Each ionogel was prepared keeping constant the 50 wt. % of polyDADMA-TFSI. Figure 2.3.a shows that the ionic conductivity has a strong dependence on the NaFSI content in the electrolyte, the more NaFSI in the ionogel the lower the ionic conductivity. When increasing the concentration of NaFSI the ionogel membrane becomes more rigid and easy to handle but lower ionic conductivity. The ionic conductivity increases from  $1.1 \cdot 10^{-3}$  S/cm (57 mol % NaFSI) to  $7.1 \cdot 10^{-3}$  S/cm (14 mol % NaFSI) at 70°C. The membranes containing high sodium salt concentration (30, 40 and 57 mol % NaFSI) possess a stronger dependence on the temperature, increasing the ionic conductivity 2 orders of magnitude (in case of 57 mol % NaFSI) when varying the temperature from 30°C to 100°C. However, in the case of the membranes with low concentration of NaFSI (14 mol % and 18 mol % NaFSI) the ionic conductivity did not vary significantly (from  $1.12 \cdot 10^{-3}$  S/cm to  $8 \cdot 10^{-2}$  S/cm over the same temperature range). The sodium transference number in these ionogels was determined using the Bruce and Vincent method at 70°C. Here, the transference number increases from 0.15 to 0.61 when NaFSI concentration increases (Figure 2.3.b). Contrary to the ionic conductivity, the increasing amount of sodium salt affects positively to the Na<sup>+</sup> transference number. It is worth to mention that these results are similar to the obtained ones by Hagiwara *et al*<sup>13</sup> and Forsyth *et al*<sup>14</sup> the variation of the Na salt has a negative impact on the ionic conductivity of ionic liquid electrolytes but on the contrary a positive one in the sodium transference number<sup>15</sup>.



**Figure 2.3. a)** Ionic conductivity of ionogel membranes containing 50 wt. % polyDADMA-TFSI and 50 wt. %  $C_3$ mpyrFSI IL with different concentrations of NaFSI salt (from 14 to 57 mol % NaFSI in the IL) at different temperatures. **b)** Sodium transference number of 50 wt. %  $C_3$ mpyrFSI ionic liquid and 50 wt. %

polyDADMA-TFSI ionogel membranes containing different concentrations of NaFSI salt (14 mol %, 18 mol %, 30 mol % and 40 mol %) at 70°C.

Inorganic nanoparticles have been widely used as fillers in polymeric electrolyte materials to improve the ionic conductivity as well as the mechanical properties.<sup>16, 17</sup> For this reason, membranes containing 50 wt. % IL (containing 40 and 57 mol % of NaFSI salt, black and green lines in figure 2.4.) were chosen to study the impact of the addition of alumina nanoparticles. Figure 2.4. shows the effect of wt% of alumina nanoparticles in the ionic conductivity of the ionogels. A small decrease in the conductivity is observed when adding 5 wt. % and 10 wt. % (from  $0.1 \cdot 10^{-4}$  S/cm to  $0.4 \cdot 10^{-4}$  S/cm in case of 40 mol % NaFSI membrane and from  $3.6 \cdot 10^{-5}$  S/cm to  $6.9 \cdot 10^{-6}$  S/cm for membrane containing 57 mol % NaFSI at 30°C). The ionic conductivity drop caused by the addition of alumina nanoparticles is small (less than  $3.3 \cdot 10^{-6}$  S/cm) and even smaller when increasing the temperature. However, the handling of the membranes improved considerably by just adding 5 wt. % of alumina nanoparticles which is a benefit for battery cell assembly showed in the next sections.



**Figure 2.4.** Ionic conductivity of 50 wt. % IL and 50 wt. % polyDADMA-TFSI ionogel membranes containing different concentrations of NaFSI salt (40 mol % and 57 mol %) with 5 wt% and 10 wt% of alumina nanoparticles.

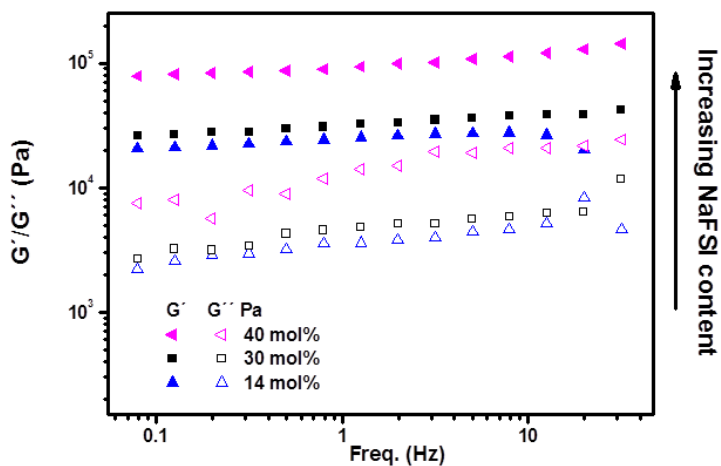
All in all, in the previous sections we investigated the effect of the different ingredients of the membranes in their ionic conductivity and sodium transference number. It is clearly seen that the IL content can improve 4 orders of magnitude the ionic conductivity from 30°C to 70°C. Ionic liquid facilitates the movility of the ions through the membrane giving much higher ionic conductivities for those membranes with high ionic liquid content ( $7.8 \cdot 10^{-3}$  S/cm). On the other hand the ionic conductivity decreases when increasing the NaFSI ( $1.5 \cdot 10^{-3}$  S/cm) but provokes and increase in the sodium transference number up to 0.61.



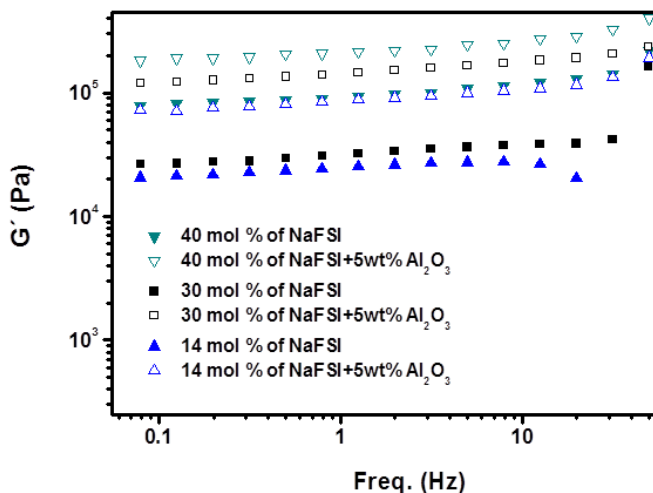
### **2.3. Rheological properties of poly(ionic liquid) ionogel membranes at different temperatures**

The mechanical properties and their stability with temperature are important parameters of polymer electrolyte solid membranes since they prevent the growth of dendrites on the metal electrodes. For this reason, we measured the rheological properties of our membranes in order to estimate its mechanical properties. Figure 2.5.a shows the  $G'$  Storage modulus and  $G''$  loss modulus for 50 wt. % IL containing different NaFSI concentration (40 mol %, 30 mol % and 14 mol % of NaFSI). The ionogel membranes were measured at 25 °C and at the typical operation temperature of a sodium battery at 70 °C. According to figure 2.5.a, the ionogel with higher NaFSI concentration presented the highest modulus probably due to the increase of the viscosity of the liquid fraction in the ionogel. This observation is in accordance with the decrease of ionic conductivity in the case of high NaFSI content ionogels. The dominance of  $G'$  across all frequency ranges indicates that the material has elastic character. For all ionogel compositions shown in figure 2.5.a cross-over between  $G'$  and  $G''$  is not observed meaning that no viscoelastic transitions are present in a wide range of frequency (from 0.06 Hz to 60 Hz). A comparison of the behaviour at both temperatures shows that the  $G'$  and  $G''$  values are very similar. This confirms that the mechanical properties observed in the membrane preparation at room temperature will be similar at the operating temperature of the battery (70 °C).

a)



b)



**Figure 2.5. a)** Rheological properties of 50 wt. % IL and 50 wt. % polyDADMA-TFSI ionogel membranes containing different concentrations of NaFSI salt (14 mol %, 30 mol % and 40 mol %) at 70°C. **b)** Rheological properties of 50 wt. %

IL and 50 wt. % polyDADMA-TFSI ionogel membranes containing different concentrations of NaFSI salt (40 mol %, 30 mol % and 14 mol %) at 70°C adding 5 wt% of alumina nanoparticles.

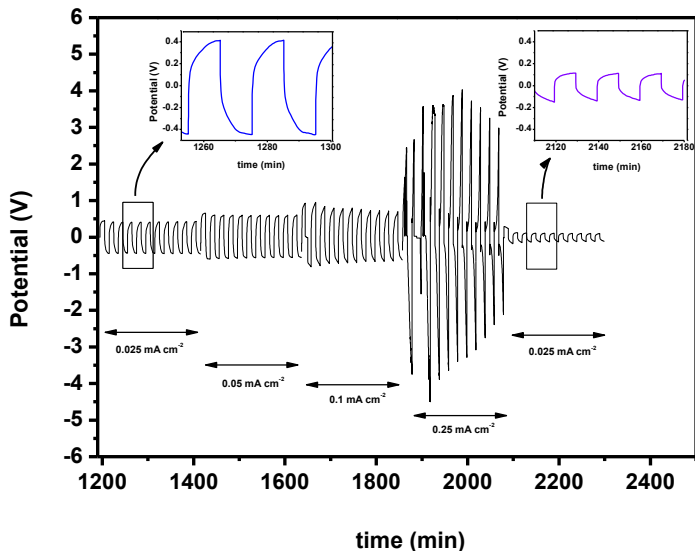
As we described previously, with the aim of increasing the mechanical stability, alumina nanoparticles were added to the ionogel membranes and therefore the equivalent rheological experiments were carried out for 50 wt. % of IL with different concentration of NaFSI salt (14, 30 and 40 mol %) and adding 5 wt% of Alumina nanoparticle. Figure 2.5.b shows that the  $G'$  has been considerably increased showing that the storage modulus improved considerably with 5 wt% of alumina nanoparticle addition. This corroborates a good balance between the ionic conductivity and mechanical properties that are required for good performance of the final battery.

## 2.4. Sodium plating and stripping

After the previous studies, the ionogel membrane with a composition 50:50wt% polyDADMA-TFSI:IL (14 mol%) + 5wt%  $Al_2O_3$  was selected for carrying out the electrochemical characterizations since showed the highest ionic conductivity and excellent mechanical stability at 70 °C. For this reason, first the electrochemical window of the ionogel was examined by cyclic voltammetry with stainless steel as the working electrode and sodium metal as the reference and counter electrode. The measurements were carried out in the potential range of -1 to 4 V (vs. Na/Na<sup>+</sup>). Sodium plating and stripping is observed as two narrow peaks at -0.8 V and -0.35 V respectively. No other significant oxidation current was observed in the operating range of the battery

(from 1.5 to 4.0 V) demonstrating a wide electrochemical window of 5.0 V. This ionogel membrane was therefore further studied in sodium cells.

Next, symmetric sodium cell experiments were carried out since they allow understanding the interface between the anodic material (sodium metal in this case) and the solid electrolyte with respect to the ability to undergo facile oxidation and reduction reactions. Thus, the stripping and plating results for the Na|ionogel|Na symmetric cell at 70 °C are shown in Figure 2.6. This cell was cycled at the following current densities of 0.025, 0.05, 0.1 and 0.25 mA cm<sup>-2</sup> followed by a return to 0.025 mA cm<sup>-2</sup> for 10 cycles at each current density. It can be seen, that the polarization remains below 0.8 V during 0.025, 0.05, 0.1 and 0.025 mA cm<sup>-2</sup> demonstrating the ability of the ionogel to support sodium oxidation and reduction reactions at these current densities. However, the voltage increases dramatically at 0.25 mA cm<sup>-2</sup> showing unstable cycling profiles indicating instability of the Na metal under these conditions. Maybe, lower polarization potentials could be reached by using thinner electrolytes when applying 10 times higher density than the initial one. Interestingly after applying high current density of 0.25 mA cm<sup>-2</sup>, when the current density decreases back to the initial level, the polarization potential drops rapidly, showing a more efficient plating and stripping process and the ability of the ionogel to recover the initial voltage again. Unfortunately, we could not compare these results to other cases of solid electrolytes. When compared with liquid electrolytes, symmetric cell containing 50 mol % NaFSI in C3mpyrFSI show lower overpotentials (less than 0.05V at 0.1 mA·cm<sup>-2</sup>) than these ionogels<sup>15</sup>, this may be due to the better mass transfer that just the liquid electrolytes can achieve comparing with the solid electrolytes.

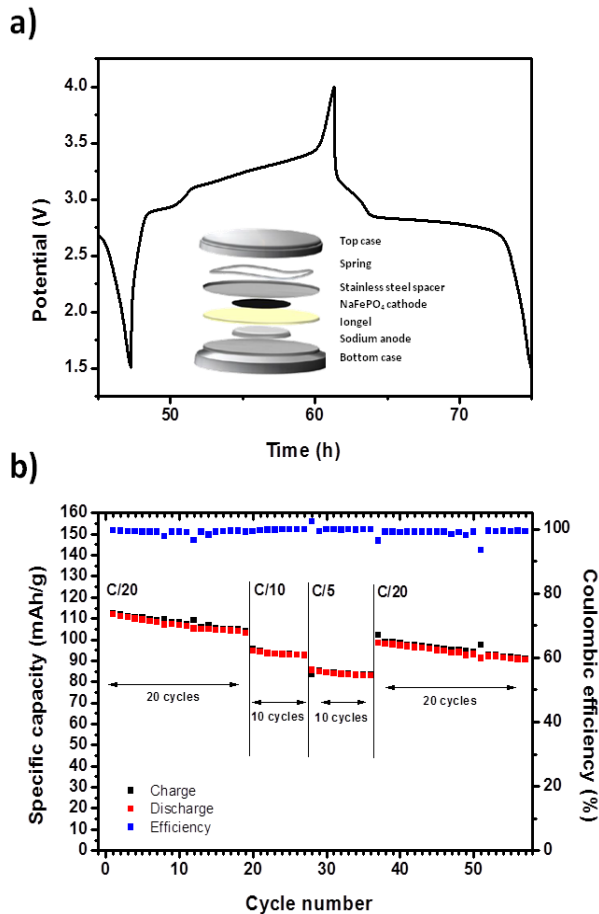


**Figure 2.6.** Plating-stripping cycles at 70 °C at different current densities (0.025, 0.05, 0.1 and 0.025 mA cm<sup>-2</sup>).

## 2.5. Electrochemical performance of the Na/NaFePO<sub>4</sub> sodium solid-state battery

Finally, the electrochemical performance of the optimum composition ionogel was evaluated in a sodium solid state battery using sodium metallic as anodic material and *olivine*-type NaFePO<sub>4</sub> as cathodic material. Among the cathode materials for sodium-ion batteries, NaFePO<sub>4</sub> has recently been identified as a potential cathode<sup>18</sup> NaFePO<sub>4</sub> possesses on the highest theoretical capacity value (154 mAhg<sup>-1</sup>) of polyanionic compounds and maintains some of the exceptional features of its Li counterpart: reaction within a

narrow voltage range inside the voltage stability window of the electrolyte, relatively high operating voltage ( $\sim 2.8$  V)<sup>19</sup>, good stability and good cyclability. Figure 2.7.a shows the charging process of olivine-type NaFePO<sub>4</sub> with the typical two plateaus separated by a voltage drop corresponding to the formation of an intermediate Na<sub>x</sub>FePO<sub>4</sub> ( $x \approx 2/3$ ) phase<sup>20, 21</sup>. Figure 2.7.b shows the rate capability measurements of a Na|ionogel|NaFePO<sub>4</sub> battery at different C-rates cycled from 1.5 to 4.0 V. The results show good capacity retention with high coulombic efficiency (>97%) at each C-rate, achieving the 70 % of the theoretical capacity of the NaFePO<sub>4</sub> at C/20 ( $\sim 115$  mAhg<sup>-1</sup>). The battery also cycled well at C/10 ( $\sim 95$  mAhg<sup>-1</sup>) and C/5 ( $\sim 85$  mAhg<sup>-1</sup>), recovering later the capacity at C/20. As mentioned before this is the first example of ionogel membrane for sodium batteries so we cannot find examples to compare with. However, these results compared favourably with other works using solid polymer electrolytes which display lower capacities at C/5 ( $\sim 80$  mAhg<sup>-1</sup>) using NaFePO<sub>4</sub> as active material<sup>22</sup> demonstrating the good performance of the ionogel to support the chemistry of the sodium in sodium batteries. However, there is still room for improvement since ionic liquid electrolytes such as butylmethylpyrrolidinium-bis(trifluoromethylsulfonyl)imide (Pyr<sub>14</sub>TFSI) ionic liquid was used as liquid electrolyte for Na/NaFePO<sub>4</sub> batteries achieving 125 mAhg<sup>-1</sup> as optimum specific capacity at C/20 (50 °C). In this paper using this ionogel, a specific capacity of 114 mAhg<sup>-1</sup> was obtained at C/20 (70°C), a very promising result considering the solid state presented here. Furthermore the ionogel is able to cycle for more than 60 cycles (more than 1400 hours) providing high capacities for long term experiments.



**Figure 2.7. a)** Charge/discharge profile during cycling at C/20. Cut-off potential: 1.5 V to 4 V **b)** Capacity values and coulombic efficiency for polyDADMA-TFSI:IL (14 mol%) 50:50wt. % + 5wt%  $\text{Al}_2\text{O}_3$  iongel at 70 °C at different c-rates (C/20, C/10 and C/5).

## 2.6. Conclusions

In this work, a new ionogel membrane has been designed based on polyDADMA-TFSI poly(ionic liquid) as polymer matrix, C<sub>3</sub>mpyrFSI as ionic liquid and NaFSI as the salt for Na-ion batteries. We optimized the composition of the ionogel membrane in order to obtain the highest ionic conductivity and sodium transference number. As expected, the ionic liquid content appeared beneficial for the ionic conductivity. Second, the effect of different NaFSI concentrations was beneficial for the sodium transference number but detrimental for the ionic conductivity of the membranes. On the other hand, the addition of alumina nanoparticles did not affect significantly the ionic conductivity of the membranes but made them easier to handle. The mechanical properties were also investigated and the membranes showed stable modulus at room temperature as well as 70 °C. All in all, the optimum composition was a membrane having 50:50wt% polyDADMA-TFSI:IL (14 mol%) + 5wt% Al<sub>2</sub>O<sub>3</sub> which showed an excellent ionic conductivity value of  $1.6 \times 10^{-3}$  S/cm at 30 °C.

The ionogel membranes presented a wide electrochemical window of 5 V which allowed its use in sodium cells. Symmetric sodium cells were investigated showing excellent sodium stripping and plating performance at 70 °C. Then, the electrochemical performance of the optimum composition ionogel was evaluated in a sodium solid state battery using a sodium metal anode and NaFePO<sub>4</sub> as cathode material. The cells show good capacity retention with high coulombic efficiency (>97%) at each C-rate achieving 114 mAhg<sup>-1</sup> at C/20. The battery also worked at C/10 and C/5, recovering later the capacity at C/20, without optimization. To the best of our knowledge this is the first report of a full solid state sodium battery based on ionogels, which demonstrates the applicability to develop sustainable and versatile batteries based on sodium



metal. Interestingly these ionogels compare favourably in values of ionic conductivity and battery performance with the solid electrolytes based on polymers previously reported.

## 2.7. Experimental part

### 2.7.1. Materials and sample preparation

N-Propyl-N-methylpyrrolidinium bis (fluorosulfonyl)imide (C<sub>3</sub>mpyrFSI, Solvionic 99.9%) and Sodium bis (fluorosulfonyl)imide (NaFSI, Solvionic 99.7%) were used as received. Poly(dimethyldiallylammonium bis(trifluoromethanesulfonyl)imide (polyDADMA-TFSI) was synthesized by anionic exchange reaction of Poly(dimethyldiallylammonium) chloride (sigma-aldrich, 20wt% in water) in the presence of lithium bis(trifluoromethanesulfonyl)imide as previously reported.<sup>23</sup>

The ionogels were prepared by dissolving polyDADMA-TFSI, neat C<sub>3</sub>mpyrFSI ionic liquid (IL) and NaFSI salt in acetone (Scharlau). Different mixtures were prepared and finally alumina nanoparticles (Al<sub>2</sub>O<sub>3</sub> <50 nm, Sigma-Aldrich) were also added to the mixture as reinforcement to improve mechanical properties of the ionogels. The mixture was stirred for 1 hour at room temperature and casted on a silicon surface. The casted films were dried for 4 hours in a fume-hood and dried overnight under vacuum at 60 °C. Finally the membranes were cut into circular disks ( $\varnothing = 14$  mm, average thickness = 250  $\mu\text{m}$ ).

## 2.7.2. Characterization

### 2.7.2.1. Ionic conductivity and sodium transference number

The ionic conductivity was measured by electrochemical impedance spectroscopy (EIS) with an Autolab 302N Potentiostat Galvanostat coupled to a Microcell HC station to control the temperature during the measurements. The sample was prepared by punching a circular membrane ( $\varnothing = 11$  mm) with a thickness of 250  $\mu\text{m}$ . The membranes were sandwiched between two stainless steel electrodes and sealed in a Microcell under inert atmosphere in a glove box to avoid contamination of the sample. The measurements were carried out between 20°C and 100°C with a step of 10°C. Before each measurement, temperature was held constant for 25 minutes to allow temperature equilibration of the sample. The frequency range was set from 0.1 MHz to 0.1 Hz and the amplitude was 10 mV. Finally, the conductivity was calculated considering the dimensions of the sample (thickness and area) and the resistance of the membrane (extracted from the Nyquist plot).

Sodium transference number measurements were carried out using a Na/ionogel/Na symmetric cell set up. These Na/ionogel/Na cells were assembled under argon atmosphere in a glove box with Na metal used as counter and working electrode. CR2032 Hohsen coin cell set up was used to test the ionogels, meaning that the ionogel and the electrodes were sandwiched between two stainless steel spacers ( $\varnothing = 16$  mm, thickness = 0.5 mm) which work as current collectors and sealed in a stainless steel bottom type case; a spring (thickness = 1.4 mm) was included to improve the contact between the electrodes and the stainless steel case. The assembling was done with a manual crimper. Sodium transference number was determined by Bruce and Vincent method<sup>24</sup> at 70°C using the following equation:

$$T_{Na^+} = \frac{I_S(\Delta V - I_0 R_0)}{I_0(\Delta V - I_S R_S)}$$

Where  $\Delta V$  is the applied voltage across the cell,  $I_0$  and  $I_S$  are initial and steady-state current, and  $R_0$  and  $R_S$  are initial and steady-state impedance of the measured cell extracted from the Nyquist plot.

### 2.7.2.2. Rheology

TA Instrument AR-G2 was used for recording the viscoelastic properties using oscillatory shear with 12 mm diameter parallel plate geometry. Measurements of the storage ( $G'$ ) and the loss ( $G''$ ) modules involved isothermal frequency scans within the range  $6^2 < \omega < 6^{-2}$  rad/s at 30°C and 70°C, cell operation temperature.

### 2.7.2.3. Electrochemical window

Na/ionogel/Stainless steel cell was used to determine the electrochemical stability of the ionogels. These cells were assembled under argon atmosphere in a glove box with Na metal and stainless steel disc as electrodes. CR2032 Hohsen coin cell set up was used to test the ionogels, meaning that the ionogel and the electrodes were sealed in a stainless steel bottom type case; a spring (thickness = 1.4 mm) was included to improve the contact between the electrodes and the stainless steel case. The assembling was done with a manual crimper. Cyclic voltammetry tests were carried out using a VMP3 Biologic potentiostat at a scan rate of 20 mV/s at 70 °C.

#### **2.7.2.4. Electrode preparation**

Sodium metal was used as anodic material. Sodium circular electrodes were prepared ( $\varnothing = 10$  mm, thickness = 300  $\mu\text{m}$ ) rolling a piece of sodium metal (Panreac) in a glove box.

For the electrode preparation, *olivine*-type  $\text{NaFePO}_4$  was used as cathode active material,  $\text{C}_{65}$  carbon as electronic conductor and polyvinylidene fluoride (PVDF, SOLEF) as binder in a weight ratio of 80:10:10. Materials were gently grinded in a hand mortar using acetone to help mixing. Once acetone was evaporated, the powder was collected and dissolved in 1-methyl-2-pyrrolidone (NMP, Sigma Aldich, 99.5%). The dispersion was stirred at RT for 1 h and the slurry was casted onto aluminium foil paper. The slurry was dried under fume hood for 45 min and finally further drying was done under vacuum at 120 °C overnight. Before the cell assembly, a drop of ionic liquid electrolyte was added to improve the contact between the electrodes which ( $\varnothing = 10$  mm) were pressed applying 2 tons for 2 min.

#### **2.7.2.5. Sodium plating and stripping**

Na/ionogel/Na symmetric cells were assembled to study the plating and stripping of the sodium in the ionogel. The Na/ionogel/Na cells were assembled under argon atmosphere in a glove box with sodium metal used as counter and working electrode. CR2032 Hohsen stainless steel coin type cell was used to

test the ionogels, meaning that the ionogel and the electrodes were sandwiched between two stainless steel spacers ( $\varnothing = 16$  mm, thickness = 0.5 mm) which work as current collectors using a spring (thickness = 1.4 mm) to improve the contact between the electrodes and the stainless steel case. The assembling was done with a manual crimper.

Na symmetrical cell cycling tests were carried out using a VMP3 Biologic potentiostat at 70 °C, increasing constant current densities ( $j = 0.025, 0.05, 0.1, 0.25$  mA cm<sup>-2</sup>) for 10 minutes both stripping and plating during 10 cycles at each current density.

#### **2.7.2.6. Electrochemical characterization of solid state battery**

Na/ionogel/NaFePO<sub>4</sub> half cells were assembled to study the electrochemical performance. *Olivine* NaFePO<sub>4</sub> electrode as cathode and sodium metal as anode were assembled under argon atmosphere in a glove box. CR2032 Hohsen coin cell set up was used to test the ionogels, meaning that the ionogel and the electrodes were sandwiched between two stainless steel spacers ( $\varnothing = 16$  mm, thickness = 0.5 mm) which work as current collectors and sealed in a stainless steel coin type cell; a spring (thickness = 1.4 mm) was included to improve the contact between the electrodes and the stainless steel case. The assembling was done with a manual crimper.

Na/ionogel/NaFePO<sub>4</sub> half cell cycling test were carried out using a VMP3 Biologic potentiostat at 70 °C. The cells were tested at different C rates (C/20, C/10 and C/5) cycled in a potential range of 1.5 V to 4 V for 60 cycles.

## 2.8. References

1. Kim, J. I., Chung, K. Y., Park, J. H., Design of a porous gel polymer electrolyte for sodium ion batteries, *Journal of Membrane Science*, **2018**, 566, 122-128.
2. Palomares, V., Serras, P., Villaluenga, I., Hueso, K. B., Carretero-González, J., Rojo, T., Na-ion batteries, recent advances and present challenges to become low cost energy storage systems, *Energy & Environmental Science*, **2012**, 5, 5884-5901.
3. Basile, A., Hilder, M., Makhlooghiyazad, F., Pozo-Gonzalo, C., MacFarlane, D. R., Howlett, P. C., Forsyth, M., Ionic Liquids and Organic Ionic Plastic Crystals: Advanced Electrolytes for Safer High Performance Sodium Energy Storage Technologies, *Advanced Energy Materials*, **2018**, 8, 1703491.
4. Pozo-Gonzalo, C., Johnson, L. R., Jónsson, E., Holc, C., Kerr, R., MacFarlane, D. R., Bruce, P. G., Howlett, P. C., Forsyth, M., Understanding of the Electrogenerated Bulk Electrolyte Species in Sodium-Containing Ionic Liquid Electrolytes During the Oxygen Reduction Reaction, *The Journal of Physical Chemistry C*, **2017**, 121, 23307-23316.
5. Casado, N., Hilder, M., Pozo-Gonzalo, C., Forsyth, M., Mecerreyes, D., Electrochemical Behavior of PEDOT/Lignin in Ionic Liquid Electrolytes: Suitable Cathode/Electrolyte System for Sodium Batteries, *ChemSusChem*, **2017**, 10, 1783-1791.
6. Ding, C., Nohira, T., Hagiwara, R., Matsumoto, K., Okamoto, Y., Fukunaga, A., Sakai, S., Nitta, K., Inazawa, S., Na[FSA]-[C3C1pyrr][FSA] ionic liquids as electrolytes for sodium secondary batteries: Effects of Na

- ion concentration and operation temperature, *Journal of Power Sources*, **2014**, 269, 124-128.
7. Salsamendi, M., Rubatat, L., Mecerreyes, D., in *Electrochemistry in Ionic Liquids: Volume 1: Fundamentals*, ed. A. A. J. Torriero, Springer International Publishing, Cham, 2015, pp. 283-315.
  8. Wang, X., Zhu, H., Girard, G. A., Yunis, R., MacFarlane, D. R., Mecerreyes, D., Bhattacharyya, A. J., Howlett, P. C., Forsyth, M., Preparation and characterization of gel polymer electrolytes using poly(ionic liquids) and high lithium salt concentration ionic liquids, *Journal of Materials Chemistry A*, **2017**, 5, 23844-23852.
  9. Fdz De Anastro, A., Casado, N., Wang, X., Rehm, J., Evans, D., Mecerreyes, D., Forsyth, M., Pozo-Gonzalo, C., Poly(ionic liquid) ionogels for all-solid rechargeable zinc/PEDOT batteries, *Electrochimica Acta*, **2018**, 278, 271-278.
  10. Tiruye, G. A., Muñoz-Torrero, D., Palma, J., Anderson, M., Marcilla, R., Performance of solid state supercapacitors based on polymer electrolytes containing different ionic liquids, *Journal of Power Sources*, **2016**, 326, 560-568.
  11. Mindemark, J., Mogensen, R., Smith, M. J., Silva, M. M., Brandell, D., Polycarbonates as alternative electrolyte host materials for solid-state sodium batteries, *Electrochemistry Communications*, **2017**, 77, 58-61.
  12. Tomé, L. C., Isik, M., Freire, C. S. R., Mecerreyes, D., Marrucho, I. M., Novel pyrrolidinium-based polymeric ionic liquids with cyano counter-anions: High performance membrane materials for post-combustion CO<sub>2</sub> separation, *Journal of Membrane Science*, **2015**, 483, 155-165.
  13. Matsumoto, K., Okamoto, Y., Nohira, T., Hagiwara, R., Thermal and Transport Properties of Na[N(SO<sub>2</sub>F)<sub>2</sub>]-[N-Methyl-N-

- propylpyrrolidinium][N(SO<sub>2</sub>F)<sub>2</sub>] Ionic Liquids for Na Secondary Batteries, *The Journal of Physical Chemistry C*, **2015**, 119, 7648-7655.
14. Yoon, H., Zhu, H., Hervault, A., Armand, M., MacFarlane, D. R., Forsyth, M., Physicochemical properties of N-propyl-N-methylpyrrolidinium bis(fluorosulfonyl)imide for sodium metal battery applications, *Physical Chemistry Chemical Physics*, **2014**, 16, 12350-12355.
  15. Forsyth, M., Yoon, H., Chen, F., Zhu, H., MacFarlane, D. R., Armand, M., Howlett, P. C., Novel Na<sup>+</sup> Ion Diffusion Mechanism in Mixed Organic–Inorganic Ionic Liquid Electrolyte Leading to High Na<sup>+</sup> Transference Number and Stable, High Rate Electrochemical Cycling of Sodium Cells, *The Journal of Physical Chemistry C*, **2016**, 120, 4276-4286.
  16. Klongkan, S., Pumchusak, J., Effects of Nano Alumina and Plasticizers on Morphology, Ionic Conductivity, Thermal and Mechanical Properties of PEO-LiCF<sub>3</sub>SO<sub>3</sub> Solid Polymer Electrolyte, *Electrochimica Acta*, **2015**, 161, 171-176.
  17. Liu, W., Liu, N., Sun, J., Hsu, P.-C., Li, Y., Lee, H.-W., Cui, Y., Ionic Conductivity Enhancement of Polymer Electrolytes with Ceramic Nanowire Fillers, *Nano Letters*, **2015**, 15, 2740-2745.
  18. Moreau, P., Guyomard, D., Gaubicher, J., Boucher, F., Structure and Stability of Sodium Intercalated Phases in Olivine FePO<sub>4</sub>, *Chemistry of Materials*, **2010**, 22, 4126-4128.
  19. Fernández-Roperó, A. J., Zarrabeitia, M., Reynaud, M., Rojo, T., Casas-Cabanas, M., Toward Safe and Sustainable Batteries: Na<sub>4</sub>Fe<sub>3</sub>(PO<sub>4</sub>)<sub>2</sub>P<sub>2</sub>O<sub>7</sub> as a Low-Cost Cathode for Rechargeable Aqueous Na-Ion Batteries, *The Journal of Physical Chemistry C*, **2018**, 122, 133-142.



20. Galceran, M., Roddatis, V., Zúñiga, F. J., Pérez-Mato, J. M., Acebedo, B., Arenal, R., Peral, I., Rojo, T., Casas-Cabanas, M., Na-Vacancy and Charge Ordering in  $\text{Na}_{2/3}\text{FePO}_4$ , *Chemistry of Materials*, **2014**, 26, 3289-3294.
21. Boucher, F., Gaubicher, J., Cuisinier, M., Guyomard, D., Moreau, P., Elucidation of the  $\text{Na}_{2/3}\text{FePO}_4$  and  $\text{Li}_{2/3}\text{FePO}_4$  Intermediate Superstructure Revealing a Pseudouniform Ordering in 2D, *Journal of the American Chemical Society*, **2014**, 136, 9144-9157.
22. Colò, F., Bella, F., Nair, J. R., Destro, M., Gerbaldi, C., Cellulose-based novel hybrid polymer electrolytes for green and efficient Na-ion batteries, *Electrochimica Acta*, **2015**, 174, 185-190.
23. Pont, A.-L., Marcilla, R., De Meazza, I., Grande, H., Mecerreyes, D., Pyrrolidinium-based polymeric ionic liquids as mechanically and electrochemically stable polymer electrolytes, *Journal of Power Sources*, **2009**, 188, 558-563.
24. Evans, J., Vincent, C. A., Bruce, P. G., Electrochemical measurement of transference numbers in polymer electrolytes, *Polymer*, **1987**, 28, 2324-2328.



# **Chapter 3. Poly(diallyldimethylammonium)- Polystyrene Block Copolymers based ionogels**

## **3.1. Introduction**

Poly(diallyldimethyl ammonium chloride) (PDADMAC) is a commercially available cationic polyelectrolyte commonly used in water purification processes.<sup>1</sup> In the last years the poly(ionic liquid) versions of PDADMAC obtained by anion exchange of the chloride anion by sulfonamide anions are being successfully investigated in different applications such as polymer electrolyte for batteries<sup>2,3</sup> and supercapacitors,<sup>4</sup> gas separation membranes,<sup>5,6</sup> flocculants for water purification, magnetic polymers or as smart-stabilizers in nanotechnology.<sup>7</sup> In most of these emerging applications a PDADMAC based poly(ionic liquid) of high molecular weight polymer is used in combination of an ionic liquid plastisizer to form a free-standing membrane. The polymer gives the mechanical properties and the good interaction with the ionic liquid avoiding its leaching, whereas the ionic liquid confers to the material the excellency in ionic conductivity or gas permeability desired for the

applications. As a limitation once the ionic liquid content is higher than 50 wt% the ionic liquid/poly(ionic liquid) material becomes too soft to form a free-standing membrane as seen in the previous chapter of this thesis. So, there is a need of PDADMAC copolymers which allow to form free-standing membranes with higher ionic liquid contents. For instance, the use of triblock copolymers was pioneered by Lodge et al. as excellent matrices for ionogels with high ionic liquid content.<sup>8</sup>

Industrially, the synthesis of PDADMAC is carried out by free radical (cylico)polymerization (FRP) of DADMAC monomer in water.<sup>9–11</sup> However, the controlled polymerization and the formation of well-defined chain lengths of PDADMAC remains difficult. The recent advances in controlled radical polymerization (CRP), as Reversible-Addition Fragmentation Transfer (RAFT) polymerization, demonstrated the possibility to control the different macromolecular parameters during the process.<sup>12–17</sup> More specifically, RAFT with the use of xanthate, namely Macromolecular Design by Interchange of Xanthate (MADIX), appeared to be well-suited for the control of less-activated monomers (LAMs), such as DADMAC.<sup>14,16,18–21</sup> Destarac *et al.* notably obtained PDADMAC having molecular weights close to 40 kg/mol in the presence of xanthate Rhodixan A1-terminated acrylamide oligomer.<sup>22</sup> Lately, Balsara and coworkers have synthesized poly(styrene)-*b*-PDADMA(OH<sup>-</sup>) copolymers by MADIX for the formation of stable hydroxide-ion transport membranes.<sup>23</sup> However, the synthetic strategy required several steps and different solvents to obtain the final copolymer, mostly due to the huge difference of hydrophobicity between the two blocks.

Polymerization-Induced Self-Assembly (PISA) is an excellent tool that allows the synthesis of amphiphilic block copolymers by controlled radical polymerization. Furthermore PISA allows the synthesis of the block

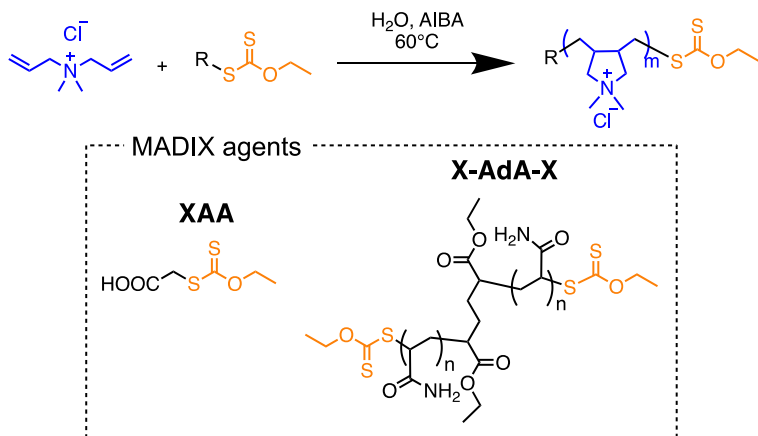
copolymer in one pot and the formation of latexes by self-assembly of the block copolymers either in forms of spheres or other morphologies, as worms, "jellyfish" or vesicles, by varying the DPs of both blocks.<sup>24-41</sup> Although PISA is receiving an enormous interest in the last years, to the best of our knowledge, the synthesis of PDADMAC block copolymers by PISA has not been reported yet. Interestingly, the synthesis of block copolymers having cationic blocks was previously demonstrated by PISA having ammonium containing acrylic blocks in combination with polystyrene or poly(methyl methacrylate). In all the cases where ionic macromonomers were used, only spherical particles were observed due to the strong electrostatic repulsion of the stabilizing chains.

In this paper, we reported the synthesis of poly(diallyldimethylammonium)-based di- and triblock copolymers by MADIX/RAFT. First, DADMAC was polymerized in water using mono- or difunctional MADIX agents at 60 °C with the water soluble diazo radical initiator. Taking advantage of the PISA technique, PDADMAC served as macroinitiator for the emulsion of styrene (S) in water at 60 °C, leading to the formation of cationic latexes, either di- or triblock copolymers. We investigated the different parameters that influence the synthesis of the morphology of the latex particles. After anion exchange, the PDADMAC poly(ionic liquid) block copolymers were dissolved in toluene and mixed with different amount of ionic liquid electrolyte commonly used in sodium batteries. Self-standing membranes were obtained by casting and the ionic conductivity was measured by electrochemical impedance spectroscopy (EIS). The ionogel based on PDADMAC block copolymers showed high ionic liquid electrolyte retention and superior properties than previously reported PDADMA/ionic liquid ionogels.

## 3.2. Synthesis of MADIX CTA

First, the controlled radical polymerization of DADMAC using MADIX agent was studied. Xanthate agents have shown excellent properties for the control of DADMAC at 60°C.<sup>15,16</sup> Here, we implemented the synthesis of controlling MADIX agent, targeting both mono- and difunctional molecules.

As monofunctional controlling agent, S-ethoxythiocarbonyl mercaptoacetic acid, namely XAA (Figure 3.1.), was chosen by reacting potassium ethyl xanthogenate and bromoacetic acid, as reported in the literature.<sup>44,45</sup> Its structure was confirmed by <sup>1</sup>H NMR. Similarly, a difunctional MADIX agent was synthesized in two steps: (1) diethyl meso-2,5-dibromoadipate was reacted with potassium ethyl xanthogenate leading to a dixanthate diester molecule (X-DiEst-X);<sup>46</sup> (2) due to the insolubility of this X-DiEst-X in water, we performed the polymerization of acrylamide in EtOH:H<sub>2</sub>O mixture in order to synthesize a water-soluble difunctional macroinitiator (X-PAm-DiEst-PAm-X). The intermediate and final products were characterized by <sup>1</sup>H NMR. MALDI mass spectrometry was realized to determine the precise molecular weight of the difunctional MADIX agent. The number averaged molecular weight of X-PAm-DiEst-PAm-X is around 1850 g/mol (1.02) and a corresponding DP of 26. To the best of our knowledge, this difunctional X-PAm-DiEst-PAm-X (X-AdA-X) MADIX agent has been synthesized for the first time.



**Figure 3.1.** Polymerization of DADMAC using mono- and difunctional MADIX agents, namely S-ethoxythiocarbonyl mercaptoacetic acid (XAA) and diester-based CTA (X-AdA-X).

### 3.3. MADIX Polymerization of DADMAC

Once both CTA MADIX agents have been synthesized, the study of DADMAC polymerization conditions was performed in water at  $60^\circ\text{C}$  using 2,2-azobis(2-methylpropionamidine) dihydrochloride (AIBA) as radical initiator and monofunctional XAA as controlling agent (Figure 3.1.A). Four PDADMAC macroinitiators (mono- and difunctional) have been synthesized and characterized by SEC, targeting different degrees of polymerization (DP) (Table 1, Entries 1-4). Due to the broad signals obtained in  $^1\text{H}$  NMR, the calculation of DPs was determined using SEC values of molecular weight. For the XAA monofunctional, we synthesized a small chain with  $M_n \text{ SEC} = 4\,600$  g/mol (PDADMAC<sub>5k</sub>,  $M_w/M_n = 1.12$ ) (Table 1, Entry 1) and a longer macroCTA

(PDADMAC<sub>18k</sub>,  $M_n$  SEC = 17 800 g/mol,  $M_w/M_n$  = 1.21) (Table 1, Entry 2). The X-AdA-X difunctional macroinitiator was used to create a difunctional macroCTA of 12 800 g/mol (PDADMAC<sub>13k</sub>,  $M_w/M_n$  = 1.38) after 1.25 h and 53% conversion (Table 1, Entry 3), while a longer difunctional macroCTA was formed with a  $M_n$  SEC = 30 900 g/mol (PDADMAC<sub>31k</sub>,  $M_w/M_n$  = 1.28) (Table 1, Entry 4).

**Table 1.** MADIX polymerization of DADMAC in water at 60°C.<sup>a</sup>

Entries	CT A <sup>b</sup>	[DAD]/[CTA]	Time (h)	$V_{H_2O}$ total (ml)	[DAD] (M)	Conv. (%) <sup>c</sup>	$M_n$ th (kg/mol) <sup>d</sup>	$M_n$ SEC (kg/mol) <sup>e</sup>	$M_w/M_n$ <sup>e</sup>	D Pt	Code
1	XA A	30	2	/	3.5	50	2.6	4.6	1.12	27	PDADMA C <sub>5k</sub>
2	XA A	400	6	/	3.5	40	27.6	17.8	1.21	11 1	PDADMA C <sub>18k</sub>
3	X- Ad A-X	49	1.2 5	/	3.5	53	6.1	12.8	1.38	68	PDADMA C <sub>13k</sub>
4	X- Ad A-X	400	5	/	3.5	51	34.7	30.9	1.28	18 0	PDADMA C <sub>31k</sub>

<sup>a</sup> Conditions: [CTA]/[AIBA] = 1/0.3.

<sup>b</sup> XAA = S-ethoxythiocarbonyl mercaptoacetic acid and X-AdA-X = X-PAM-DiEst-PAM-X (Scheme 1).

<sup>c</sup> Determined by <sup>1</sup>H NMR in D<sub>2</sub>O.

<sup>d</sup> Determined via the conversion.

<sup>e</sup> Determined by SEC in H<sub>2</sub>O (CH<sub>3</sub>COOH/CH<sub>3</sub>COONa 0.2/0.3M)

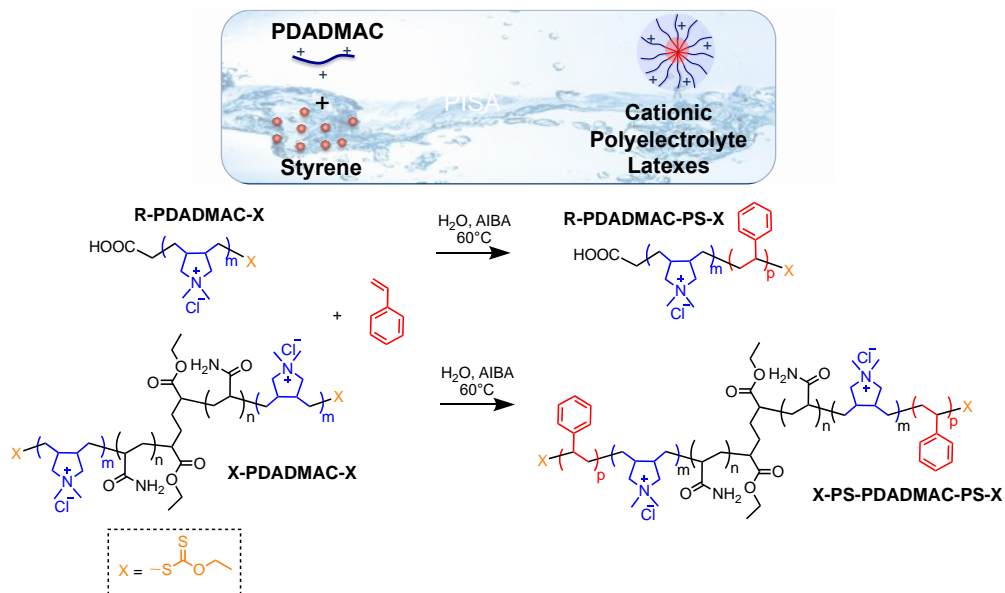
<sup>f</sup> Calculated via  $M_n$  SEC.

### 3.4. PISA of Styrene

Cationic polyelectrolyte latexes synthesis was performed by PISA of styrene in aqueous emulsion. As shown in figure 3.2., mono- and difunctional PDADMAC macroinitiators were used in water to polymerize styrene as hydrophobic monomer in a total solid content of 12 wt%. After MADIX emulsion



polymerization, diblock and triblock nanoparticles (NPs) were created with a poly(styrene) block located in the core of the latexes and PDADMAC block constituting the shell of the NPs (Figure 3.2.).



**Figure 3.2.** Synthetic scheme of PISA of styrene in water using monofunctional (R-PDADMAC-X) and difunctional PDADMAC-based macroCTA (X-PDADMAC-X).

The conversion of styrene was measured gravimetrically and 100% was achieved after 6h of polymerization for both macroinitiators (Figure 3A). Regarding the monofunctional PDADMAC<sub>18k</sub> macroininitiator (Table 1, Entry 2), an analysis of the reaction medium showed an increase in the turbidity between 0.5 and 4h of polymerization (Figure 3.3.B), confirmed by Transmission electron microscopy (TEM) images that clearly showed higher diameters ( $145 \pm 30$  nm) at 4h. After 24h, TEM images showed white stable latex solutions with spherical

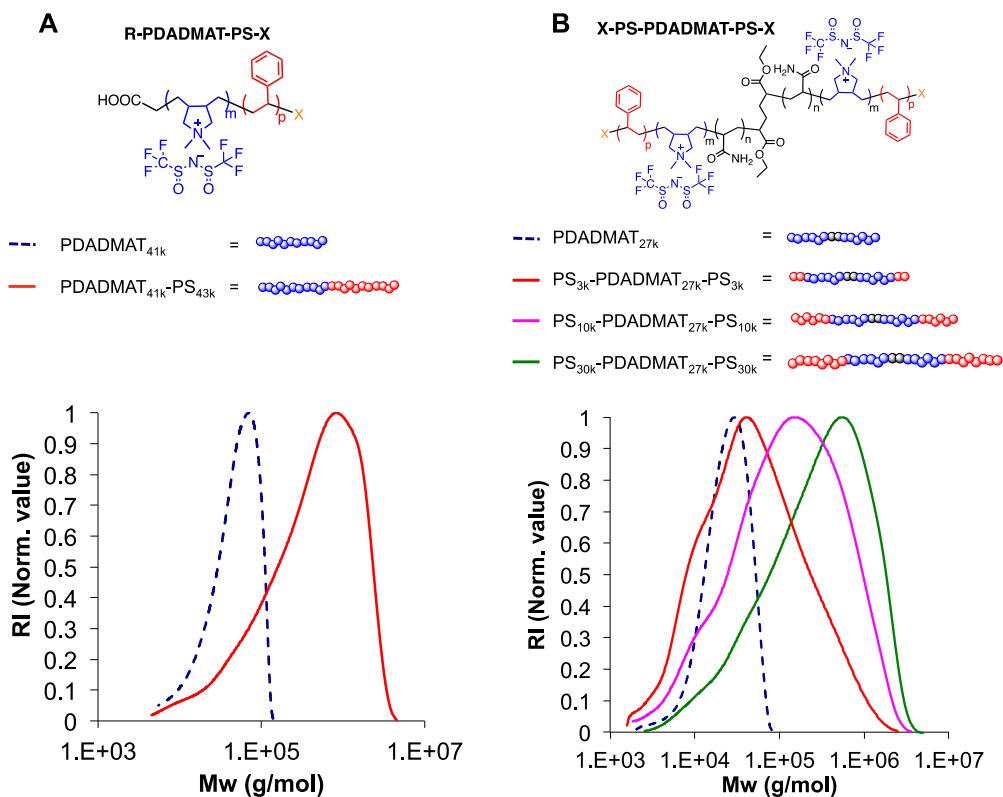


**Figure 3.3.** PISA of styrene using monofunctional PDADMAC<sub>18k</sub> and difunctional PDADMAC<sub>31k</sub>: (A) Kinetics plot of conversion of styrene vs time with (B) the corresponding pictures of the reactor and TEM images of the latex nanoparticles (scale bare: 1 $\mu$ m).

As reported in the literature, the characterization of PILs by SEC has to be realized in a good solvent containing a 0.1 M of the anion salt of the polymer.<sup>47</sup> Therefore, anion exchange was realized in water to allow a solubilization of both blocks for SEC analysis. An excess of lithium bis(trifluoromethylsulfonyl)imide] (LiTFSI) salt was added to the latex solution and a white precipitate appeared after 2h due to the insolubility of the PDADMATFSI (or PDADMAT) in water. SEC in DMF with 0.1 M lithium bis(trifluoromethylsulfonyl)imide] (LiTFSI) salt was performed on the both di- and triblock copolymers (Figure 3.4.). Due to the absence of available standards having similar nature of PDADMAT (PMMA standards were used here), the obtained molecular weight was not in accordance with the targeted one. For this reason, we will preferably focus on the shift of SEC traces towards higher molecular weights (Figure 3.4.) instead of values of  $M_n$  and  $M_w/M_n$ . Figure 3.4.A shows SEC chromatograms of the monofunctional PDADMAT<sub>41k</sub> and the centrifuged BCP with PS block, namely PDADMAT<sub>41k</sub>-PS<sub>43k</sub>. A clear shift to higher molecular weight was observed when the PS block is formed. By comparing crude and centrifuged diblock copolymer (Figure 3.4.A), centrifugation clearly showed a disappearance of the remaining macroCTA from the crude mixture.

Similarly, difunctional macroinitiators were synthesized and same behavior was observed with the formation of the ABA-type triblock copolymers (Figure 3.4.B). As shown in Figure 4B, we targeted the formation of three different BCPs

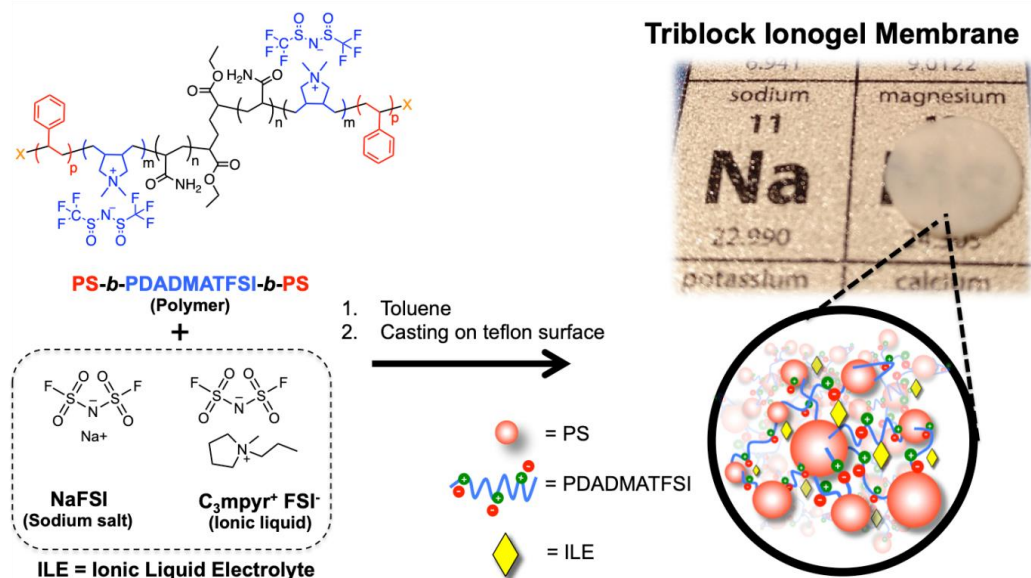
having different PDADMAT:PS  $M_n$  ratios, 1:1 (pink curve), 1:2 (green curve) and 4:1 (red curve) respectively. From PDADMAT<sub>27k</sub> macroinitiator (dotted blue line), a shift to higher  $M_n$  values was noticed in all cases. Again, SEC traces of centrifuged BCPs appeared without tailing of the remaining macroCTA, contrary to the ones of crude BCPs. A controlled process for the formation of these BCPs is undoubtedly not reached here, however the clear shift to higher molecular weight indicates the incorporation of PS, assuming the partial formation of BPCs.



**Figure 3.4.** Anion-exchanged PDADMATFSI-based (co)polymers and the SEC traces of the formation of centrifuged BCPs with their targeted molecular weights: (A) diblock and (B) triblock copolymers.

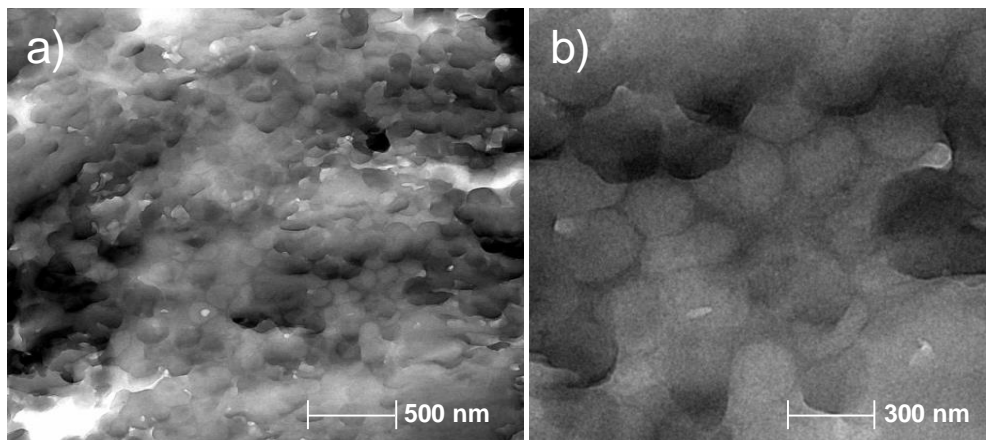
### 3.5. PDADMA-based Ionogel Membranes

Four different BCPs were selected and used to make ionogel membranes: PDADMAT<sub>41k</sub>-PS<sub>43k</sub>, PS<sub>37k</sub>-PDADMAT<sub>69k</sub>-PS<sub>37k</sub>, PS<sub>10k</sub>-PDADMAT<sub>27k</sub>-PS<sub>10k</sub> and PS<sub>30k</sub>-PDADMAT<sub>27k</sub>-PS<sub>30k</sub>. For the preparation of ionogel membranes, each polymer was dissolved in toluene and mixed with the ionic liquid electrolyte (ILE), made of sodium salt (NaFSI) and ionic liquid (C<sub>3</sub>mpyr<sup>+</sup>FSI) (Figure 3.5.). The block copolymer matrix was used to give flexible and solid character to the membranes while the ILE was used to give ionic conductivity and particularly Na<sup>+</sup> diffusion. The composition/properties dependence of the ionogel was examined by variation of the different ratio of block copolymer:ILE. As first observation, all triblocks copolymers were able to form self-standing solid flexible membranes. However, with PDADMAT<sub>41k</sub>-PS<sub>43k</sub> diblock, no membrane was formed, even at different ILE concentrations (10-20 wt. % of ILE) and only viscous liquid electrolyte was obtained. As general statement, increasing the ILE fraction in the membrane provides more flexible and softer membranes. The three triblock copolymers (PS<sub>37k</sub>-PDADMAT<sub>69k</sub>-PS<sub>37k</sub>, PS<sub>10k</sub>-PDADMAT<sub>27k</sub>-PS<sub>10k</sub> and PS<sub>30k</sub>-PDADMAT<sub>27k</sub>-PS<sub>30k</sub>) can withstand a maximum amount of 80 wt.% of ILE in a self-standing membrane. At higher amounts of ionic liquid, the membranes were too soft to be handled becoming a viscous paste.



**Figure 3.5.** Ionogel membrane formation.

According to previous work done in this group, pure PDADMATFSI polymer was used to make ionogels achieving a maximum ILE content of 50 wt%.<sup>43</sup> In this case, the styrene block gives more strength and robustness to the ionogel membrane, so that increase the ILE content can rise up to 80 wt%. At the same time, PDADMATFSI block retains the ILE fraction due to its ionic nature, avoiding any leaching of the ILE from the ionogel membrane. Figure 3.6. shows a TEM picture of an ionogel membrane composed by 70 wt.% of ILE and 30 wt.% of PS<sub>37k</sub>-PDADMAT<sub>69k</sub>-PS<sub>37k</sub>. Interestingly the spherical nanoparticles synthesized in the PISA polymerization are congregated forming a self-standing membrane and keeping up to 70 wt.% of ILE between them.

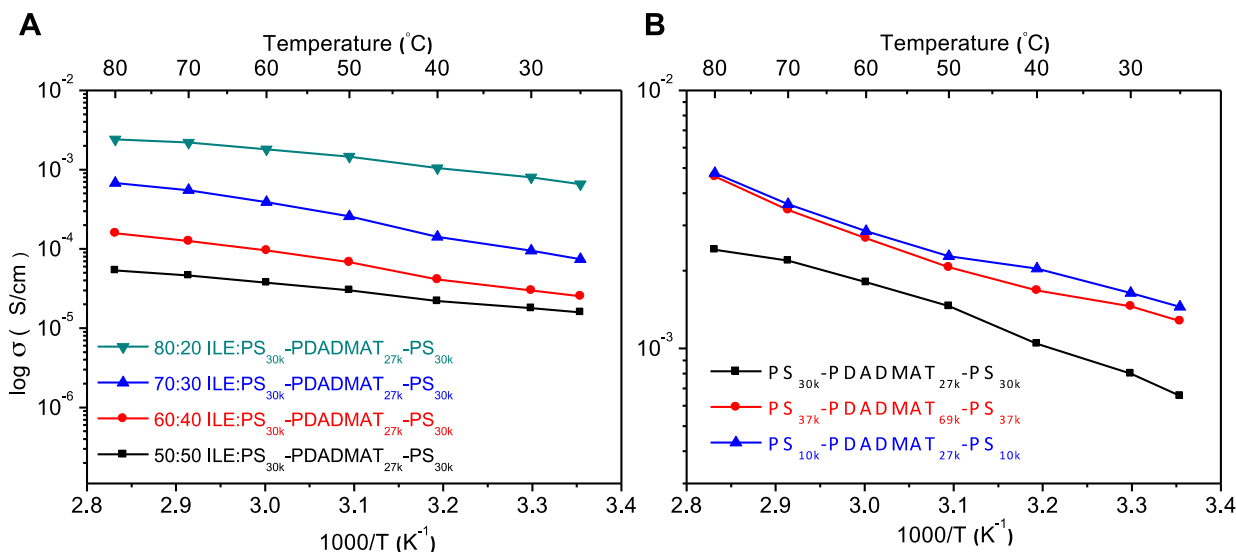


**Figure 3.6.** TEM picture of an ionogel membrane composed by 70 wt.% of ILE and 30 wt.% of  $\text{PS}_{37\text{k}}\text{-PDADMAT}_{69\text{k}}\text{-PS}_{37\text{k}}$ . at different magnification.

### 3.6. Ionic conductivity

Among several parameters that prove the suitability of ionogel electrolyte membrane to be used for sodium batteries, the ionic conductivity is one of the most studied and most important one. Ionic conductivity was measured by impedance spectroscopy at different temperatures, for this purpose. Therefore, different membranes were prepared varying the amount of ILE ( $\text{C}_3\text{mpyrFSI} + 18$  mol % of  $\text{NaFSI}$ ) and the triblock copolymer composition:  $\text{PS}_{37\text{k}}\text{-PDADMAT}_{69\text{k}}\text{-PS}_{37\text{k}}$ ,  $\text{PS}_{10\text{k}}\text{-PDADMAT}_{27\text{k}}\text{-PS}_{10\text{k}}$  and  $\text{PS}_{30\text{k}}\text{-PDADMAT}_{27\text{k}}\text{-PS}_{30\text{k}}$ . First, we studied the effect of the ILE content in the ionogel membranes on ionic conductivity at different temperatures. Four different composition ionogel were prepared varying the ILE content with the PS block copolymer as hosting polymer. Figure 3.7.A represents ionic conductivities of four different

composition ionogel membranes (80:20, 70:30, 60:40 and 50:50) in which we can observe a strong dependence of the ionic conductivity with the increase of the ILE content (or the decrease of  $\text{PS}_{30\text{k}}\text{-PDADMAT}_{27\text{k}}\text{-PS}_{30\text{k}}$  triblock copolymer content). An increase of the ILE content in the ionogel leads to increase the ionic conductivity from  $1.1 \cdot 10^{-5}$  S/cm to  $1.0 \cdot 10^{-3}$  S/cm at  $30^\circ\text{C}$  when 80 wt% of ILE is added.



**Figure 3.7.** Ionic conductivity of different ionogel membranes of (A) PDADMATFSI-based triblock copolymer ( $\text{PS}_{30\text{k}}\text{-PDADMAT}_{27\text{k}}\text{-PS}_{30\text{k}}$ ) mixed with ILE in different ratios (80:20, 70:30, 60:40 and 50:50 in wt.%) at different temperatures and (B) ILE:polyDADMATFSI triblock  $\text{PS}_{37\text{k}}\text{-PDADMAT}_{69\text{k}}\text{-PS}_{37\text{k}}$ ,  $\text{PS}_{10\text{k}}\text{-PDADMAT}_{27\text{k}}\text{-PS}_{10\text{k}}$  and  $\text{PS}_{30\text{k}}\text{-PDADMAT}_{27\text{k}}\text{-PS}_{30\text{k}}$  mixed with 80 wt.% of ILE ionogel membranes.

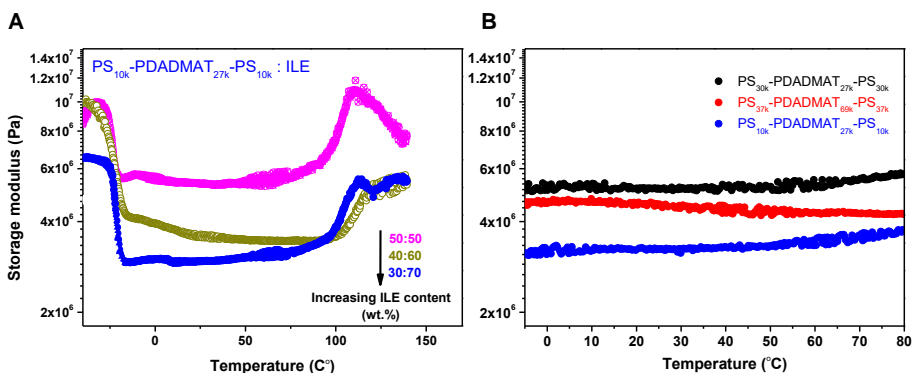


In order to compare the triblock copolymers, three different ionogel membranes were prepared containing 80 wt.% of ILE and using the three triblock copolymers as hosting materials. In figure 3.6.B is represented the ionic conductivity of each ionogel at different temperatures. As it is observed in figure 3.7.B, highest ionic conductivity is achieved with the ionogel composed by the low molecular weight PS<sub>10k</sub>-PDADMAT<sub>27k</sub>-PS<sub>10k</sub> triblock ( $1.9 \cdot 10^{-3}$  S/cm at 30°C), comparing with the other two hosting triblock copolymers, higher molecular weights and higher styrene content prevent ion diffusion due to an increase off the glass transition.

### **3.7. Dynamic mechanical thermal analysis (DMTA) of the ionogel membranes**

High elastic modulus and good mechanical properties of ionogel electrolyte membranes are known to prevent the growth of dendrites on the metal electrodes.<sup>48</sup> For this reason, we measured the rheological properties of three different ionogels (containing 80 wt. % of ILE) using different BCPs: PS<sub>37k</sub>-PDADMAT<sub>69k</sub>-PS<sub>37k</sub>, PS<sub>10k</sub>-PDADMAT<sub>27k</sub>-PS<sub>10k</sub> and PS<sub>30k</sub>-PDADMAT<sub>27k</sub>-PS<sub>30k</sub>. At first sight, these three ionogel membranes were exhibiting self-standing properties but different flexibility and robustness. DMTA analysis was performed at different temperatures to evaluate storage modulus of each membrane. According to Figure 3.8 a/b the three ionogels presents a very stable storage modulus from -5 °C to 80 °C, this is particularly interesting for battery operation since it demonstrates that the membrane maintains its mechanical properties at different temperatures (from -5 °C to 80 °C). Before -10 °C the storage modulus decreases dramatically due to the melting of the ionic liquid and it keeps

constant until 85 °C where the storage modulus increases dramatically. This unusual behaviour is due to the loss of the ionic liquid fraction during the DMTA analysis. Beyond this temperature the ionogel loses the ionic liquid fraction and just the storage modulus of the hosting polymer is measured (higher storage modulus are measured). This limits the use of this ionogels from -5 °C to 80 °C. As it is observed in Figure 3.8 b, the highest modulus was achieved with the PS<sub>30k</sub>-PDADMAT<sub>27k</sub>-PS<sub>30k</sub> 5.9·10<sup>6</sup> Pa, this triblock copolymer, is the polymer with highest styrene content comparing with the other two block copolymers, the styrene block gives strength to the polymer and the ionogel due to its higher glass transition (≈110 °C) comparing with the DADMA-TFSI block. On the other hand, comparing same composition but different molecular weight triblock copolymers, the ionogel composed by the higher molecular weight triblock has the highest storage modulus (4.5·10<sup>6</sup> Pa). High molecular weight generally gives strength to the polymer and this is what we can observe in this case.



**Figure 3.8.** Dynamic mechanical thermal analysis (DMTA) of the ionogel membranes (A) of three different ionogels containing 50,60 and 70 wt.% of ILE mixed PS<sub>10k</sub>-PDADMAT<sub>27k</sub>-PS<sub>10k</sub> (B) DMTA of different ionogel membranes at different temperatures composed by PS<sub>37k</sub>-PDADMAT<sub>69k</sub>-PS<sub>37k</sub>, PS<sub>10k</sub>-PDADMAT<sub>27k</sub>-PS<sub>10k</sub> and PS<sub>30k</sub>-PDADMAT<sub>27k</sub>-PS<sub>30k</sub> mixed with 80 wt.% of ILE ionogel membranes.

Interestingly it can be observed a correlation between ionic conductivity and mechanical properties, when ionic conductivity increases the mechanical properties decrease probably due to the increase of the  $T_g$  of the bloc copolymer host, in any case, this three ionogels present a good balance between the ionic conductivity and mechanical properties that are required for a good performance in a final sodium battery.

## 3.8. Conclusions

As conclusion, we performed the MADIX polymerization of DADMAC using both mono- and difunctional xanthate CTAs. Well-defined macroinitiators having different molecular weights were synthesized, characterized and used for the formation of BCPs by emulsion PISA. Cationic latexes made of PDADMAC and PS BCPs were treated with LiTFSI for anion-exchange and later used for casted ionogel membrane formation. Once mixed with the ionic liquid electrolyte (ILE), made of sodium salt (NaFSI) and ionic liquid ( $C_3\text{mpyr}^+\text{FSI}$ ), triblock copolymers revealed to be ideal for the formation of self-standing membranes, unlike diblock copolymers. Composition up to 80 wt % of ILE was loaded for the membrane formation. Among the different triblocks,  $PS_{10k}\text{-PDADMAT}_{27k}\text{-PS}_{10k}$  BCP provided the highest values of conductivity around  $1.9 \cdot 10^{-3}$  S/cm at  $30^\circ\text{C}$ . This study aims to broaden the research on the formation of charged ABA-type triblock copolymers and their particular properties, notably in terms of physical cross-linking via the external blocks. Further investigations will be dedicated to reach a higher level of control of the second block in the future.

## 3.9. Experimental part

### 3.9.1. Materials

Sodium hydroxide pellets (Fisher), bromoacetic acid (Acros, 99%), ammonium chloride (Acros), potassium hydrogen carbonate (Fisher), ethanol (EtOH, Scharlab, 96%), acetone (Scharlab, tech. grade), HCl (tech. grade, Fisher), Lithium bis(trifluoromethanesulfonyl)imide ( $\text{LiNTf}_2$ , Solvionic, 99.9%)

were all used as received. Diallyldimethylammonium chloride solution (DADMAC sol., 65 wt. % in H<sub>2</sub>O), 2,2-azobis(2-methylpropionamide) dihydrochloride (AIBA, 97%), potassium ethyl xanthogenate (96%), 2-bromopropionyl bromide (97%), styrene (St, >99%) magnesium sulfate (MgSO<sub>4</sub>, >99.5%), triethylene glycol (EG<sub>3</sub>, 99%), pyridine (99.5%), acrylamide (>98%) and all deuterated solvents (D<sub>2</sub>O, CDCl<sub>3</sub>) were all purchased from Sigma Aldrich and used as received. Propyl-N-methylpyrrolidinium bis(fluorosulfonyl)imide (C<sub>3</sub>mpyrFSI, Solvionic 99.9%), sodium bis(fluorosulfonyl)imide (NaFSI, Solvionic 99.7%) were used as received.

### 3.9.2. Nuclear Magnetic Spectroscopy (NMR) analysis

The different RAFT agents were analyzed by <sup>1</sup>H NMR with a Bruker Advance 300 MHz in CDCl<sub>3</sub>.

The conversion of MADIX/RAFT polymerization of DADMAC was monitored by <sup>1</sup>H NMR with a Bruker Advance 300 MHz in D<sub>2</sub>O. The estimation of the conversion of DADMAC was calculated via this formula using the integration of monomer and polymers:

$$\text{conv.}_{DADMAC} (\%) = \frac{\int_{0.95 \text{ ppm}}^{1.85 \text{ ppm}} \text{CH}_2(PDADMAC)}{(\int_{5.50 \text{ ppm}}^{5.80 \text{ ppm}} \text{CH}_2(DADMAC) + \int_{0.95 \text{ ppm}}^{1.85 \text{ ppm}} \text{CH}_2(PDADMAC))} \times 100$$

### 3.9.3. Gravimetric analysis

The conversion of St in PISA polymerization was evaluated gravimetrically following this formula:

$$conv_{.St} (\%) = \frac{m_{dry} - (m_{liq} \times \frac{m_{macroCTA}}{m_{TOT}} \times 100)}{m_{liq}} \times \frac{m_{TOT}}{m_{St}} \times 100 \quad (2)$$

Where  $m_{dry}$  is the mass of solid after drying in oven overnight;  $m_{liq}$  is the mass of the liquid sample;  $m_{macroCTA}$ ,  $m_{AIBA}$  and  $m_{St}$  correspond respectively to the initial masses of the macroCTA, radical initiator AIBA and styrene;  $m_{TOT}$  is the sum of  $m_{macroCTA}$ ,  $m_{AIBA}$ ,  $m_{St}$  and  $m_{H_2O}$ .

### 3.9.4. DMF LiTFSI Size Exclusion Chromatography (SEC)

A 1200 Infinity gel permeation chromatograph (GPC, Agilent Technologies) was used to determine  $M_n$ ,  $M_w$  and PDI of the polymers. The chromatograph was equipped with an integrated IR detector, a PLgel 5 mm MIXED-D column and a PLgel guard column (Agilent Technologies). The eluent was a 0.1 M Li(CF<sub>3</sub>SO<sub>2</sub>)<sub>2</sub>N solution in DMF and the flow rate was of 1.0 mL min<sup>-1</sup> at 50°C. PMMA standards (Agilent Technologies,  $M_p = 0.55 - 1568 \times 10^3$ ) were used to perform calibration.

### 3.9.5. Transmission Electron Microscopy (TEM)

Particle size and morphologies were determined by transmission electron microscopy (TEM) using a JEOL TM-1400 Plus series 120 kV electron microscope. To determine the particle morphology, a drop of the diluted latexes was deposited on copper grids and let to evaporate. Then, the samples were

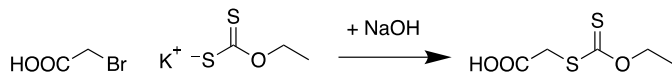
stained with a vapor of RuO<sub>4</sub> for 20 min. For the film morphologies, slices of films were prepared with a microtome, equipped with a diamond knife, at -25 °C and then the slides were deposited on copper grids.

### **3.9.6. Dynamic Mechanical Thermal Analysis (DMTA)**

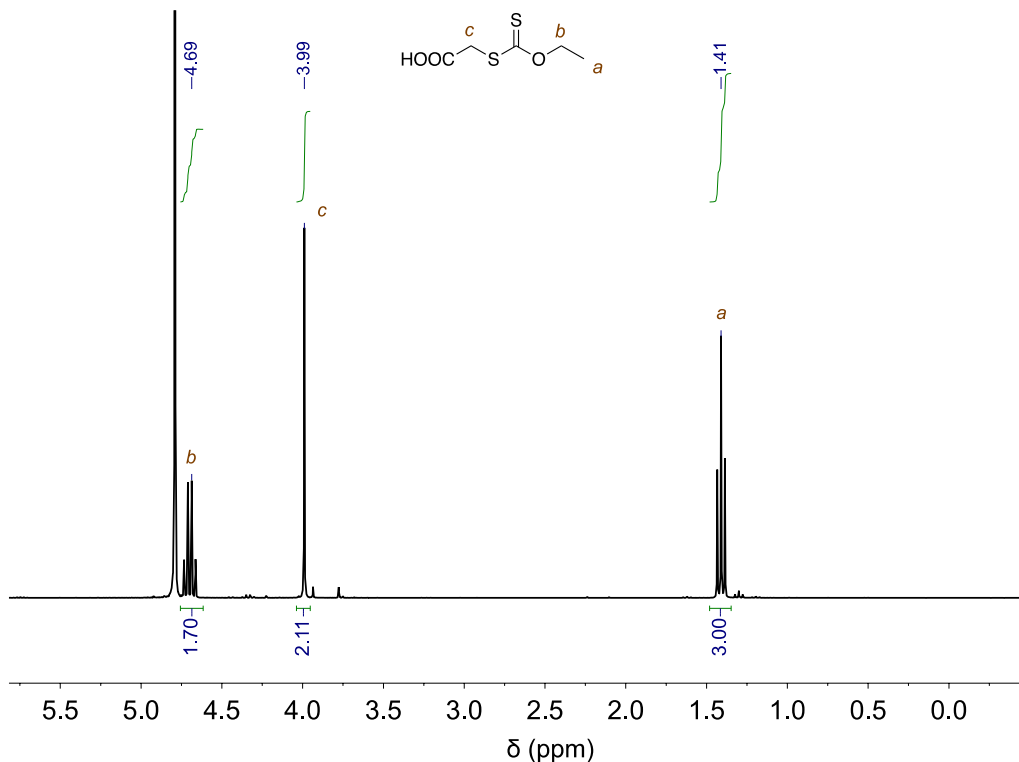
Mechanical properties of the ionogels were analyzed by dynamic mechanical thermal analysis (DMTA) conducted in compressing mode in a Dynamic Mechanical Analyser, Triton 2000 DMA (Triton Technology). Circular samples (diameter = 10 mm) were heated from -80°C to 100°C at a constant heating rate of 4 °C/min and a frequency of 1.0 Hz.

### **3.9.7. Synthesis of Monofunctional Chain Transfer Agent (CTA): Ethoxythiocarbonyl Mercaptoacetic Acid (XAA)**

The synthetic procedure has been modified from the literature.<sup>1,2</sup> NaOH (2.5g, 62.4 mmol) was first dissolved in chilled MilliQ water (100 mL), followed by addition of bromoacetic acid (1 eq, 8.67 g, 62.4 mmol) until reaching a clear solution. Potassium ethyl xanthogenate (1 eq, 10 g, 62.4 mmol) was then added portion wise to the mixture with a spatula. The solution was stirred at room temperature for 24h, followed by acidification with 4 M HCl<sub>aq</sub> to pH ~ 1. The resulting mixture was then extracted with chloroform (3 × 150 mL). The combined organic extract was dried over anhydrous MgSO<sub>4</sub>, filtered twice, and concentrated under vacuum. The solid was dried in oven at rt under vacuum to give the final brown product (8.67 g, 77% yield). <sup>1</sup>H NMR (300 MHz, CDCl<sub>3</sub>) δ (ppm): 1.43 (t, 3H, CH<sub>3</sub>), 3.97 (s, 2H, CH<sub>2</sub>), 4.65 (q, 2H, CH<sub>2</sub>).



**Scheme S1.** Synthesis of monofunctional CTA: XAA.



**Figure S1.** <sup>1</sup>H NMR (300 MHz, D<sub>2</sub>O) of monofunctional CTA: XAA.

### 3.9.8. Synthesis of difunctional CTA: X-Pam-DiEst-Pam-X (X-AdA-X)

#### A. Synthesis of X-DiEst-X.

The following procedure was inspired from a patent developed in Rhodia



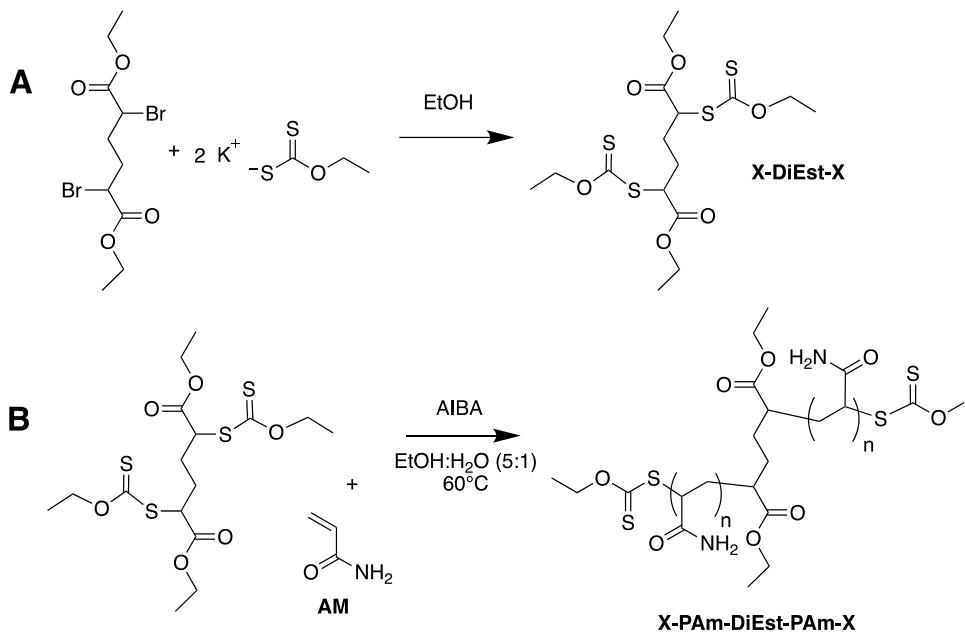
Industries.<sup>4</sup> In a round bottom flask of 500 mL, diethyl meso-2,5-dibromoadipate (10 g ; 27.7 mmol) is dissolved in EtOH (96%) (250 mL) at room temperature. After dissolution, potassium ethyl xanthogenate (11.11 g ; 69.3 mmol) is added in the medium with a spatula during 90 min. The reaction takes place at room temperature during 4h. When the reaction is finished, potassium bromide salt is filtered and EtOH evaporated under vacuum. The product is solubilized in DCM and washed three times in distilled H<sub>2</sub>O to remove the excess of potassium ethyl xanthogenate. After evaporation of DCM, the product is dried under vacuum during 24h. A yellow liquid is obtained with a yield of 90 % (11.02 g).

<sup>1</sup>H NMR (300 MHz, CDCl<sub>3</sub>) δ (ppm): 4,65-4,61 (q, 4H, -S=C-O-CH<sub>2</sub>-CH<sub>3</sub>); 4,42-4,38 (m, 2H, -CH<sub>2</sub>-CH-CO-O-); 4,25-4,17 (q, 4H, -O=C- O-CH<sub>2</sub>-CH<sub>3</sub>); 2,17-1,97 (m, 4H, -CH-CH<sub>2</sub>-); 1,46-1,43 (t, 6H, -S=C-O-CH<sub>2</sub>-CH<sub>3</sub>); 1,33-1,25 (t, 6H, - O=C- O-CH<sub>2</sub>-CH<sub>3</sub>).

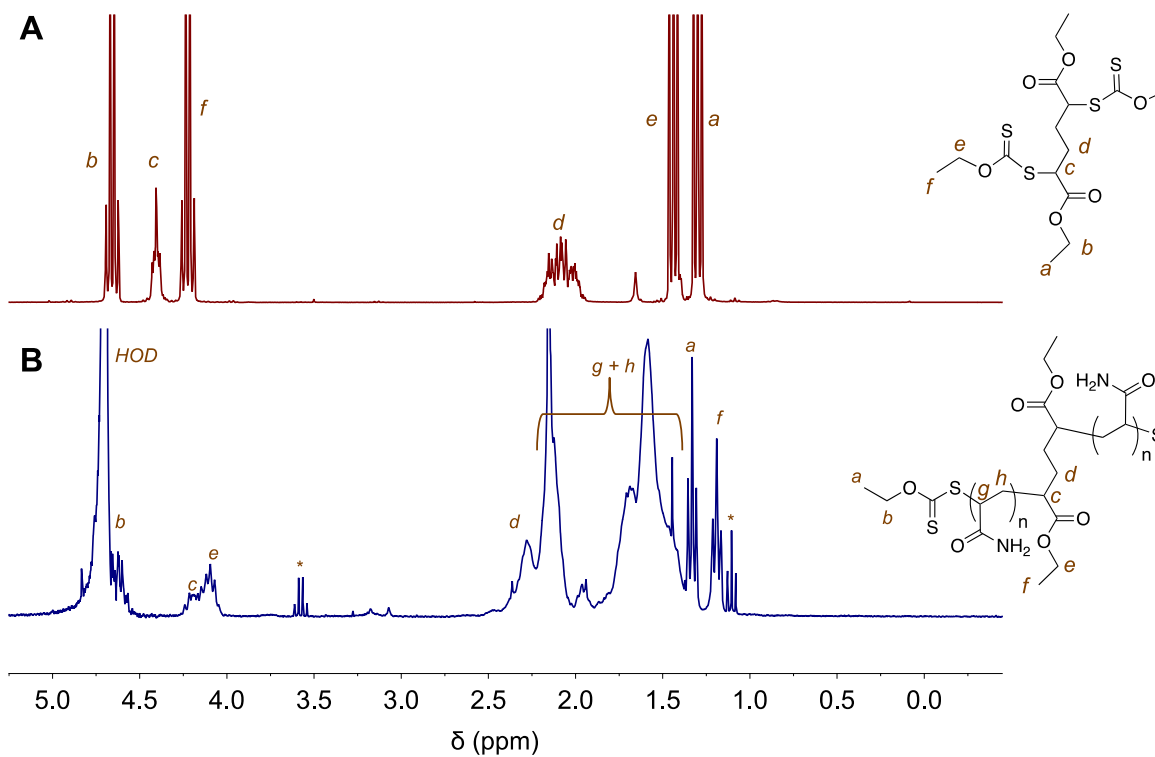
#### *B. Synthesis of X-PAm-DiEst-PAm-X (X-AdA-X).*

X-DiEst-X (1 eq, 2.496 g, 5.64 mmol), acrylamide (20 eq, 8.01g, 112.8 mmol) and radical initiator AIBA (0.04 eq, 0.069 g, 0.25 mmol) were placed in a 50 ml Schlenck and dissolved in 5 ml of water and 22 ml of EtOH. The polymerization was followed by <sup>1</sup>H NMR in D<sub>2</sub>O and stopped after 1h with the formation of a white precipitate at the bottom of the Schlenck and reaching a conversion close to 50%. The polymer was first dissolved in water (20 ml) and precipitated twice in acetone and dried under vacuum to obtain a clear yellow powder. The polymer was then analyzed by <sup>1</sup>H NMR, SEC and MALDI-TOF. The related molecular weight of the X-PAm-DiEst-PAm-X MacroCTA with the corresponding method is M<sub>n</sub> NMR = 2850, DP<sub>NMR</sub> = 34; M<sub>n</sub> MALDI = 1850, Đ<sub>MALDI</sub> = 1.02, DP = 26.

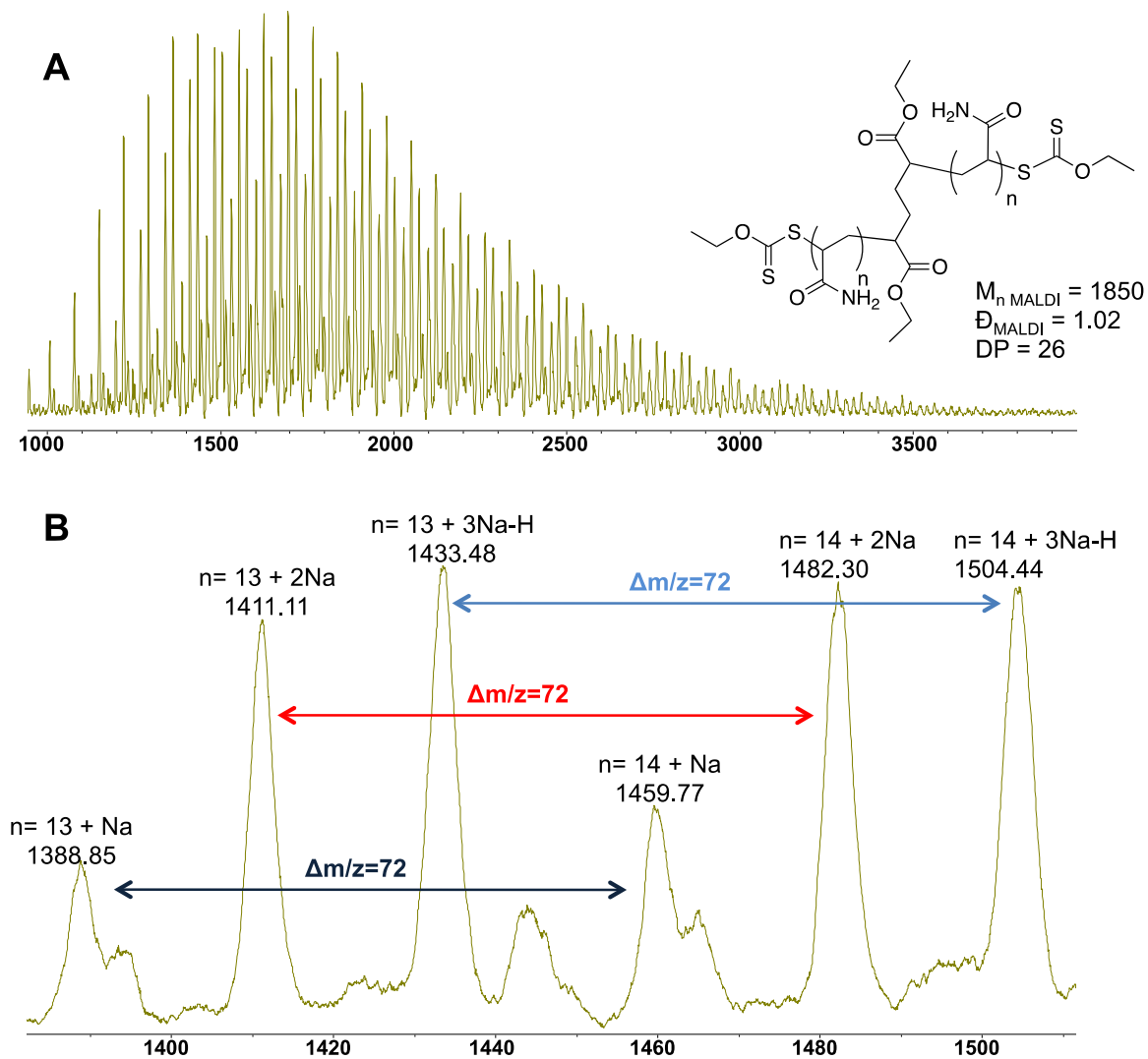
$^1\text{H}$  NMR (300 MHz,  $\text{D}_2\text{O}$ )  $\delta$  (ppm): 4.67-4.55 (q, 4H,  $-\text{S}=\text{C}-\text{O}-\text{CH}_2-\text{CH}_3$ ), 4.26-4.16 4,42-4,38 (m, 2H,  $-\text{CH}_2-\text{CH}-\text{COO}-$ ), 4.16-4 (t, 2H of the last unit of PAm,  $-\text{S}-\text{CH}(\text{CONH}_2)-\text{CH}_2-$ ), 4.16-4.02 (m, 4H,  $\text{O}=\text{C}-\text{O}-\text{CH}_2-\text{CH}_3$ ), 2.66-2.23 (m, 4H,  $-\text{CH}-\text{CH}_2-$ ), 2.23-1.38 (m, 3H of PAm units,  $-\text{CH}(\text{CONH}_2)-\text{CH}_2-$ ), 1.38-1.28 (t, 6H,  $\text{S}=\text{C}-\text{O}-\text{CH}_2-\text{CH}_3$ ), 1.28-1.14 (t, 6H, (m, 4H,  $\text{O}=\text{C}-\text{O}-\text{CH}_2-\text{CH}_3$ )).



**Scheme S2.** Synthesis of Difunctional CTA: X-PAm-DiEst-PAm-X (X-PAm-X)



**Figure S2.**  $^1\text{H}$  NMR (300 MHz) of difunctional CTA: (A) X-DiEst-X in  $\text{CDCl}_3$  and (B) X-PAm-DiEst-PAm-X in  $\text{D}_2\text{O}$  (\* indicates the remaining ethanol from the purification).

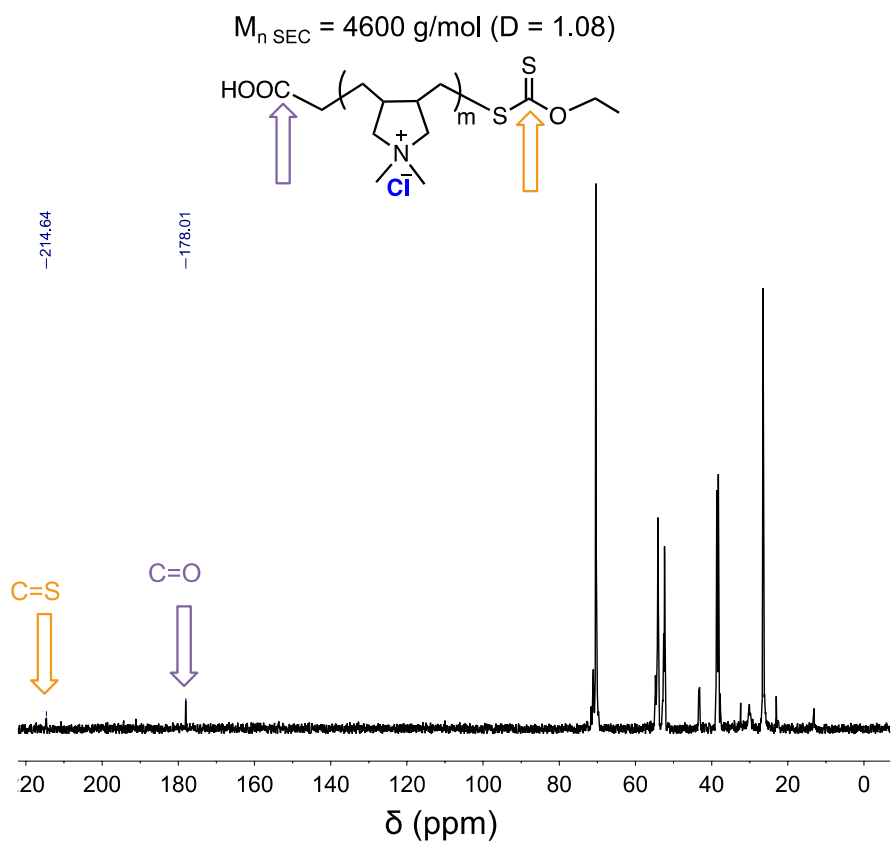


**Figure S3.** MALDI-ToF analysis of X-PAm-DiEst-PAm-X (X-AdA-X)

### 3.9.9. MADIX/RAFT Polymerization of DADMAC in water

In a typical experiment, RAFT CTA (XAA) (1 eq, 0.041 g, 0.23 mmol) and radical initiator AIBA (0.3 eq, 0.019 g, 0.07 mmol) were placed in a 50 ml Schlenk tube and solubilized with 8 ml of water. A commercial solution of 65% wt. of DADMAC (175 eq, 10 ml, 6.5 g, 40.37 mmol) is then added in the Schlenk and the mixture is stirred and degassed under N<sub>2</sub> during 30 min. pH of the mixture is close to 5 and the concentration ratio was  $[DADMAC]/[CTA]/[AIBA] = 175/1/0.3$ . The polymerization started by immersing the Schlenk in the oil bath pre-heated to 60°C. Aliquots were taken every hour for conversion values calculated by <sup>1</sup>H NMR (See Equation 1) and for molecular weights by GPC, until reaching a maximum conversion of 75%. The final polymer was precipitated in a 1:1 mixture of EtOH:Acetone, the solid was filtrated and placed under vacuum at 40°C to remove the solvents. The precipitated polymer was then analyzed by <sup>1</sup>H NMR in D<sub>2</sub>O.

The same procedure was applied varying the concentration ratio and the type of the CTA, *i.e.* X-PAm-X.



**Figure S4.**  $^{13}\text{C}$  NMR (300 MHz) of small molecular weight PDADMAC.

### **3.9.10. Synthesis of Poly(Styrene) block copolymer latexes by Polymerization Induced Self-Assembly (PISA) using PDADMAC macroCTA**

All emulsions were carried out in a 50 ml round-bottom flask equipped with a three-way stopcock to avoid the entry of oxygen and allow the sampling. Two main parameters were studied in this section: the type of macroCTA (mono- or difunctional) and the chain length of Poly(Styrene) (PS) by changing the ratio of styrene compared to the macroCTA.

In a typical PISA experiment, monofunctional macroCTA (17 800 g/mol, 0.944 g, 0.053 mmol), AIBA (0.003 g, 0.01 mmol) and 25 ml of MilliQ water were transferred in the round-bottom flask and degassed with N<sub>2</sub> during 30 min. In another flask, distilled styrene was slowly bubbled with N<sub>2</sub> during 30 min. Styrene (2.5 ml, 21.78 mmol) was then transferred in the round-bottom flask, giving a global mixture with a concentration ratio of [St]/[macroCTA]/[AIBA] = 410/1/0.3 and a 88% wt of St solution. The polymerization started by immersing the flask in the oil bath pre-heated to 60°C. Samples were withdrawn to calculate the conversion of St by gravimetric analysis (See Equation 2). After 24h (100% conversion St), the white emulsion is maintained as crude solution in water at + 6°C. Samples from the crude solution were analyzed by TEM and DLS analysis for the determination of the particles size and morphology. Anion exchange is then performed on the final polymer latexes by adding a water solution (5 ml) composed of an excess of LiNTf<sub>2</sub> salts (1.1 eq compared to initial amount of macroCTA). This solution was stirred overnight to allow the complete anion exchange and the precipitated polymer is filtrated and washed on filter

with water. The molecular weight of the latex ( $M_n = 30.1$  g/mol;  $M_w/M_n = 1.72$ ) was calculated by SEC in 0.01 M LiTf<sub>2</sub> DMF solution after anion exchange of the copolymer (Cl<sup>-</sup>/Tf<sub>2</sub>N<sup>-</sup>) and using PMMA standards.

Similar procedure was used for difunctional macroCTAs (formation of triblocks) and all data of SEC are mentioned in Table S1.

**Table S1.** PISA and anion exchange data of the block copolymers.<sup>a</sup>

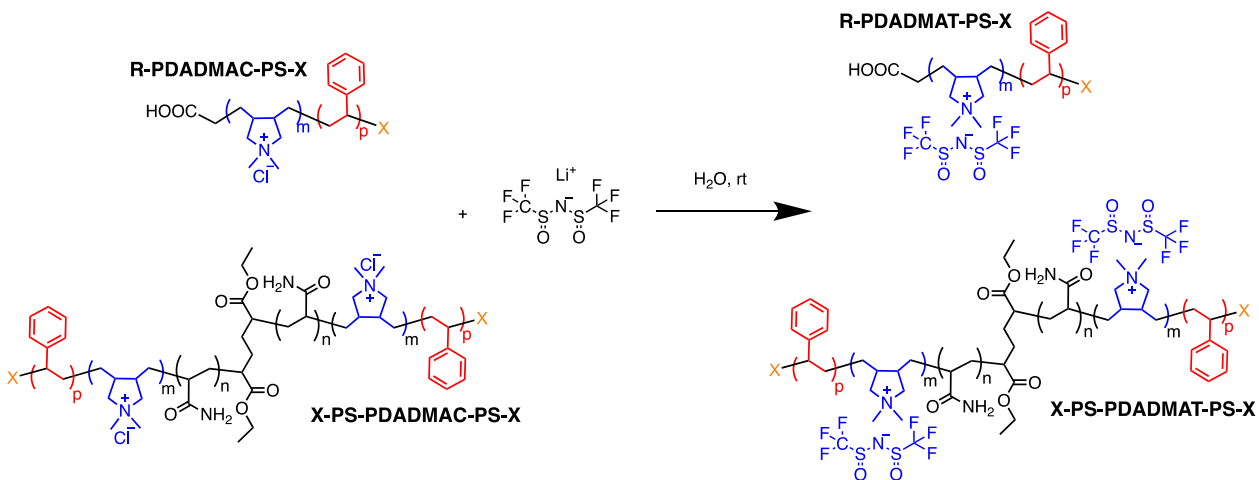
Entries	PISA	Anion exchanged Block copolymers with TFSI anions		
	PDADMAC CTA ( $M_{n,SEC}$ ) <sup>b</sup>	Block copolymers (Target $M_n$ )	$M_n$ PDADMAT <sub>SEC</sub> (kg/mol) [ $M_w/M_n$ ] <sup>c</sup>	$M_n$ block copo <sub>SEC</sub> (kg/mol) [ $M_w/M_n$ ] <sup>c</sup>
1	PDADMAC <sub>18k</sub> <sup>2</sup>	PDADMAT <sub>41k</sub> -PS <sub>43k</sub>	30.1 [1.72]	96.3 [6.83]
2	PDADMAC <sub>31k</sub> <sup>2</sup>	PS <sub>37k</sub> -PDADMAT <sub>69k</sub> -PS <sub>37k</sub>	68.2 [1.64]	90.8 [7.23]
3	PDADMAC <sub>13k</sub> <sup>2</sup>	PS <sub>10k</sub> -PDADMAT <sub>27k</sub> -PS <sub>10k</sub>	18 [1.46]	31.1 [7.59]
4	PDADMAC <sub>13k</sub> <sup>2</sup>	PS <sub>3k</sub> -PDADMAT <sub>27k</sub> -PS <sub>3k</sub>	18 [1.46]	18.3 [3.48]
5	PDADMAC <sub>13k</sub> <sup>2</sup>	PS <sub>30k</sub> -PDADMAT <sub>27k</sub> -PS <sub>30k</sub>	18 [1.46]	66.6 [6.93]

<sup>a</sup> Conditions: solid content = 12 % wt., Time = 24h.

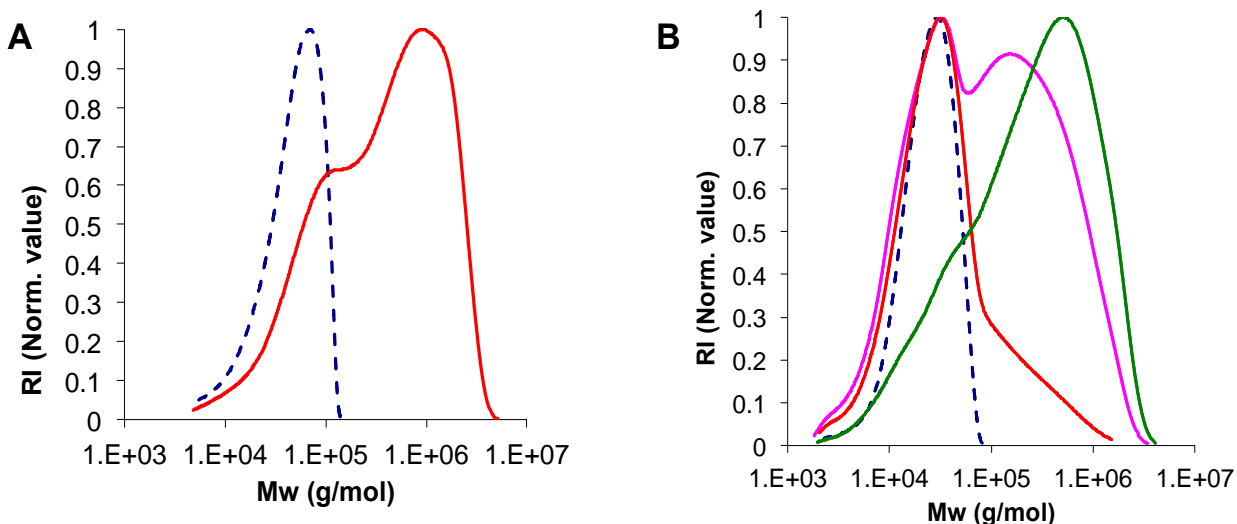
<sup>b</sup> Determined by SEC in H<sub>2</sub>O (CH<sub>3</sub>COOH/CH<sub>3</sub>COONa 0.2/0.3M)

<sup>c</sup> Determined by SEC in DMF (0.1M LiTFSI)





**Scheme S3.** Anion exchange of PDADMAC with  $\text{LiNTf}_2$  salt.



**Figure S5.** SEC traces of BCPs before centrifugation: (A) formation diblock PDADMAT<sub>41k</sub>-PS<sub>43k</sub> and (B) formation triblocks PS<sub>10k</sub>-PDADMAT<sub>27k</sub>-PS<sub>10k</sub> (pink), PS<sub>3k</sub>-PDADMAT<sub>27k</sub>-PS<sub>3k</sub> (red), PS<sub>30k</sub>-PDADMAT<sub>27k</sub>-PS<sub>30k</sub> (green).

### 3.9.11. Ionogel membranes preparation

NaFSI was dissolved in C<sub>3</sub>mpyrFSI ionic liquid to make the initial ionic liquid electrolyte (ILE) solution. After, ionogel membranes were synthesized by mixing the PS<sub>10k</sub>-PDADMAT<sub>27k</sub>-PS<sub>10k</sub> with the ILE solution in different ratio. Both ILE and PS<sub>10k</sub>-PDADMAT<sub>27k</sub>-PS<sub>10k</sub> were mixed in 0.5ml of toluene and stirred for 10 hours. Once the mixture was homogeneous the solubilised ionogel was casted on a Teflon surface and dried under the fume hood for 4 hours. Finally, the ionogel membranes were fully dried at 70°C under vacuum for 10 hours before using them. White self-standing flexible membranes were obtained as it is shown in Figure S6. As a first observation, increasing the ionic liquid concentration in the membrane, results in more flexible and softer membranes. The PS<sub>10k</sub>-PDADMAT<sub>27k</sub>-PS<sub>10k</sub> can withstand a maximum amount of 70-80 wt.% of ILE solution in a self-standing membrane. Beyond this point the ionogel became soft and not easy to handle it.

### 3.9.12. Ionic conductivity

The ionic conductivity was measured by electrochemical impedance spectroscopy (EIS) using a Autolab 302N Potentiostat Galvanostat coupled to a Microcell HC station to control the temperature during the measurements. Circular ionogel membranes were cut and used for the measurements (diameter = 11 mm) with a thickness of 150 µm. The membranes were sandwiched between two stainless steel electrodes and sealed in Teflon Microcell under argon atmosphere in a glove box. The measurements were carried out from 20°C to 80°C with a step of 10°C holding the temperature for 20 minutes before each temperature to allow temperature equilibration. The frequency range was 100

set from 0.1 MHz to 0.1 Hz and the amplitude was 10 mV. Finally, the conductivity was calculated following this equation:

$$\sigma = \frac{l}{A} \frac{1}{R_b}$$

Where  $l$  the thickness of the sample is,  $A$  is the surface of the membrane in contact with the electrode and  $R_b$  is the bulk resistance of the sample extracted from the Nyquist plot.

### 3.10. References

- 1 C. Wandrey, J. Hernandez-Barajas and D. Hunkeler, *Adv. Polym. Sci.*, 1999, **145**, 123–182.
- 2 A.-L. Pont, R. Marcilla, I. De Meatza, H. Grande and D. Mecerreyes, *J. Power Sources*, 2009, **188**, 558–563.
- 3 X. Wang, F. Chen, G. M. A. Girard, H. Zhu, D. R. MacFarlane, D. Mecerreyes, M. Armand, P. C. Howlett and M. Forsyth, *Joule*, 2019.
- 4 G. A. Tiruye, D. Munoz-Torrero, J. Palma, M. Anderson and R. Marcilla, *J. Power Sources*, 2016, **326**, 560–568.
- 5 L. C. Tome, D. Mecerreyes, C. S. R. Freire, L. P. N. Rebelo and I. M. Marrucho, *J. Memb. Sci.*, 2013, **428**, 260–266.
- 6 R. M. Teodoro, L. C. Tome, D. Mantione, D. Mecerreyes and I. M. Marrucho, *J. Memb. Sci.*, 2018, **552**, 341–348.
- 7 M. Dobbelin, V. Jovanovski, I. Llarena, L. J. C. Marfil, G. Cabanero, J. Rodriguez and D. Mecerreyes, *Polym. Chem.*, 2011, **2**, 1275–1278.
- 8 T. P. Lodge and T. Ueki, *Acc. Chem. Res.*, 2016, **49**, 2107–2114.
- 9 G. B. Butler, *Acc. Chem. Res.*, 1982, **15**, 370–378.
- 10 G. B. Butler and R. L. Bunch, *J. Am. Chem. Soc.*, 1949, **71**, 3120–3122.
- 11 J. E. Lancaster, L. Baccei and H. P. Panzer, *J. Polym. Sci. Polym. Lett. Ed.*, 1976, **14**, 549–554.
- 12 E. I. Du Pont de Nemours & Co., USA; Le, Tam Phuong; Moad, Graeme; Rizzardo, Ezio; Thang, San Hoa ., *PCT Int. Appl.*, 1998, 88 pp.
- 13 G. Moad, E. Rizzardo and S. H. Thang, *Aust. J. Chem.*, 2006, **59**, 669–692.
- 14 M. H. Stenzel, L. Cummins, G. E. Roberts, T. P. Davis, P. Vana and C. Barner-Kowollik, *Macromol. Chem. Phys.*, 2003, **204**, 1160–1168.

- 15 C. Barner-Kowollik, T. P. Davis, J. P. A. Heuts, M. H. Stenzel, P. Vana and M. Whittaker, *J. Polym. Sci. Part A Polym. Chem.*, 2003, **41**, 365–375.
- 16 S. Perrier and P. Takolpuckdee, *J. Polym. Sci. Part A Polym. Chem.*, 2005, **43**, 5347–5393.
- 17 H. Chaffey-Millar, M. H. Stenzel, T. P. Davis, M. L. Coote and C. Barner-Kowollik, *Macromolecules*, 2006, **39**, 6406–6419.
- 18 Y. Assem, H. Chaffey-Millar, C. Barner-Kowollik, G. Wegner and S. Agarwal, *Macromolecules*, 2007, **40**, 3907–3913.
- 19 Y. Assem, A. Greiner and S. Agarwal, *Macromol. Rapid Commun.*, 2007, **28**, 1923–1928.
- 20 J. P. Blinco, A. Greiner, C. Barner-Kowollik and S. Agarwal, *Eur. Polym. J.*, 2011, **47**, 111–114.
- 21 M. G. Kochameshki, A. Marjani, M. Mahmoudian and K. Farhadi, *Chem. Eng. J. (Amsterdam, Netherlands)*, 2017, **309**, 206–221.
- 22 M. Destarac, A. Guinaudeau, R. Geagea, S. Mazieres, E. Van Gramberen, C. Boutin, S. Chadel and J. Wilson, *J. Polym. Sci. Part A Polym. Chem.*, 2010, **48**, 5163–5171.
- 23 P. Cotanda, N. Petzetakis, X. Jiang, G. Stone and N. P. Balsara, *J. Polym. Sci. Part A Polym. Chem.*, 2017, **55**, 2243–2248.
- 24 J. Rieger, G. Osterwinter, C. Bui, F. Stoffelbach and B. Charleux, *Macromolecules*, 2009, **42**, 5518–5525.
- 25 N. J. Warren and S. P. Armes, *J. Am. Chem. Soc.*, 2014, **136**, 10174–10185.
- 26 J. Rieger, *Macromol. Rapid Commun.*, 2015, **36**, 1458–1471.
- 27 S. L. Canning, G. N. Smith and S. P. Armes, *Macromolecules*, 2016, **49**, 1985–2001.
- 28 A. Blanazs, A. J. Ryan and S. P. Armes, *Macromolecules*, 2012, **45**,

- 5099–5107.
- 29 A. Blanazs, J. Madsen, G. Battaglia, A. J. Ryan and S. P. Armes, *J. Am. Chem. Soc.*, 2011, **133**, 16581–16587.
- 30 A. Blanazs, R. Verber, O. O. Mykhaylyk, A. J. Ryan, J. Z. Heath, C. W. I. Douglas and S. P. Armes, *J. Am. Chem. Soc.*, 2012, **134**, 9741–9748.
- 31 B. Charleux, G. Delaittre, J. Rieger and F. D’Agosto, *Macromolecules*, 2012, **45**, 6753–6765.
- 32 M. J. Derry, L. A. Fielding and S. P. Armes, *Prog. Polym. Sci.*, 2016, **52**, 1–18.
- 33 W.-D. He, X.-L. Sun, W.-M. Wan and C.-Y. Pan, *Macromolecules*, 2011, **44**, 3358–3365.
- 34 J. Tan, H. Sun, M. Yu, B. S. Sumerlin and L. Zhang, *ACS Macro Lett.*, 2015, **4**, 1249–1253.
- 35 I. Chaduc, A. Crepet, O. Boyron, B. Charleux, F. D’Agosto and M. Lansalot, *Macromolecules*, 2013, **46**, 6013–6023.
- 36 I. Chaduc, M. Girod, R. Antoine, B. Charleux, F. D’Agosto and M. Lansalot, *Macromolecules*, 2012, **45**, 5881–5893.
- 37 W. Zhang, F. D’Agosto, P.-Y. Dugas, J. Rieger and B. Charleux, *Polymer*, 2013, **54**, 2011–2019.
- 38 J. Lesage de la Haye, X. Zhang, I. Chaduc, F. Brunel, M. Lansalot and F. D’Agosto, *Angew. Chemie, Int. Ed.*, 2016, **55**, 3739–3743.
- 39 S. Binauld, L. Delafresnaye, B. Charleux, F. D’Agosto and M. Lansalot, *Macromolecules*, 2014, **47**, 3461–3472.
- 40 N. J. W. Penfold, Y. Ning, P. Verstraete, J. Smets and S. P. Armes, *Chem. Sci.*, 2016, **7**, 6894–6904.
- 41 F. Boujioui, F. Zhuge and J.-F. Gohy, *Macromol. Chem. Phys.*, 2019, Ahead of Print.
- 42 H. R. Kricheldorf and G. Schwarz, *J. Macromol. Sci. Part A Pure Appl.*

*Chem.*, 2007, **44**, 625–649.

- 43 J. Cao, D. Siefker, B. A. Chan, T. Yu, L. Lu, M. A. Saputra, F. R. Fronczek, W. Xie and D. Zhang, *ACS Macro Lett.*, 2017, **6**, 836–840.
- 44 M. Destarac and W. Bzducha, *PCT Int. Appl.*, 2003.
- 45 H. He, M. Zhong, B. Adzima, D. Luebke, H. Nulwala and K. Matyjaszewski, *J. Am. Chem. Soc.*, 2013, **135**, 4227–4230.
- 46 A. Fdz De Anastro, N. Lago, C. Berlanga, M. Galcerán, M. Hilder, M. Forsyth and D. Mecerreyes, *J. Memb. Sci.*, 2019, **582**, 435–441.





# **Chapter 4. UV-crosslinked Ionogels for All Solid-State Rechargeable Sodium Batteries**

## **4.1. Introduction**

Sodium-ion batteries are one of the most promising post-lithium battery technologies of the energy storage portfolio<sup>1</sup>. Sodium is widely available whereas lithium resources are unevenly distributed across the planet. However, sodium is a larger ion than lithium and the current intercalation electrode materials and the electrolyte materials developed over the years for lithium ion batteries do not perform as in the lithium case. For this reason, new materials need to be designed to act as battery components in order to compete with lithium-ion batteries for capacity, speed of charge, energy and power density. Among the different battery components that need to be developed, the polymer electrolyte membrane is a crucial one, in particular in a battery configuration that uses sodium metal as anode. The use of sodium as anode shows advantages in terms of specific capacity and power density of the battery, however, brings about important safety issues due to the high reactivity of sodium metal. For this reason, electrolytes with low or zero flammability such as ionic liquids and

polymers are ideal candidates in the case of sodium metal batteries<sup>2-4</sup>. Recently a phosphonate gel system imbued with an organic electrolyte has been demonstrated to support SnS<sub>2</sub> as an anode and NaVP as a cathode, achieving stable cycling whilst offering low flammability and thus enhanced safety due to the extinguishing properties of the phosphonate polymer<sup>5</sup>. However, the liquid electrolyte components typically used in such gels are not environmentally friendly nor safe, being based on either NaClO<sub>4</sub> or NaPF<sub>6</sub> and carbonates or glymes. Moreover, such electrolytes are not able to support stable Na metal cycling which is still a holy grail for higher energy density.

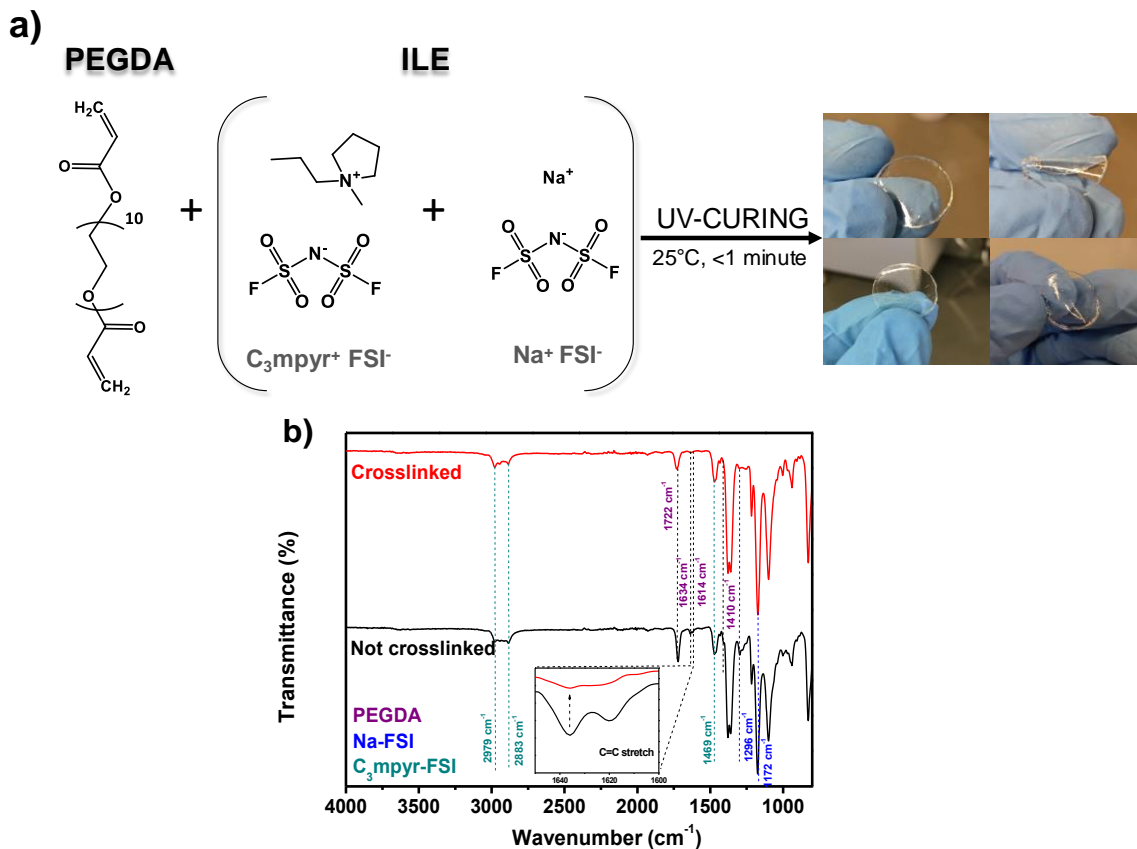
On the other hand ionic liquid based electrolytes have been developed showing excellent performance in both Na-ion and Na-metal batteries<sup>6, 7</sup>. Several electrolyte formulations have been reported using ammonium, phosphonium, imidazolium and pyrrolidonium ionic liquids having mostly fluorinated sulphonamide anions such as TFSI and FSI combined with NaFSI or NaTFSI salts<sup>8-10</sup>. These anions, as well as many ionic liquids used in potential battery electrolytes, are more recyclable which is of great importance when considering next generation energy storage and the circular economy principles<sup>11</sup>. Some of those electrolytes also show excellent ability to support sodium electrochemistry and long term stability over sodium metal. However, their liquid nature brings about some disadvantages such as the need of a porous separator and the potential leaking of the electrolyte. To overcome this issue, the preparation of solid gel electrolytes such as the so-named ionogel, ionic liquid gel or ionogel electrolytes encapsulating the ionic liquid within a polymer network would be ideal<sup>12, 13</sup>. Although, the use of ionogels is a very popular solution for lithium batteries and other technologies such as supercapacitors<sup>12</sup> or Zn-batteries<sup>14</sup> to the best of our knowledge there are only two reports relating to the development of ionogel membranes for Na-ion

batteries<sup>15, 16</sup>. In one case, the ionic liquid N-Propyl-N-methylpyrrolidinium bis(fluorosulfonyl)imide (C<sub>3</sub>mpyrFSI) and 0.8m sodium bis(fluorosulfonyl)imide salt (NaFSI) were incorporated within PVDF-co HFP copolymer (94%IL: 6%polymer) which was also supported on a glass fibre mat and a Na/ionogel/NVP battery was cycled successfully and safely reaching just over 80mAh/g capacity. On other hand we recently used the polydiallyldimethylammonium-bis(trifluoromethane)sulfonimide (PDADMA-TFSI) polymer to incorporate up to 50% of a similar ILE based on C<sub>3</sub>mpyrFSI and 20mol% NaFSI. This relatively low ILE content in the (PDADMA-TFSI) retains the mechanical properties of the ionogel, however it limits the ionic conductivity values of the final polymer electrolyte. In this paper, we present a simple way of preparing ionogel membranes for sodium metal batteries which show superior solid electrolyte parameters (mechanical properties, thermal stability, ionic conductivity and sodium transference number) and battery performance. We also show that incorporating a higher NaFSI content in the ionogel allows higher rate capability of Na cycling.

## 4.2. Membrane preparation

The preparation pathway towards ionogel electrolytes is shown in Figure 4.1. The ionogels were prepared by UV-curing photopolymerization due to its previous success for making elaborating ionogels for lithium batteries<sup>17</sup>. The ionogels were made by UV-curing of poly(ethylene glycol diacrylate) (PEGDA) within an ionic liquid electrolyte (ILE) composed of N-Propyl-N-methylpyrrolidinium bis(fluorosulfonyl)imide (C<sub>3</sub>mpyrFSI) ionic liquid and sodium

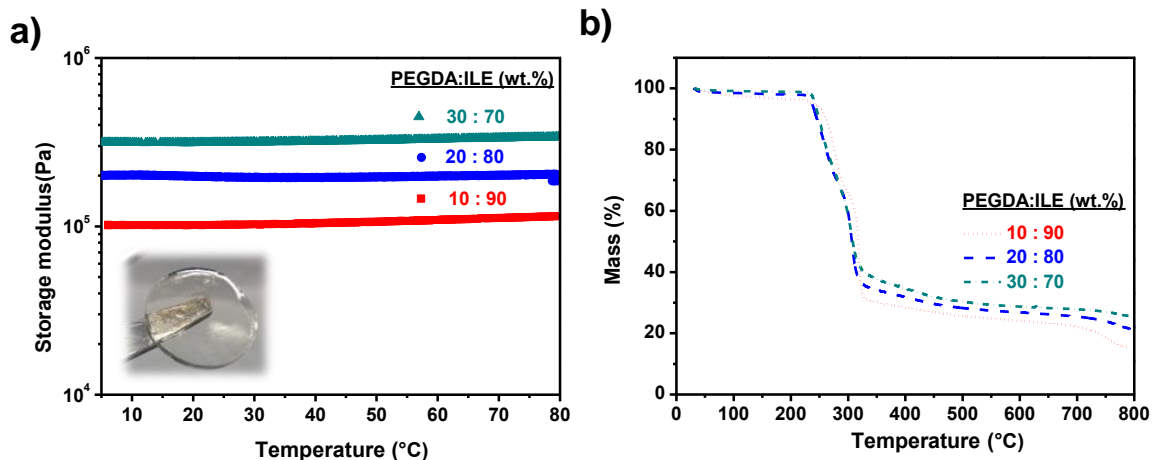
bis(fluorosulfonyl)imide salt (NaFSI) using 2-Hydroxy-2-methylpropiophene (DAROCUR) as a radical photoinitiator. We varied the amount of PEGDA crosslinker between 10 and 30 wt%. Six different ionogels were prepared containing 10, 20 and 30 wt% of PEGDA combined with 90, 80 and 70 wt% of ionic liquid electrolyte (ILE) that contained 20 and 50 mol% of NaFSI dissolved in  $C_3mpyrFSI$ . The obtained ionogels were self-standing membranes easily handled and flexible as shown in Figure 4.1.a). At higher amounts of ionic liquid (>90wt %) the membranes were too soft to be handled becoming as honey. The photopolymerization process is very fast as confirmed by the optical appearance of the ionogel membranes which became solid flexible materials after 1 minute. By Fourier Transform Infrared Radiometer (FTIR) we could observe how the bands at 1634 and 1614  $cm^{-1}$  associated to the acrylate double bond disappeared almost completely which indicated also the high extent of the photopolymerization process (Figure 4.4..1.b).



**Figure 4.1.** a) Synthetic representation of the preparation of the ionogels by UV-Curing; b) FTIR of the ionogel before and after curing showing the disappearance of the acrylate functionalities of an ionogel containing an initial composition of 20 wt% of PEGDA and 80 wt% of ionic liquid electrolyte.

### 4.3. Mechanical properties and thermal stability

The mechanical properties and thermal stability of the membranes were also evaluated. Figure 4.2.a) shows the dynamic mechanical thermal analysis (DMTA) of three different ionogels prepared with initial composition in PEGDA based polymer network 10, 20 and 30 wt% and ionic liquid electrolyte that contained 50 mol% of NaFSI dissolved in C<sub>3</sub>mpyrFSI. As expected the storage modulus of the membranes increases while increasing the PEGDA polymer content showing values between 10<sup>5</sup> to 5x10<sup>5</sup> Pa. More interestingly, the storage modulus of the membranes is constant between room temperature and 80 °C probably due to the cross-linking in the material. This is particularly interesting for battery operation since it demonstrates that the membrane maintains its mechanical properties at different temperatures. Figure 4.2.b shows the thermogravimetric analysis of the same ionogels and indicates that they do not present any degradation until temperatures higher than 250 °C. This high thermal stability is typical of ionic liquids and this data shows that the stability is directly transferred to the ionogels. Similar DMTA and TGA results were obtained with the ionogels having lower concentration of NaFSI.



**Figure 4.2.** a) DMTA analysis of three different membranes composed by 10, 20 and 30 wt% of PEGDA based polymer network with 90, 80, 70 wt% of ionic liquid electrolyte that contained 50 mol% of NaFSI dissolved in  $\text{C}_3\text{mpyrFSI}$ , b) TGA Analysis under nitrogen at 10  $^{\circ}\text{C}/\text{min}$  of the same ionogels.

#### 4.4. Ionic conductivity and sodium transference number

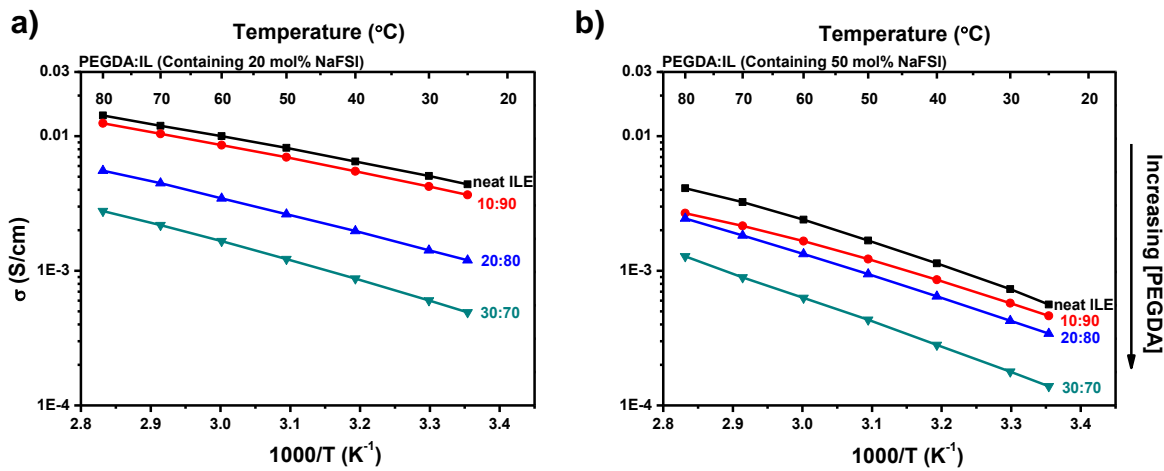
The effect of the composition on the ionic conductivity of the polymer electrolyte membranes was also investigated. For this purpose, the ionic conductivity was measured by impedance spectroscopy at different temperatures in the case of six different ionogels with initial compositions of 10, 20 and 30 wt% of PEGDA based polymer network combined with 90, 80, 70 wt% of ILE that contained 20 and 50 mol% of NaFSI dissolved in  $\text{C}_3\text{mpyrFSI}$ . These ionogels were compared with the neat ionic liquid electrolytes. According

to Figure 4.3.a) for the lower concentration NaFSI ionogel, the ionic conductivity increases steadily when increasing the IL content towards the value of neat ionic liquid electrolytes. As expected, the ionic conductivity increases with the temperature and both slope and shape of the curves are very similar to those of the ionic liquid electrolytes. It is remarkable that the ionic conductivity of the ionogel having 90 wt% of ionic liquid electrolyte shows very high values ( $6.5 \cdot 10^{-3} \text{ S} \cdot \text{cm}^{-1}$  at  $50 \text{ }^\circ\text{C}$ ) which are very similar to the ones of the ionic liquid electrolyte ( $7.8 \cdot 10^{-3} \text{ S} \cdot \text{cm}^{-1}$ ). Following this, we investigated the effect on conductivity of increasing the concentration of NaFSI salt in the ionogels (figures 4.3.b), from which it is clearly observed that the ionic conductivity decreases at higher NaFSI concentrations in the electrolyte ( $6.5 \cdot 10^{-3} \text{ mS} \cdot \text{cm}^{-1}$  value as compared to  $1.5 \cdot 10^{-3} \text{ S} \cdot \text{cm}^{-1}$  at  $50 \text{ }^\circ\text{C}$ ), this phenomenon can be explained with the calculation of the activation energies in which is shown that the dynamics are harder in case of the more concentrated ionogel. This was also previously observed in the related ionic liquid electrolytes and is attributed to the increase of the viscosity of the liquid electrolyte when working with high NaFSI salt content systems<sup>2</sup>. It is also interesting to note that there appears to be a more dramatic effect of the PEGDA on the conductivity of the ILE at 10% PEGDA content in comparison with the 20mol% NaFSI whereas the effect is less evident at higher PEGDA loadings. This could reflect an interaction between the  $\text{Na}^+$  ions in the ILE and the ether functional groups in the polymer which would also suggest good compatibility between the components.

When considering the optimum solid electrolyte to incorporate into an electrochemical cell, normally, one would think that the lower NaFSI concentrations are more desirable for given their higher conductivities, however, as was shown by several other works in both IL and organic solvents, the higher concentrations in fact lead to better electrochemical performance<sup>18, 19</sup>. One



reason for this is thought to be due to the increased  $\text{Na}^+$  transport number in the concentrated IL but another may be to do with the nature of the SEI that forms in these higher concentration systems.



**Figure 4.3.** Ionic conductivity vs temperature of ionic liquid electrolytes and ionogels having 90, 80, 70 wt% of ionic liquid  $\text{C}_3\text{mpyrFSI}$  electrolyte containing a) 20 mol% of NaFSI and b) 50 mol% of NaFSI.

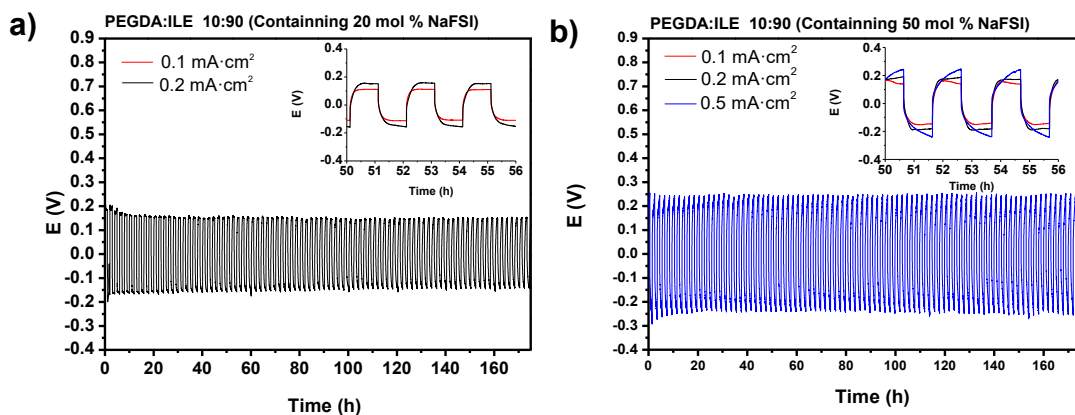
The sodium transference number in these ionogels (containing 10 wt% of PEGDA combined with 90 wt% of IL that contained 20 and 50 mol% of NaFSI) was determined using the equation proposed by Watanabe et al at 50°C<sup>20, 21</sup>, which showed more consistency than the famous Vincent and Bruce equation. The increasing concentration of the NaFSI in the ionogels leads to an

increase of the  $t_{Na^+}$  from 0.3 to 0.49. According to Forsyth *et al* transference number in C<sub>3</sub>mpyrFSI/NaFSI liquid electrolyte system may imply different sodium ion transport mechanism in higher NaFSI concentration systems; this fact explains the dramatic increase of the transference number for these ionogels since they have very similar physico-chemical and electrochemical properties compared with their analogous liquid electrolyte systems.

### 4.5. Symmetric sodium cell

Symmetric sodium cell experiments were carried out to determine the performance of the ionogels at the Na electrode that was used as anode in a solid-state battery. Plating/stripping cycles for these Na|ionogel|Na symmetric cells at 50 °C are shown in Figure 4.4. Two different ionogels with an initial composition of 10 wt% of PEGDA polymer network combined with 90 wt% of ILE that contained 20 (Figure 4.4.a) and 50 mol% (Figure 4.4.b) of NaFSI dissolved in C<sub>3</sub>mpyrFSI were chosen to investigate the effect of the higher ionic conductivity values in these ionogels. Symmetric cell experiments were performed at 0.1, 0.2 and 0.5 mA·cm<sup>-2</sup> (1h both plating and stripping) for 175 cycles. Polarization profiles for each composition are presented as an inset in Figure 4.4.a and 4b to better appreciate the increase of the polarization potential with the increase of the current density although interestingly it is not very significant considering a 5 fold increase in current density (from 0.1 to 0.5 mA/cm<sup>2</sup>). Both compositions show good performance at 0.1 and 0.2 mA·cm<sup>-2</sup> for more than 160 hours with a stable polarization potential of 0.17 and 0.18V at 0.2 mA·cm<sup>-2</sup> for 20 and 50 mol% NaFSI salt content ionogel respectively. Both ionogels present stable interface during sodium plating/stripping after 10 cycles according to the impedance spectra recorded every 10 cycles. Interestingly only

the ionogel containing 50 mol% of NaFSI salt can support the higher current density cycling ( $0.5 \text{ mA}\cdot\text{cm}^{-2}$ ), demonstrating good sodium cycling stability for more than 150 cycles. These results corroborate previous observations with liquid electrolytes based on  $\text{C}_3\text{mpyrFSI/NaFSI}$  where high concentration of NaFSI facilitates cycling at high current densities despite their lower ionic conductivity. It is worth remarking that the cycling results shown here for both ionogels at lower current densities are very similar to the previously reported ones for ionic liquid electrolytes ( $\sim 0.15\text{V}$  of overpotential at  $0.1 \text{ mA}\cdot\text{cm}^{-2}$ ) with the additional advantage of their soft solid nature<sup>22</sup>.

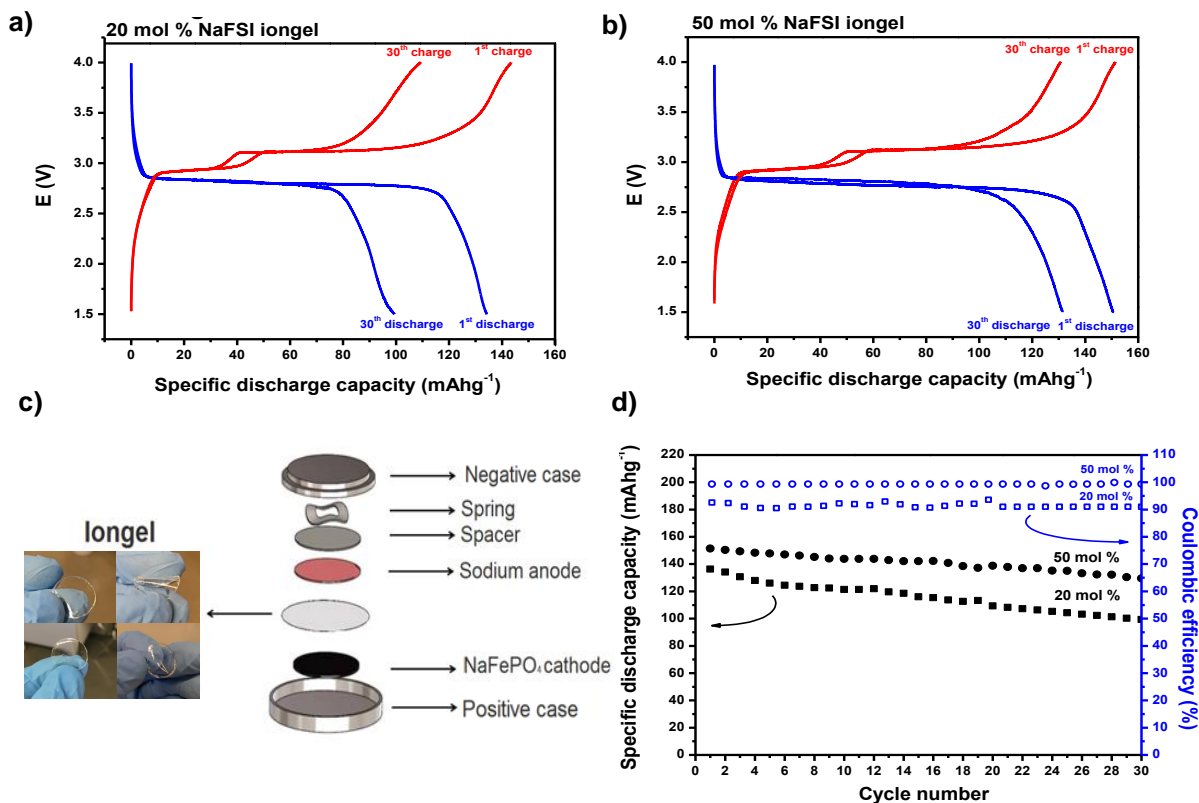


**Figure 4.4.** Plating/stripping cycles of sodium symmetric cells having the ionogel electrolytes composed of 90wt % ionic liquid electrolyte having a) 20 mol% NaFSI and b) 50 mol % NaFSI. Cycling was carried out at  $50 \text{ }^\circ\text{C}$  at different current densities ( $0.1, 0.2$  and  $0.5 \text{ cm}^{-2}$ ).

## 4.6. Sodium metal solid state battery

Finally, the two different ionogels were tested in a sodium metal solid state battery (Figure 4.5.a and 5b). These cycling measurements were carried out in a CR2032 coin cell type set up (Figure 4.5.c) using a sodium metal disc as anode and *olivine*-type  $\text{NaFePO}_4$  as cathode material (theoretical capacity of  $154 \text{ mAhg}^{-1}$ ). All  $\text{Na}|\text{ionogel}|\text{NaFePO}_4$  batteries were cycled between 1.5 and 4V at a rate of C/20 at  $50^\circ\text{C}$ . Figure 4.5.a) and 4.5.b) show the charge and discharge curves (potential vs specific capacity) of the two ionogel compositions, delivering in both batteries a specific capacity 98% and 90% of the theoretical one, respectively. Interestingly after the 30<sup>th</sup> cycle the capacity of the 20 mol% NaFSI containing ionogel decreases from  $137 \text{ mAhg}^{-1}$  to  $100 \text{ mAhg}^{-1}$  (from 90% to 65% of the theoretical specific capacity) while the capacity of the 50 mol% NaFSI containing ionogel decreases from  $152 \text{ mAhg}^{-1}$  to  $131 \text{ mAhg}^{-1}$  (from 99% to 85% of the theoretical specific capacity). In addition, higher coulombic efficiency is achieved when using the NaFSI concentrated ionogel, >99% (high NaFSI concentration) versus >91% (low NaFSI concentration). Thus we observe that, the ionogel containing higher salt concentration shows better performance (higher specific capacity, higher columbic efficiency and better capacity retention) corroborating the previous observations in the symmetric cells. The capacities observed in this work of  $152 \text{ mAhg}^{-1}$  and  $131 \text{ mAh g}^{-1}$  at 1<sup>st</sup> and 30<sup>th</sup> cycle respectively are to the best of our knowledge the highest reported in the literature, for an all solid-state solid metal sodium battery. In fact, there are not many examples of solid polymer electrolytes to compare with, with the exception of the PDADMA-TFSI recently reported<sup>16</sup> which presented  $125 \text{ mAh g}^{-1}$  at C/20 in a similar  $\text{Na}|\text{ionogel}|\text{NaFePO}_4$  metal battery. Furthermore, these results are even better than those reported for the related ionic liquid electrolytes like  $\text{C}_4\text{mpyrTFSI}/\text{NaTFSI}$  system, in which lower specific capacity is reported ( $125$

mAhg<sup>-1</sup>) using same cell set up (Na/NaFePO<sub>4</sub>) at C/20 at 50 °C<sup>23</sup> and Ferdousi's recent work in the case where the C<sub>3</sub>mpyrFSI/NaFSI is soaked into Solupor<sup>24</sup>. One interesting thing to consider here is that when assembling the full cell, the soft solid electrolyte makes excellent contact with the electrodes in the cell and in particular due to wetting and penetration for the electrolyte into the cathode. This efficient contact may provide better charge transport characteristics for improved cell performance.



**Figure 4.5.** Charge and discharge curves profile at the 1<sup>st</sup> and 30<sup>th</sup> cycle of ionogels composed by 10 wt. % of PEGDA combined with 90wt % ionic liquid electrolyte having a) 20 mol % NaFSI and b) 50 mol % NaFSI at 50 °C at C/20. c) scheme of CR2032 coin cell configuration and d) Specific discharge capacity values and coulombic efficiency ionogels composed by 10 wt% of PEGDA combined with 90wt % ionic liquid electrolyte having 20 and 50 mol % NaFSI respectively.

## 4.7. Versality of UV-crosslinked ionogels

Ionogels can be very versatile materials since different ionic liquid and polymer matrix can be used depending on the application that we are looking for. In this chapter we have mainly focused in C<sub>3</sub>mpyrFSI ionic liquid based ionogels, but different ionic liquids can be used to elaborate new UV-crosslinked ionogel membranes.

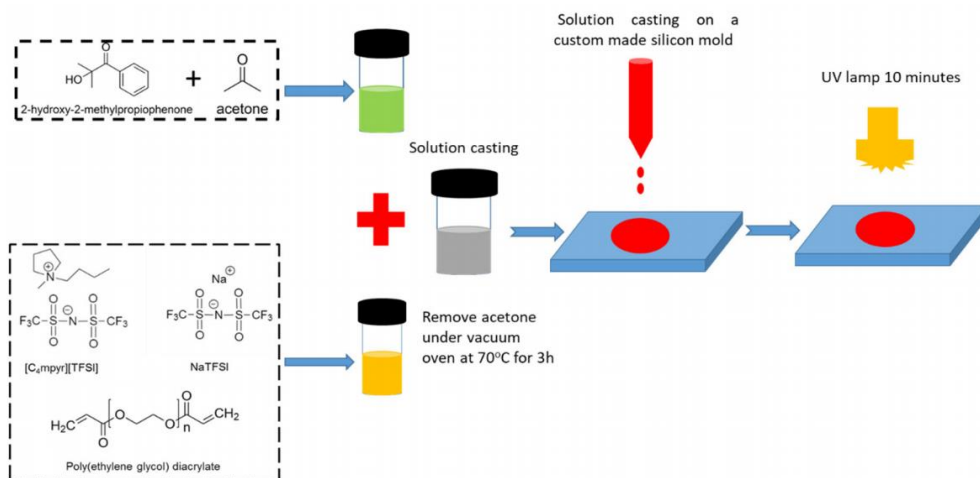
### 4.7.1. UV-crosslinked ionogels for Na-O<sub>2</sub> batteries

As an example, ionogels based on N-butyl-N-methylpyrrolidinium bis(trifluoromethylsulfonyl)imide [C<sub>4</sub>mpyr][TFSI] in poly(methylmethacrylate) (70:30 wt%)<sup>28</sup> and same ionic liquid in poly(vinylidene fluoride-co-hexafluoropropylene) (70:30 wt%)<sup>29</sup> have been reported for Li-O<sub>2</sub> cells, promoting the formation of a more stable and conductive solid electrolyte interface (SEI) on the Li metal anode accompanied with the construction of an effective barrier to protect the Li anode. These promising results open up new alternatives that can be transferred to other metal-O<sub>2</sub> chemistries. However, to the best of our knowledge, ionogels in Na-O<sub>2</sub> cells have not yet been studied or reported.

In this thesis we went one step further by using a bilayer electrolyte composed of an ionogel and an ionic liquid. The ionogel composition has a higher ionic liquid content (0.5 M NaTFSI in [C<sub>4</sub>mpr][TFSI]), in poly(ethylene glycol) diacrylate (PEGDA) (90: 10 wt%)) than the aforementioned ionogel

compositions, aimed to promote mass transport across the electrolyte layers. Such a bilayer electrolyte combination should limit the crossover of oxygen electrogenerated species to the metallic anode, and hence the corrosion of the sodium metal.

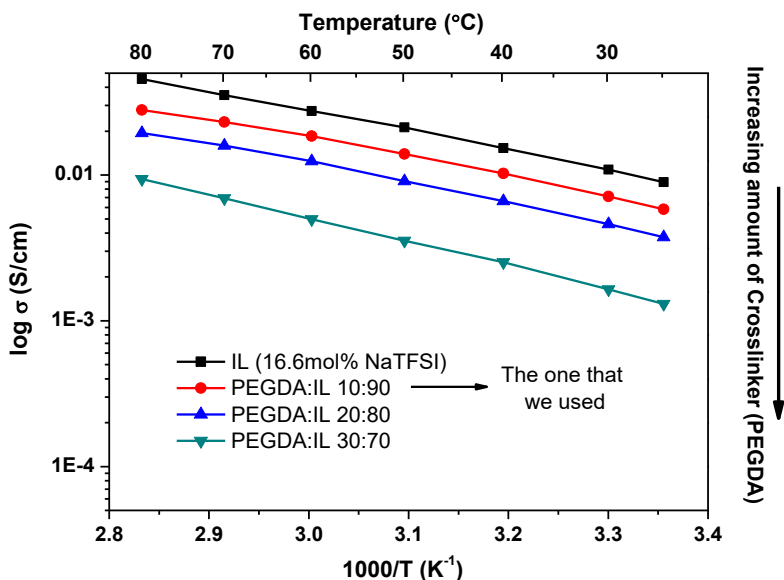
The ionogels were prepared by mixing a solution containing 16.6 mol % NaTFSI in C4mpyrTFSI with PEGDA and DAROCUR in acetone in two different concentrations (e.g. 0.49M and 0.13M, respectively). Once the mixture became homogeneous (after 1 hour stirring), the acetone was removed in an oven for 3 hours under vacuum at 70 °C. After that, the mixture was casted on a custom made silicon mold with circular shape ( $\varnothing = 16$  mm, average thickness = 250  $\mu\text{m}$ ) and was irradiated with a UV lamp for 10 minutes. Then, the casted membranes were dried for 4 hours in a fume-hood and dried for 24 hours under vacuum at 70 °C before using them.



**Figure 4.6.** Scheme of the UV polymerization process.



Similar to previous ionogels mentioned in this chapter, these ionogels were able to withstand a 90 wt. % of ionic liquid with reasonable robustness to be used in a sodium-air battery. Three composition membranes were prepared varying the amount of IL ( $C_4\text{mpyrTFSI}$ ) from 70 to 90 wt. %, afterwards the ionic conductivity was measured (figure 4.7.) at different temperatures and they were compared with the neat ILE (without any PEGDA).



**Figure 4.7.** Ionic conductivity vs temperature of ionic liquid electrolyte and ionogels having 90, 80, 70 wt% of ionic liquid  $C_4\text{mpyrTFSI}$  content.

The ionic conductivity increases steadily when increasing the IL content towards the value of neat ionic liquid electrolytes (Figure 4.7.). As expected, the ionic conductivity increases with the temperature and both slope and shape of the curves are very similar to those of the ionic liquid electrolytes. It is

remarkable that the ionic conductivity of the ionogel having 90 wt% of ionic liquid electrolyte shows very high values ( $0.9 \cdot 10^{-2} \text{ S} \cdot \text{cm}^{-1}$  at  $50 \text{ }^\circ\text{C}$ ) which are very similar to the ones of the ionic liquid electrolyte ( $2.1 \cdot 10^{-2} \text{ S} \cdot \text{cm}^{-1}$ ).

In conclusion, we have developed a new ionogel suitable for sodium-oxygen batteries. We have used this ionogel to develop a strategy to reduce the side product formation in sodium-oxygen cells by protecting the sodium metal anode with a bilayer ionogel/ionic liquid electrolyte by limiting the oxygen crossover of electrogenerated species to the sodium metal, corrosion of the sodium anode is prevented, and subsequently the formation of film-like side products that passivate the air cathode are eliminated. Such strategy resulted in higher coulombic efficiency (close to 100 %) and lower charge overpotential, in comparison to the monolayer electrolyte.

### **4.7.2. Phosponium ionic liquid based ionogels**

Many studies about ionic liquids for sodium metal batteries have been focused in the use of  $\text{C}_3\text{mpyrFSI}$  but some studies have demonstrated that not only pyrrolidinium base ionic liquids are good candidates, but also phosponium cation ionic liquids like trimethyl isobutyl phosponium bis(fluorosulfonyl)imide ( $\text{P}_{11114}\text{FSI}$ ). This ionic liquid combined with  $\text{NaFSI}$  has demonstrated to outperform commonly used solvent based electrolytes in terms of capacity, elevated temperature performance, cycle stability and safety.

In this thesis  $\text{P}_{11114}\text{FSI}$  is used to make new ionogels for sodium metal batteries. These ionogels were synthesized by the same UV curing process that is described in this chapter. Similar to previous ionogels mentioned in this chapter, these ionogels were able to withstand a 90 wt. % of ionic liquid as well with

reasonable robustness to be used in a sodium-air battery. Three composition membranes were prepared varying the amount of IL ( $P_{11114}$ FSI) from 70 to 90 wt. %, afterwards the ionic conductivity was measured (figure 4.8.) at different temperatures and they were compared with the neat ILE (without any PEGDA).

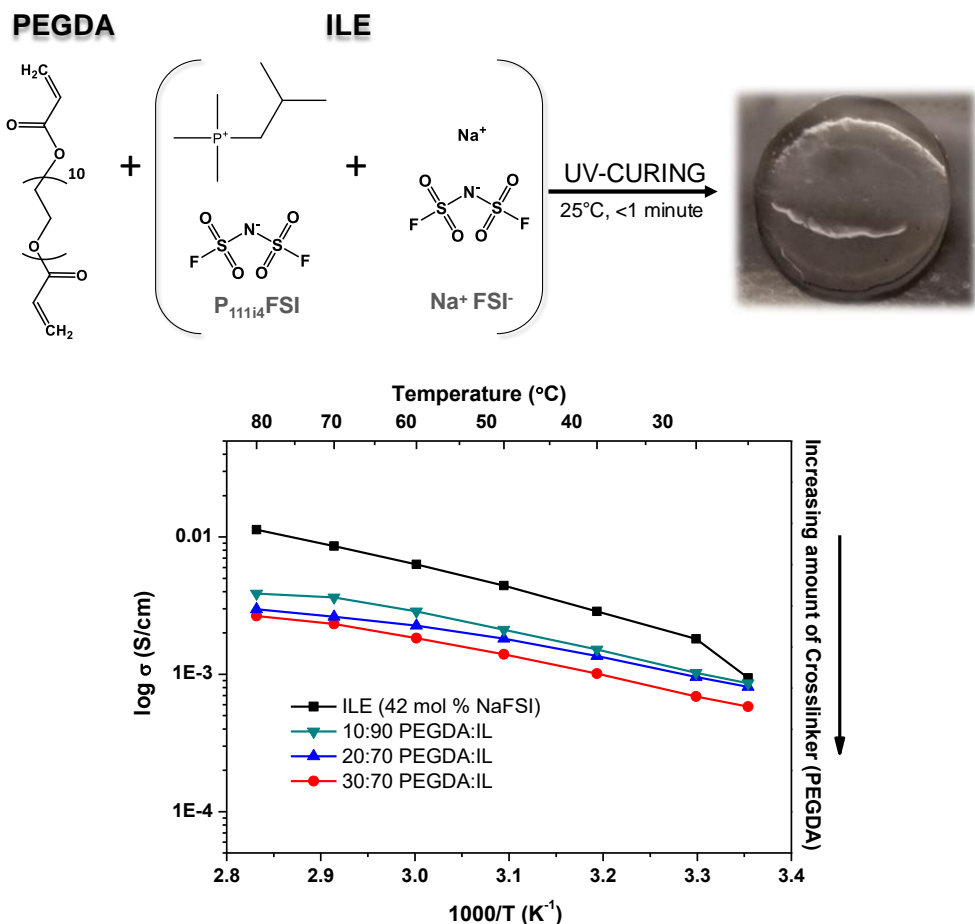


Figure 4.8. **Top:**Composition of the ionogel. **Bottom:** Ionic conductivity vs temperature of ionic liquid electrolyte and ionogels having 90, 80, 70 wt% of ionic liquid  $P_{11114}$ FSI content.

The ionic conductivity increases steadily when increasing the IL content towards the value of neat ionic liquid electrolytes (Figure 4.8.). As expected, the ionic conductivity increases with the temperature and both slope and shape of the curves are very similar to those of the ionic liquid electrolytes. It is remarkable that the ionic conductivity of the ionogel having 90 wt% of ionic liquid electrolyte shows very high values ( $2.2 \cdot 10^{-3} \text{ S} \cdot \text{cm}^{-1}$  at  $50 \text{ }^\circ\text{C}$ ) which are very similar to the ones of the ionic liquid electrolyte ( $4.3 \cdot 10^{-3} \text{ S} \cdot \text{cm}^{-1}$ ).

### 4.8. Conclusions

In conclusion, ionogel solid electrolytes with excellent properties for all solid-state rechargeable sodium batteries are presented. These ionogels were easily prepared by fast (<1 min) UV photopolymerization of commercially available poly(ethyleneglycol diacrylate) in the presence of an ionic liquid electrolyte (ILE) based on N-Propyl-N-methylpyrrolidinium bis(fluorosulfonyl)imide ( $\text{C}_3\text{mpyrFSI}$ ) ionic liquid and sodium bis (fluorosulfonyl)imide ( $\text{NaFSI}$ ) salt. The ionogels are flexible, self-standing membranes with very high ionic conductivity values (up to  $6.5 \cdot 10^{-3} \text{ S} \cdot \text{cm}^{-1}$  at  $50 \text{ }^\circ\text{C}$ ) which are dependent on the relative amount of polymer network and ionic liquid electrolytes. The studies show that high salt concentration in the ionogels was beneficial for the sodium transference number but slightly detrimental for the ionic conductivity of the membranes. These ionogels showed excellent performance both in sodium symmetric cells and all-solid battery using a sodium metal anode and  $\text{NaFePO}_4$  as the cathode material. In fact the results presented here for ionogels are even somewhat superior to

the previously reported ones with ionic liquid electrolytes soaked in Solupor separator, with the additional advantage of their solid nature which brings intrinsic advantages for battery fabrication and security.

In addition, It has been demonstrated the effectiveness of the UV-polymerization of the PEGDA to form different ionic liquid based ionogels with different properties for different batteries such as sodium metal or sodium oxygen.

## **4.9. Experimental part**

### **4.9.1. Materials and sample preparation**

N-Propyl-N-methylpyrrolidinium bis(fluorosulfonyl)imide ( $C_3\text{mpyrFSI}$ , Solvionic 99.9%), sodium bis(fluorosulfonyl)imide (NaFSI, Solvionic 99.7%), Poly(ethylene glycol) diacrylate (PEGDA, average  $M_n$  575, Aldrich) and 2-Hydroxy-2-methylpropiophene (DAROCUR 1173, Aldrich 97%) were used as received.

The ionogels were prepared by mixing different volumes of a solution of NaFSI in  $C_3\text{mpyrFSI}$  (20 and 50 mol%) and two solutions of PEGDA and DAROCUR 1173 (photoinitiator) in acetone (0.49M and 0.13M respectively). The mixture was stirred for 1 hour, until the mixture became homogeneous, and the acetone was removed in an oven for 3 hours under vacuum at 70°C. When the final solution became viscous (due to the evaporation of the acetone), it was casted on a silicon mold and was irradiated with a UV lamp for 45 seconds. The cast films were dried for 4 hours in a fume-hood and dried for 24hours under vacuum at 70 °C before transferring the samples to an Argon filled glove box. The obtained membranes were circular disks (diameter = 14 mm, average thickness = 250  $\mu\text{m}$ ).

### **4.9.2. Photo-Differential Scanning Calorimetry (DSC) and FTIR**

A Perkin Elmer 8500 DSC equipped with an ultraviolet lamp was used for this experiment to characterize the curing process and the conversion of the ionogels. 5 mg of sample were placed in an open crucible that was irradiated by ultraviolet light. All the experiments were performed under nitrogen flow in isothermal conditions at 25°C.

Chemical characterization was studied using Fourier transform infrared spectroscopy (FTIR, Bruker Alpha I Spectrometer). FTIR measurements were taken by keeping the measuring probe on the bare sample at room temperature.

### **4.9.3. Thermo-mechanical properties**

Thermal degradation of the ionogels was analyzed by Thermal Gravimetric Analysis employing a TGA Q 500 (TA instruments). About 10 mg of sample were heated from 40 to 800 °C at a heating rate of 10 °C/min under nitrogen flux of 90 mL/min. At 800 °C air flux was introduced for 15 minutes to remove the organic part of the sample.

Mechanical properties of the ionogels were analyzed by dynamic mechanical thermal analysis (DMTA) conducted compressing mode in a Dynamic Mechanical Analyser, Triton 2000 DMA (Triton Technology). Circular samples (diameter = 11 mm) were heated from 5°C to 80°C at a constant heating rate of 4 °C/min and a frequency of 1.0 Hz.

#### 4.9.4. Electrochemical characterization

The ionic conductivity was measured by electrochemical impedance spectroscopy (EIS) using a Autolab 302N Potentiostat Galvanostat coupled to a Microcell HC station to control the temperature during the measurements. Circular membranes were used for the measurements (diameter = 11 mm) with a thickness of 200  $\mu\text{m}$ . The membranes were sandwiched between two electrodes made of stainless steel and sealed in a Microcell under argon atmosphere in a glove box. The measurements were carried out from 20°C to 80°C with a step of 10°C holding the temperature for 20 minutes before each temperature to allow temperature equilibration. The frequency range was set from 0.1 MHz to 0.1 Hz and the amplitude was 10 mV. Finally, the conductivity was calculated following this equation:

$$\sigma = \frac{l}{A R_b}$$

Where  $l$  the thickness of the sample is,  $A$  is the surface of the membrane in contact with the electrode and  $R_b$  is the bulk resistance of the sample extracted from the Nyquist plot.

The Na transference number of these ionogels was carried out using a sodium symmetric cell set up. For this set up the ionogels and the Na electrodes were sandwiched between two stainless steel spacers (diameter = 16 mm, thickness = 0.5 mm) which worked as current collectors and sealed in a stainless steel bottom type case; Na metal electrodes worked as counter and working electrode. These cells were assembled under argon atmosphere in a glove box in a CR2032 Hohsen coin cell set up. A spring (thickness = 1.4 mm) was

included to improve the contact between the electrodes and the stainless steel case and finally the cells were assembled using a manual crimper. Sodium transference number was measured by direct current (DC) polarization technique proposed by Watanabe et al. According to this method an external potential step  $+\Delta V$  (0.02 V in this case) is applied across the sample that is sandwiched between the two Na metal electrodes and the resulting current is monitored as a function of time. Finally  $t_{Na^+}$  is estimated using the following equation<sup>21</sup>:

$$t_{Na^+} = \frac{R_{bS}}{\left[\frac{\Delta V}{I_S} - R_{iS}\right]}$$

Where  $\Delta V$  is the applied voltage across the cell,  $I_S$  is the current reached in the steady-state for sample polarized,  $R_{bS}$  is the resistance of bulk after polarization and  $R_{iS}$  is the interfacial resistance(SEI) after polarization.

For this experiment a Na symmetric cell set up was used and a potential step was applied. Then, the resulting current was monitored and all parameters were substituted in Watanabe's equation to extract  $t_{Na^+}$  number.

### 4.9.5. Electrode preparation

Sodium circular electrodes were punched (diameter = 10 mm, 0.785 cm<sup>2</sup>, thickness = 250  $\mu$ m) from a rolled piece of sodium metal (Panreac) in a glove box. These sodium metal electrodes were used as anode. The mass loading of the NaFePO<sub>4</sub> is 1,06 mg per electrode corresponding to a charge of 0.163 mAh.



For the cathode preparation, *olivine*-type  $\text{NaFePO}_4$  was used as cathode active material, polyvinylidene fluoride (PVDF, SOLEF) as binder and  $\text{C}_{65}$  carbon as electronic conductor and in a weight ratio of 80:10:10. The sodium iron phosphate ( $\text{NaFePO}_4$ ) was synthesized and characterized in CIC energigune. Materials were gently grinded in a hand mortar using acetone to help mixing. The powder was collected after the acetone was evaporated and dissolved in 1-methyl-2-pyrrolidone (NMP, Sigma Aldrich, 99.5%). The dispersion was stirred at RT for 1 h and the slurry was casted onto aluminium foil paper. The slurry was dried on the fume hood for 1 h and further drying was done under vacuum at 100 °C overnight.

#### **4.9.6. Sodium plating and stripping**

Na symmetric cells were used to study the interface between the sodium and the ionogel. For this set up the ionogels and the Na electrodes were sandwiched between two stainless steel spacers (diameter = 16 mm, thickness = 0.5 mm) which worked as current collectors and sealed in a stainless steel CR2032 Hohsen coin type cell; Na metal electrodes worked as counter and working electrode. These cells were assembled under argon atmosphere in a glove. A spring (thickness = 1.4 mm) was included to improve the contact between the electrodes and the stainless steel case and finally the cells were assembled using a manual crimper.

Na symmetrical cell cycling tests were carried out using a VMP3 Biologic potentiostat at 50 °C, at different current densities ( $I = 0.1, 0.2, 0.5 \text{ mA}\cdot\text{cm}^{-2}$ ) for 1h both stripping and plating during 175 cycles at each current density.

### 4.9.7. Solid state battery

Na|ionogel|NaFePO<sub>4</sub> half cells were assembled to study the electrochemical performance. *Olivine* NaFePO<sub>4</sub> electrode as cathode and sodium metal as anode were used for setting up these cells. The ionogel and the electrodes were sandwiched between two stainless steel spacers ( $\varnothing = 16$  mm, thickness = 0.5 mm) which work as current collectors and sealed in a stainless steel CR2032 Hohsen coin type cell. These cells were assembled under argon atmosphere in a glove box. A spring (thickness = 1.4 mm) was included to improve the contact between the electrodes and the stainless steel case and finally the cells were assembled using a manual crimper.

Na|ionogel|NaFePO<sub>4</sub> half cell cycling test were carried out using a VMP3 Biologic potentiostat at 50 °C. The cells were tested at C/20 cycled in a potential range of 1.5 V to 4 V for 30 cycles.

## 4.10. References

1. Palomares, V., Serras, P., Villaluenga, I., Hueso, K. B., Carretero-Gonzalez, J., Rojo, T., Na-ion batteries, recent advances and present challenges to become low cost energy storage systems, *Energy & Environmental Science*, **2012**, 5, 5884-5901.
2. Basile, A., Hilder, M., Makhlooghiyazad, F., Pozo-Gonzalo, C., MacFarlane, D. R., Howlett, P. C., Forsyth, M., Ionic Liquids and Organic Ionic Plastic Crystals: Advanced Electrolytes for Safer High Performance Sodium Energy Storage Technologies, *Advanced Energy Materials*, **2018**, 8, 1703491.
3. Forsyth, M., Porcarelli, L., Wang, X., Goujon, N., Mecerreyes, D., Innovative Electrolytes Based on Ionic Liquids and Polymers for Next-Generation Solid-State Batteries, *Accounts of Chemical Research*, **2019**, 52, 686-694.
4. Vignarooban, K., Kushagra, R., Elango, A., Badami, P., Mellander, B. E., Xu, X., Tucker, T. G., Nam, C., Kannan, A. M., Current trends and future challenges of electrolytes for sodium-ion batteries, *International Journal of Hydrogen Energy*, **2016**, 41, 2829-2846.
5. Zheng, J., Zhao, Y., Feng, X., Chen, W., Zhao, Y., Novel safer phosphonate-based gel polymer electrolytes for sodium-ion batteries with excellent cycling performance, *Journal of Materials Chemistry A*, **2018**, 6, 6559-6564.
6. Wu, F., Zhu, N., Bai, Y., Liu, L., Zhou, H., Wu, C., Highly Safe Ionic Liquid Electrolytes for Sodium-Ion Battery: Wide Electrochemical Window and Good Thermal Stability, *ACS Applied Materials & Interfaces*, **2016**, 8, 21381-21386.

7. Fukunaga, A., Nohira, T., Kozawa, Y., Hagiwara, R., Sakai, S., Nitta, K., Inazawa, S., Intermediate-temperature ionic liquid NaFSA-KFSA and its application to sodium secondary batteries, *Journal of Power Sources*, **2012**, 209, 52-56.
8. Matsumoto, K., Taniki, R., Nohira, T., *Inorganic-Organic Hybrid Ionic Liquid Electrolytes for Na Secondary Batteries*, 2014.
9. Wongittharom, N., Wang, C.-H., Wang, Y.-C., Yang, C.-H., Chang, J.-K., Ionic Liquid Electrolytes with Various Sodium Solutes for Rechargeable Na/NaFePO<sub>4</sub> Batteries Operated at Elevated Temperatures, *ACS Applied Materials & Interfaces*, **2014**, 6, 17564-17570.
10. Makhlooghiyazad, F., Guazzagaloppa, J., O'Dell, L. A., Yunis, R., Basile, A., Howlett, P. C., Forsyth, M., The influence of the size and symmetry of cations and anions on the physicochemical behavior of organic ionic plastic crystal electrolytes mixed with sodium salts, *Physical Chemistry Chemical Physics*, **2018**, 20, 4721-4731.
11. Valdés Vergara, M. A., Lijanova, I. V., Likhanova, N. V., Olivares Xometl, O., Jaramillo Viguera, D., Morales Ramirez, A. J., Recycling and recovery of ammonium-based ionic liquids after extraction of metal cations from aqueous solutions, *Separation and Purification Technology*, **2015**, 155, 110-117.
12. Yang, Q., Zhang, Z., Sun, X.-G., Hu, Y.-S., Xing, H., Dai, S., Ionic liquids and derived materials for lithium and sodium batteries, *Chemical Society Reviews*, **2018**, 47, 2020-2064.
13. Singh, V. K., Shalu, Chaurasia, S. K., Singh, R. K., Development of ionic liquid mediated novel polymer electrolyte membranes for application in Na-ion batteries, *RSC Advances*, **2016**, 6, 40199-40210.
14. Fdz De Anastro, A., Casado, N., Wang, X., Rehmen, J., Evans, D., Mecerreyes, D., Forsyth, M., Pozo-Gonzalo, C., Poly(ionic liquid) ionogels

- for all-solid rechargeable zinc/PEDOT batteries, *Electrochimica Acta*, **2018**, 278, 271-278.
15. Mendes, T. C., Zhang, X., Wu, Y., Howlett, P. C., Forsyth, M., Macfarlane, D. R., Supported Ionic Liquid Gel Membrane Electrolytes for a Safe and Flexible Sodium Metal Battery, *ACS Sustainable Chemistry & Engineering*, **2019**, 7, 3722-3726.
  16. Fdz De Anastro, A., Lago, N., Berlanga, C., Galcerán, M., Hilder, M., Forsyth, M., Mecerreyes, D., Poly(ionic liquid) iongel membranes for all solid-state rechargeable sodium-ion battery, *Journal of Membrane Science*, **2019**.
  17. Porcarelli, L., Shaplov, A. S., Bella, F., Nair, J. R., Mecerreyes, D., Gerbaldi, C., Single-Ion Conducting Polymer Electrolytes for Lithium Metal Polymer Batteries that Operate at Ambient Temperature, *ACS Energy Letters*, **2016**, 1, 678-682.
  18. Basile, A., Ferdousi, S. A., Makhlooghiazad, F., Yunis, R., Hilder, M., Forsyth, M., Howlett, P. C., Beneficial effect of added water on sodium metal cycling in super concentrated ionic liquid sodium electrolytes, *Journal of Power Sources*, **2018**, 379, 344-349.
  19. Hilder, M., Howlett, P. C., Saurel, D., Gonzalo, E., Basile, A., Armand, M., Rojo, T., Kar, M., MacFarlane, D. R., Forsyth, M., The effect of cation chemistry on physicochemical behaviour of superconcentrated NaFSI based ionic liquid electrolytes and the implications for Na battery performance, *Electrochimica Acta*, **2018**, 268, 94-100.
  20. Pożyczka, K., Marzantowicz, M., Dygas, J. R., Krok, F., IONIC CONDUCTIVITY AND LITHIUM TRANSFERENCE NUMBER OF POLY(ETHYLENE OXIDE):LiTFSI SYSTEM, *Electrochimica Acta*, **2017**, 227, 127-135.

21. Watanabe, M., Nagano, S., Sanui, K., Ogata, N., *Estimation of Li<sup>+</sup> transport number in polymer electrolytes by the combination of complex impedance and potentiostatic polarization measurements*, 1988.
22. Forsyth, M., Yoon, H., Chen, F., Zhu, H., MacFarlane, D. R., Armand, M., Howlett, P. C., Novel Na<sup>+</sup> Ion Diffusion Mechanism in Mixed Organic–Inorganic Ionic Liquid Electrolyte Leading to High Na<sup>+</sup> Transference Number and Stable, High Rate Electrochemical Cycling of Sodium Cells, *The Journal of Physical Chemistry C*, **2016**, 120, 4276-4286.
23. Wongittharom, N., Lee, T.-C., Wang, C.-H., Wang, Y.-C., Chang, J.-K., Electrochemical performance of Na/NaFePO<sub>4</sub> sodium-ion batteries with ionic liquid electrolytes, *Journal of Materials Chemistry A*, **2014**, 2, 5655-5661.
24. Ferdousi, S. A., Hilder, M., Basile, A., Zhu, H., O'Dell, L. A., Saurel, D., Rojo, T., Armand, M., Forsyth, M., Howlett, P. C., Water as an Effective Additive for High-Energy-Density Na Metal Batteries? Studies in a Superconcentrated Ionic Liquid Electrolyte, *ChemSusChem*, **2019**, 12, 1700-1711







## Chapter 5. Conclusions

In this PhD thesis we synthesized different innovative ionogels to use them in sodium metal batteries. Overall, we demonstrated that using different pathways to synthesize ionogels, ionic liquid fraction can be enhanced achieving high ionic liquid content ionogels (up to 90 wt. %). In addition physico-chemical and electrochemical properties can be modulated as it will be shown.

In the second chapter of this thesis, we showed a new ionogel electrolyte with excellent properties for an all solid-state rechargeable sodium batteries. This ionogel membrane is based on the poly(dimethyldiallylammonium) polyDADMA-TFSI poly(ionic liquid), N-Propyl-N-methylpyrrolidinium bis(fluorosulfonyl)imide (C<sub>3</sub>mpyrFSI) and sodium bis (fluorosulfonyl)imide (NaFSI) the salt. PolyDADMA-TFSI can incorporate up to 50 wt% of C<sub>3</sub>mpyrFSI ionic liquid content in a self-standing membrane with high ionic conductivity. The increasing the NaFSI concentration in this electrolyte was beneficial for the sodium transference number but detrimental for the ionic conductivity of the membranes. The addition of alumina nanoparticles further improved the membrane mechanical robustness without affecting significantly the ionic conductivity. The ionogel membranes presented a wide electrochemical window of 5 V thereby supporting sodium electrochemistry as demonstrated by excellent symmetric sodium cell cycling at 70 °C for 60

cycles. Finally, the electrochemical performance of the optimum composition ionogel was evaluated in sodium all solid-state battery using a sodium metal anode and  $\text{NaFePO}_4$  as the cathode material. The cells show good capacity retention with high coulombic efficiency (>97%) at C rates between C/20 and C/5 achieving  $110 \text{ mAhg}^{-1}$  at C/20.

In the third chapter of this thesis, the synthesis of poly(diallyldimethylammonium)-based block copolymers (BCPs) was investigated by MADIX/RAFT. DADMAC was firstly polymerized in water using mono- or difunctional MADIX agent at  $60^\circ\text{C}$  with the water-soluble azoinitiator. Then, Polymerization-Induced Self-Assembly (PISA) was implemented using PDADMAC as macroinitiator and styrene (S) for the emulsion phase, leading to cationic latexes made of di- or triblock copolymers. Taking advantage of the self-standing properties of the PS segment, these BCPs appeared to be ideal for ionogel membranes. After anion exchange between chloride and bis(trifluoromethanesulfonyl)imide, the BCPs were mixed with ionic liquid electrolyte (ILE) composed by a mixture of propyl-N-methylpyrrolidinium bis(fluorosulfonyl)imide ionic liquid ( $\text{C}_3\text{mpyrFSI}$ ) and sodium bis(fluorosulfonyl)imide salt ( $\text{NaFSI}$ ) in various ratio. Once casted, self-standing membranes were obtained and the ionic conductivity was measured. Compared to diblock, triblock copolymers showed the best self-standing properties, which is hypothetically related to the physical cross-linking of the two external PS blocks. High conductivity values were obtained for these PDADMATFSI-based membranes composed of up to 80 wt % in ILE meaning only 20 wt % in BPCs.

In the fourth chapter of this thesis, a simple method to prepare a mechanically robust ionogel film by fast (<1 min) UV photopolymerization of poly(ethylenglycol diacrylate) in the presence of an ionic liquid electrolyte (ILE) based on N-Propyl-N-methylpyrrolidinium bis(fluorosulfonyl)imide (C<sub>3</sub>mpyrFSI) IL and sodium bis (fluorosulfonyl)imide (NaFSI) salt is demonstrated. The ionogels can incorporate up to 90 wt% of ILE with very high ionic conductivity at 50 °C ( $6.5 \cdot 10^{-3} \text{ S} \cdot \text{cm}^{-1}$ ) close to the liquid counterpart ( $7.8 \cdot 10^{-3} \text{ S} \cdot \text{cm}^{-1}$ ). Two compositions of ionogel electrolytes were compared having different NaFSI salt concentration (20 and 50 mol %). High salt concentration in the ionogels was beneficial for the sodium transference number although slightly detrimental for the ionic conductivity of the ionogels. The ionogel with high NaFSI concentration delivers the best performance in the symmetric sodium cell, showing long-term plating and stripping experiments at 50 °C for more than 150 cycles at 0.1, 0.2 and 0.5 mA·cm<sup>-2</sup>. Furthermore, Na/ionogel/NaFePO<sub>4</sub> full cells were easily assembled with the high ILE loading of the ionogel providing excellent interfacial compatibility and wetting of the cathode to deliver a high specific capacity of 152 mAhg<sup>-1</sup> at 50 °C with good capacity (88 % retained after 30 cycles). Furthermore, we extended this synthetic methodology to ionogels containing different ionic liquids electrolytes which can be tailored for Sodium-air and sodium metal batteries.

Last, we would like to finish this section by comparing the different ionogels prepared in the different chapters. In chapters 2, 3 and 4 different types of ionogels has been synthesized for sodium metal rechargeable batteries. Different parameters have been studied using different ionic liquids and

hosting polymers, leading to different performance and behaviour. We can summarize these materials in table 5.1.

Table 5.1. Ionogels synthesized in chapters 2, 3 and 4 and their properties.

Ionogel #	Polymer Host	Ionic Liquid/Salt	ILE (wt.%)	Ionic conductivity at 30°C (S cm <sup>-1</sup> )	Storage modulus (Pa)
1	PolyDADMA-TFSI	C <sub>3</sub> mpyrFSI/NaFSI	50-60	1.6·10 <sup>-3</sup>	2.1·10 <sup>4</sup>
2	PS <sub>10k</sub> <sup>-</sup> PDADMAT <sub>27k</sub> <sup>-</sup> PS <sub>10k</sub>	C <sub>3</sub> mpyrFSI/NaFSI	70-80	2.1·10 <sup>-3</sup>	3.2·10 <sup>6</sup>
3	PS <sub>37k</sub> <sup>-</sup> PDADMAT <sub>69k</sub> <sup>-</sup> PS <sub>37k</sub>	C <sub>3</sub> mpyrFSI/NaFSI	80	1.9·10 <sup>-3</sup>	4.5·10 <sup>6</sup>
4	PS <sub>30k</sub> <sup>-</sup> PDADMAT <sub>27k</sub> <sup>-</sup> PS <sub>30k</sub>	C <sub>3</sub> mpyrFSI/NaFSI	80	8.8·10 <sup>-4</sup>	5.9·10 <sup>6</sup>
5	PEGDA	C <sub>3</sub> mpyrFSI/NaFSI	90	6.3·10 <sup>-3</sup>	0.4·10 <sup>5</sup>
6	PEGDA	C <sub>4</sub> mpyrTFSI/NaTFSI	90	9.2·10 <sup>-3</sup>	-----
7	PEGDA	P <sub>111i4</sub> FSI/NaFSI	90	1.7·10 <sup>-3</sup>	-----

According to table 5.1., UV crosslinked ionogels (5,6 and 7) are the membranes with the highest ionic liquid fraction. This higher ionic liquid

capacity retention is possibly due to the more dense network achieved with the UV crosslinking systems. These ionogels possess high ionic conductivities, very close to the ionic conductivity of the neat ionic liquid with the advantage of handling a solid state polymer electrolyte. On the other hand, it can be observed that copolymerizing polyDADMA-TFSI poly(ionic liquid) with polystyrene the ionic liquid fraction is enhanced as well; polystyrene block gives strength to the polymer and higher ionic liquid fraction can be incorporated leading to higher ionic conductivities.

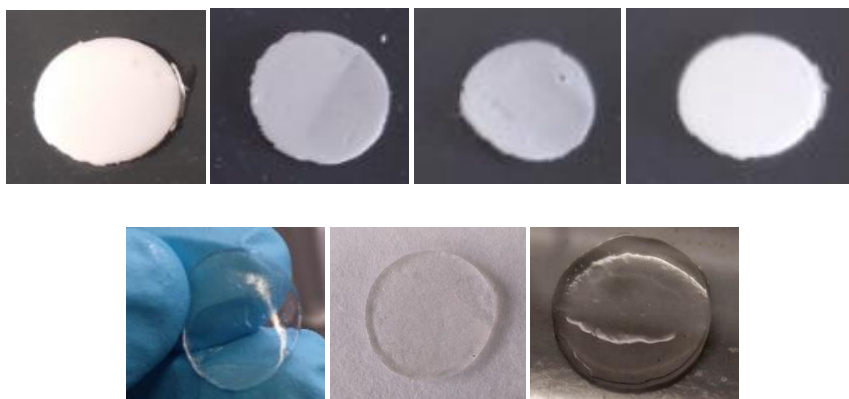


Figure 5.1.. Pictures of different ionogel membranes corresponding to ionogels 1,2,3,4,5,6,and7 consequently.

Another parameter to be compared is the leaching phenomenon. It has been observed that some ionic liquids encapsulated in certain polymers can escape from the matrix due to the lack of interaction between them; this behavior known as leaching of the ionic liquid can change the properties of

the membranes. In figure 5.1. are shown different pictures of the ionogel membranes after keeping them at 70 °C for two hours. As it is observed in these pictures UV crosslinked ionogels show a shiny appearance due to the leaching of the ionic liquid. This effect can be explained with to the lack of ionic interaction between the ionic liquid and the neutral PEGDA network. Although there is a small leach of the ionic liquid the electrochemical performance of the ionogel is excellent as it is proved in chapter 4. Interestingly, ionogels based on polyDADMA-TFSI and polyDADMA-TFSI/Styrene copolymers don't show any leaching effect even at high temperatures. Due to the ionic character of the poly(ionic liquids) like PolyDADMAC-TFSI, the chemical interaction with the ionic liquid is much higher than in other ionogels and this cause a mayor retention of the ionic liquids inside the membrane.

In terms of mechanical properties the most robust materials are the ionogels produced in chapter 3 based on triblock copolymers (ionogel 2, 3 and 4). These ionogels have the ionic affinity properties (due to the polyDADMA-TFSI segment) and the mechanical strength of the polystyrene block having an excellent compromise between mechanical properties and ionic conductivity. However, these block copolymer based ionogels lose the ionic liquid fraction at temperatures higher than 85 °C changing their mechanical properties. UV-photopolymerized ionogels, can be more suitable for temperatures beyond 85 °C because of their stable mechanically properties even at higher temperatures.

In addition, UV-crosslinked ionogels (ionogel 6) have higher ionic conductivity than the ionogel based on just polyDADMA-TFSI due to its higher ionic liquid fraction and higher storage modulus because of its crosslinked jelly like behaviour. All these features are summarized in different radar chart plots represented in figure 5.2. Each ionogel has a particular radar chart showing different compromise between all its features making each ionogel suitable for a certain application.

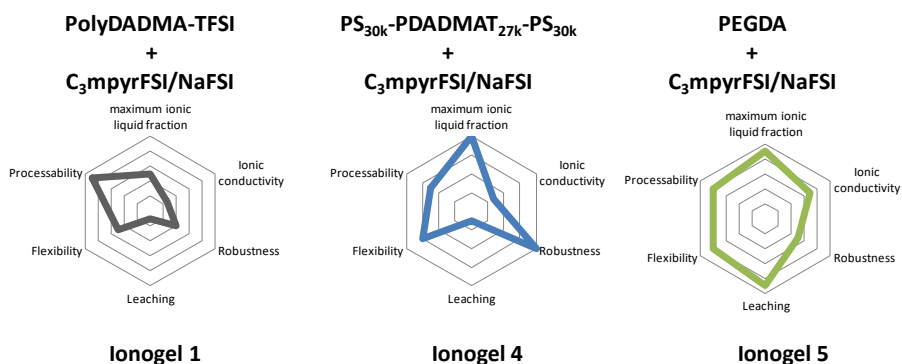


Figure 5.2.. Radar chart of different features for different ionogels.

In conclusion, this comparison has shown that the higher ionic liquid fraction and ionic conductivities has been achieved with the UV-crosslinked ionogels. On the other hand, poly(DADMAC-TFSI)-polyStyrene block copolymers ionogels has shown very interesting compromise between mechanical robustness, absence of leaching effect and ionic conductivity. We believe that this information is useful and for different applications (batteries or gas membranes for instance) the best ionogel system may be different.





# List of acronyms

<b>LIB</b>	Lithium ion batteries
<b>NFP</b>	Sodium iron phosphahate
<b>SEI</b>	Solid electrolyte interphase
<b>PC</b>	Propylene carbonate
<b>EC</b>	Ethylene carbonato
<b>IL</b>	Ionic liquid
<b>NaFSI</b>	Sodium bis(fluorosulfonyl)imide
<b>NaTFSI</b>	Sodium bis(trifluoromethanesulfonyl)imide
<b>C<sub>4</sub>mpyrTFSI</b>	<i>N</i> -methyl- <i>N</i> -propylpyrrolidinium bis(trifluoromethanesulfonyl)imide
<b>C<sub>3</sub>mpyrFSI</b>	<i>N</i> -methyl- <i>N</i> -buthylpyrrolidinium bis(fluorosulfonyl)imide
<b>PEO</b>	Poly(ethylene oxide)
<b>PMMA</b>	Poly(methyl meta)acrylate
<b>PVDF</b>	Polyvinylidene fluoride
<b>PolyDADMAC</b>	Poly(ionic liquid) poly(dimethyldiallylammonium) chloride
<b>CV</b>	Cyclic voltammetry
<b>NMP</b>	1-methyl-2-pyrrolidone

<b>RAFT</b>	Reversible-Addition Fragmentation Transfer
<b>MADIX</b>	Macromolecular Design by Interchange of Xanthate
<b>PS</b>	Polystyrene
<b>PISA</b>	Polymerization-Induced Self-Assembly
<b>AIBA</b>	2,2-azobis(2-methylpropionamide) dihydrochloride
<b>DP</b>	Degree of polymerization
<b>SEC</b>	Size exclusion chromatography
<b>DMTA</b>	Dynamic Mechanical Thermal Analysis
<b>CTA</b>	Chain transfer agent
<b>PolyDADMA-TFSI</b>	polydiallyldimethylammonium-Bis(trifluoromethane)sulfonimide
<b>PEGDA</b>	Poly(ethylene glycol diacrylate)
<b>ILE</b>	Ionic liquid electrolyte
<b>DAROCUR</b>	2-Hydroxy-2-methylpropiophene
<b>FTIR</b>	Fourier Transform Infrared Radiometer
<b>P<sub>11114</sub>FSI</b>	Isobutyl phosphonium bis(fluorosulfonyl)imide
<b>DSC</b>	Differential Scanning Calorimetry
<b>EIS</b>	Electrochemical impedance spectroscopy
<b>TGA</b>	Thermal gravimetric analysis

# List of publications, conference presentations and collaborations

## PUBLICATIONS

1. Fdz De Anastro, A., Casado, N., Wang, X., Rehmen, J., Evans, D., Mecerreyes, D., Forsyth, M., Pozo-Gonzalo, C., Poly(ionic liquid) ionogels for all-solid rechargeable zinc/PEDOT batteries, *Electrochimica Acta*, 2018, 278, 271-278.
2. Fdz De Anastro, A., Lago, N., Berlanga, C., Galcerán, M., Hilder, M., Forsyth, M., Mecerreyes, D., Poly(ionic liquid) iongel membranes for all solid-state rechargeable sodium-ion battery, *Journal of Membrane Science*, 2019.
3. Fdz De Anastro, A., Porcarelli, L., Hilder, M., Berlanga, C., Galceran, M., Howlett, P., Forsyth, M., Mecerreyes, D., UV-Cross-Linked Ionogels for All-Solid-State Rechargeable Sodium Batteries, *ACS Applied Energy Materials*, 2019, 2, 6960-6966.
4. Gomez, I., Anastro, A., Leonet, O., Blazquez, J., Grande, H. J., Pyun, J., Mecerreyes, D., Sulfur Polymers Meet Poly(ionic liquid)s: Bringing New Properties to Both Polymer Families, *Macromol. Rapid Commun.*, 2018, 39.

5. Ha, T., Anastro, A., Ortiz-Vitoriano, N., Fang, J., Macfarlane, D., Forsyth, M., Mecerreyes, D., Howlett, P., Pozo-Gonzalo, C., High Coulombic Efficiency Na-O<sub>2</sub> Batteries Enabled by a Bilayer Ionogel/Ionic Liquid, *J. Phys. Chem. Lett.*, 2019, 2019.

## CONFERENCE PRESENTATIONS

1. Fdz De Anastro, A., Casado, N., Wang, X., Rehmen, J., Evans, D., Mecerreyes, D., Forsyth, M., Pozo-Gonzalo, C., Poly(ionic liquid) ionogels for all-solid rechargeable zinc/PEDOT batteries. 15<sup>th</sup> International Symposium on Polymer Electrolytes 2016. Uppsala, Sweden (poster presentation).
2. Fdz De Anastro, A., Lago, N., Berlanga, C., Galcerán, M., Hilder, M., Forsyth, M., Mecerreyes, D., Poly(ionic liquid) iongel membranes for all solid-state rechargeable sodium-ion battery. Jóvenes Investigadores en Polímeros “JIP”. La Pineda, Spain (oral presentation).
3. Fdz De Anastro, A., Lago, N., Berlanga, C., Galcerán, M., Hilder, M., Forsyth, M., Mecerreyes, D., Poly(ionic liquid) iongel membranes for all solid-state rechargeable sodium-ion battery. “Power Our Future” organized by CIC energiGUNE 2018. Vitoria-Gasteiz, Spain (poster presentation).
4. Fdz De Anastro, A., Porcarelli, L., Hilder, M., Berlanga, C., Galceran, M., Howlett, P., Forsyth, M., Mecerreyes, D., UV-Cross-Linked Ionogels for All-Solid-State Rechargeable Sodium Batteries. 16<sup>th</sup> International Symposium on Polymer Electrolytes 2018. Yokohama, Japan (poster and flash presentation).

## COLLABORATIONS

This thesis has been done in close collaboration with various universities and research centres. The electrochemical characterization and the battery tests of the 2. Chapter has been carried out in CIC energigUNE (Vitoria-Gasteiz, Spain) under the supervision of Prof. Montse Galcerán, where I regularly moved to perform different experiments.

On the other hand, Chapter 3. Was carried out under the supervision of Prof. Cristina Pozo-Gonzalo and Prof. Maria Forsyth at Deakin University in Melbourne (Australia) where I stayed for 11 months in two stays during the PhD.

